Comparing Model Calculated Groundwater Volumes with Alternative Methods in a Mining Environment.

by

Elida Boshoff

THESIS

Submitted in fulfilment of the requirements for the degree of

Masters of Science

in the Faculty of Natural Science and Agriculture

Institute of Groundwater Studies

University of the Free State, Bloemfontein

September 2012

Promoter: Prof. Gerrit van Tonder
External co-supervisor: Prof. Ingrid Dennis

Declaration of own words

I, Elida Boshoff, hereby declare that this dissertation submitted for the degree Magister Scientiae in the Faculty of Science, Institute for Groundwater Studies, University of the Free State, Bloemfontein, South Africa, is my own work and have not been submitted to any other institution of higher education. I further declare that all sources cited are indicated in references.

E. Boshoff
2012/09/01

Keywords

Analytical calculations

Numerical estimations

Groundwater inflow

Aquifer recharge

Correlation

Comparison

Opencast mine

Acknowledgements

First and most importantly I am eternally thankful to God for providing me with all the talents and gifts that I have received over the past 27 years. My strength is in You.

To my parents; thank you for all the love, support and motivation all through my life. You have provided me with the perfect example of what I should strive for in life and my love for you is endless. I am today what I am because of you.

To the rest of my family and friends; thank you for always showing interest in my work and progress. I am privileged to have people like you in my life.

To my employer, Gerhard Steenekamp and his family; thank you for the opportunities you have given me and the guidance and support over the past five years.

To my promoter, Prof. Gerrit van Tonder and all the staff at the IGS; thank you for your support in my studies and providing me with the knowledge to build a career.

Thanks to Exarro Coal for handing me the opportunity to use the study site and information for this thesis.

Content

List of Figures

List of Tables

List of acronyms and abbreviations

LOM - Life of Mine

l/hr - litres per hour

M - meter

MAP - Mean Annual Precipitation

mamsl- meters above mean seal level

mbs - meter below surface

Model 10% - Numerical model at 10% recharge

Model 12.5% - Numerical model at 12.5% recharge

Model 20% - Numerical model at 20% recharge

m/d - meter per day

m^3/day - cubic meter per day

Q - groundwater inflow (m^3/day)

R - Radius of influence

RCH - Recharge

Sf - Storativity of fracture

Sm - Storativity of matrix

SDSL - Sandstone and shale interlaminated

SHLE - Shale

SNDS - Sandstone

SVF - Saturated volume fluctuations

Tf - Transmissivity of fracture

Tm - Transmissivity of matrix

WL - Water level

X-coord - X coordinate

Y-coord - Y coordinate

1. Introduction

The coal mining industry is one of the major contributors to the economy of South Africa. In terms of coal mining nations, South Africa is the fifth largest producer of coal in the world. It is estimated that more than 200 million tonnes of coal are mined per annum in the country (Figure 1). The country is dependent on the coal mining industry for the majority of its power supply. An estimated 92% of the energy that is produced in South-Africa is dependent on coal (Figure 3). An interesting fact is that South Africa is fourth on the list of coal consumers while Australia that is the fourth largest coal producer only plot tenth on the consumers list (Figure 2). Coal is not only used for local power supply but is also exported to other countries. (World Coal Institute, 2005)

Coal is known as a fossil fuel. It is formed when plant material is covered by soil and sedimentary material. This covering causes high temperatures and pressure which leads to the material changing in terms of physical and chemical properties. These changes will result in the formation of coal. (World Coal Institute, 2005)

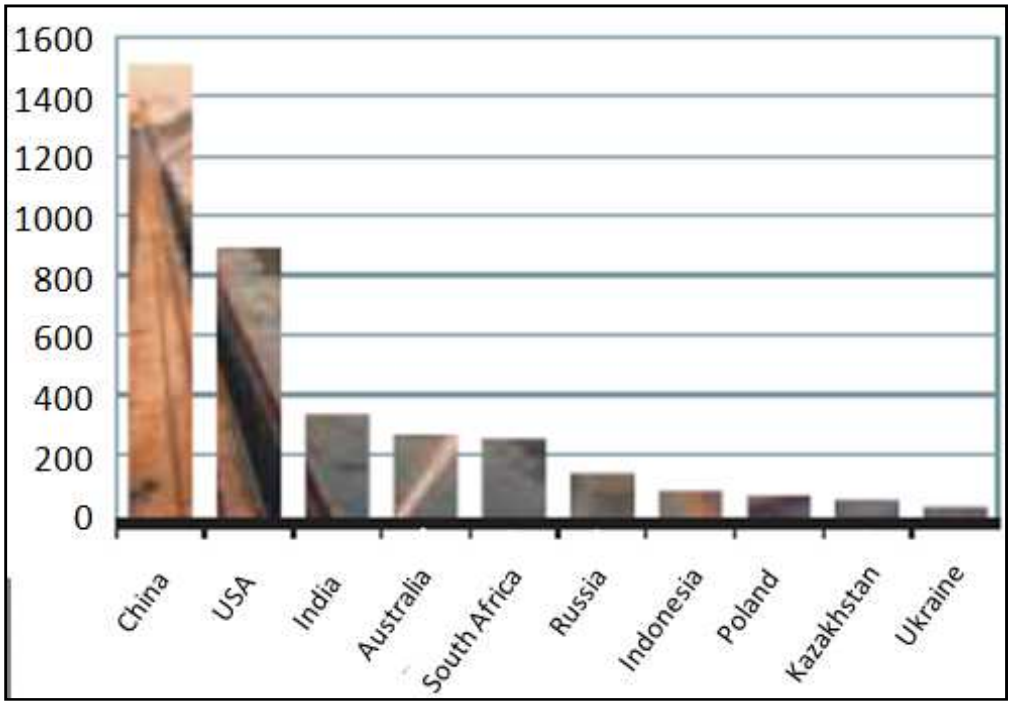

Figure 1: Top ten coal producing countries in 2003 (Mt/a). (World Coal Institute, 2005).

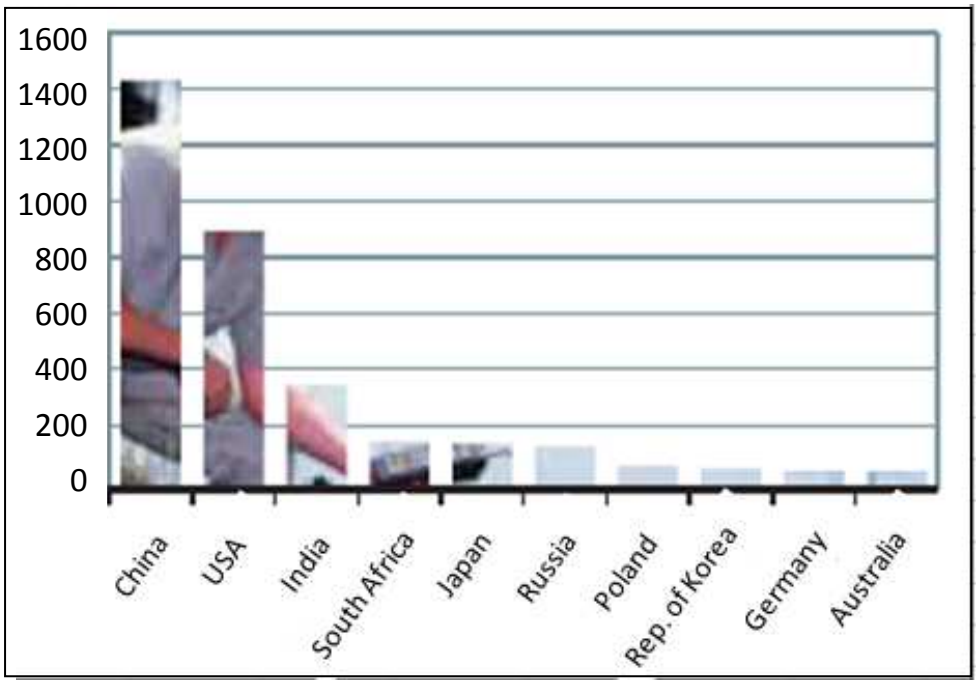

Figure 2: Top coal consumers in the world in 2003, (Mt/a) (World Coal Institute, 2005).

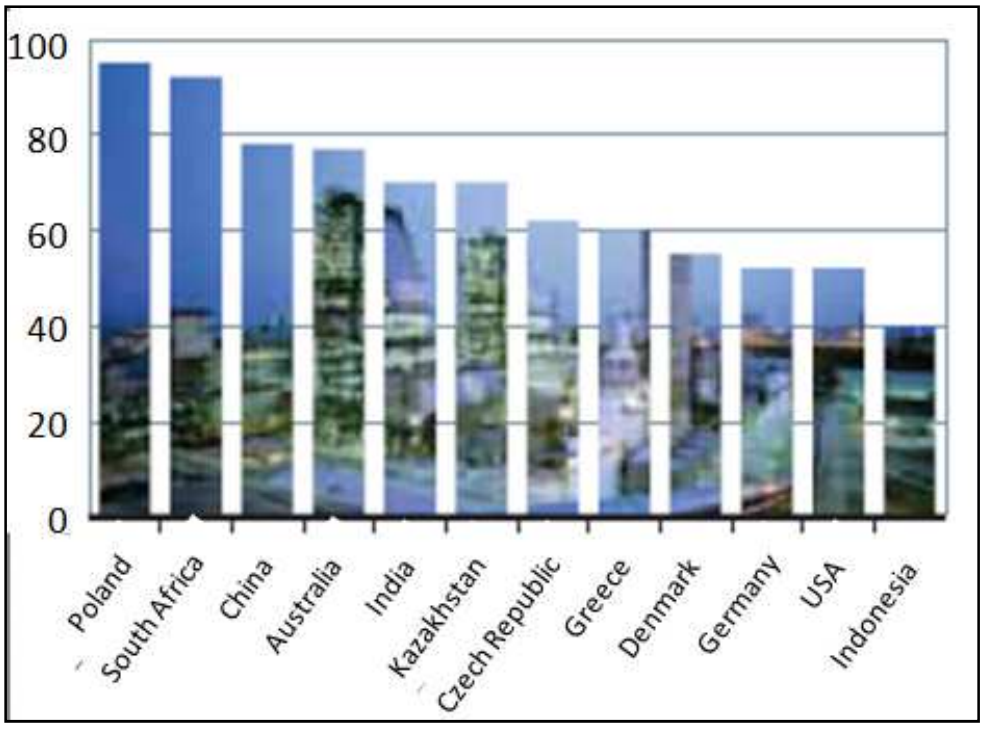

Figure 3: Percentage of electricity generated from coal (World Coal Institute, 2005).

A new opencast coal mining operation is proposed in the Belfast region in Mpumalanga, South Africa. This proposed operation is the study site that will be investigated in this thesis. The site is situated in the Witbank Coalfield which in 2001 contributed approximately 52% of the total coal production in the country. The Witbank Coalfield together with the Highveld and Waterberg Coalfields contribute more than 70% of the total coal reserves of South Africa. The Witbank Coalfield is however nearing exhaustion. (Jeffrey, 2005)

Table 1: Estimated remaining coal reserves at the end of 2000, (Jeffrey, 2005).

Coalfield	Reserves (Mt)		
	Recoverable	ROM Production (1982-2000)	Remaining (2000)
Witbank	12460.00	2320.23	10139.77
Highveld	10979.00	972.49	10006.51
Waterberg (Ellisras)	15487.00	384.00	15103.00
Vereeniging-Sasolburg	2233.00	334.91	1898.09
Ermelo	4698.00	101.11	4596.89
Klip River	655.00	85.26	569.74
Vryheid	204.00	81.80	122.20
Utrecht	649.00	64.47	584.53
South Rand	730.00	22.03	707.97
Somkhele & Nongoma	98.00	15.18	82.82
Soutpansberg	267.00	6.11	260.89
Kangwane	147.00	0.96	146.04
Free State	4919.00	0.22	4918.78
Springbok Flats	1700.00	0.00	1700.00
Limpopo	107.00	0.00	107.00
Total	**55333.00**	**4388.77**	**50944.23**

The Belfast opencast operation is expected to be operational for 29 years and coal from mainly the number 2 seam will be mined and to a small extent the number 3 and 4 seams where these two seams are present. The number 2 seam is known to have the best quality coal. It can consist of coal zones of different quality (Jeffrey, 2005). Mining in the study area will be performed by the conventional truck-and-shovel mining method.

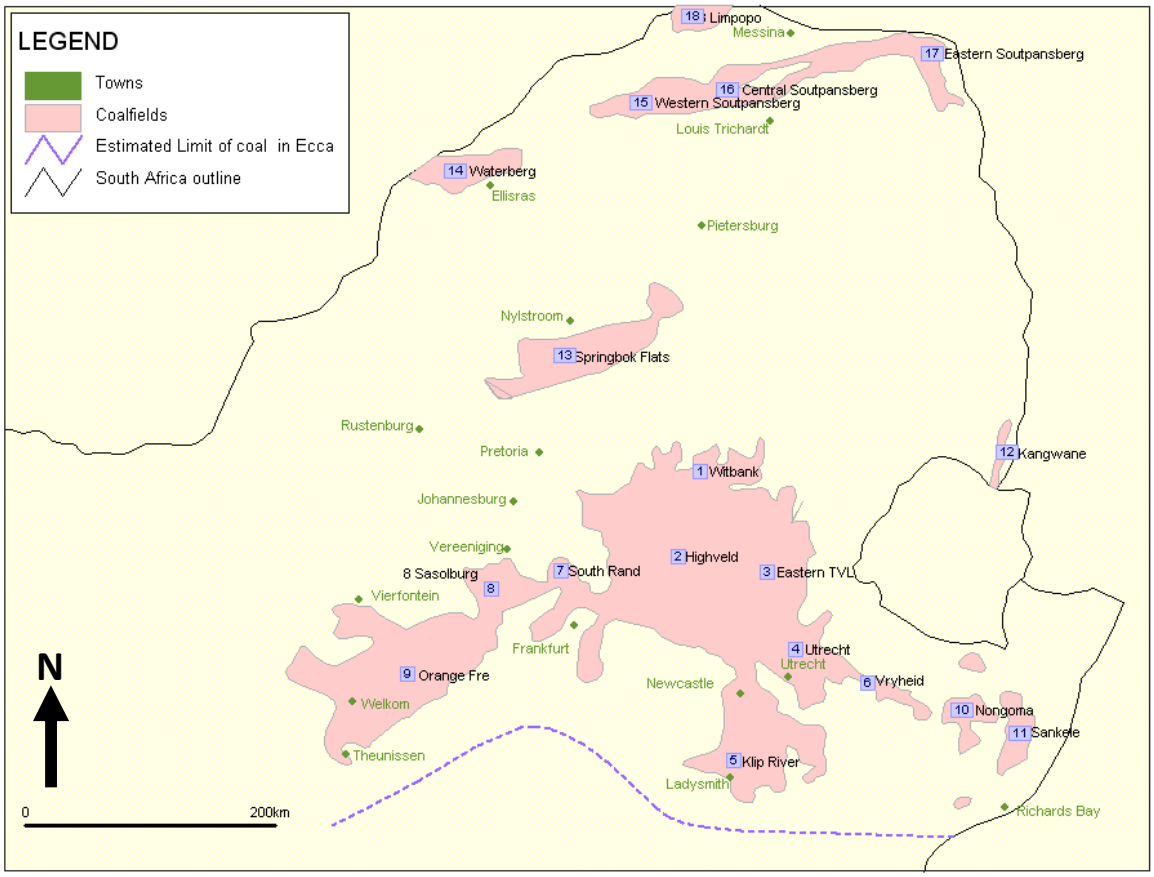

Figure 4: Coalfields of South Africa (Aquila Resources, 2010)

During the operational phase of a mining operation, water is pumped from the mine to ensure safe and dry mining conditions. The dewatering of the mining void causes the water levels within a certain radius of the mine to decrease. Since the majority of the coal mining operations are situated on agricultural land, dewatering often causes a drop in the water levels in the boreholes of surrounding farmers. It is therefore critical to evaluate and determine the impacts of the mining operation before mining commences. To determine to what extent the groundwater level will be affected around the opencast pits in the study area, a numerical groundwater model will be constructed for the site.

The rate at which groundwater flows into the mine voids are important to estimate before mining commences since this will determine at what rate groundwater needs to be pumped from the mining pits to ensure dry and safe working conditions. The inflow rate of the groundwater will be determined in this thesis by

using both analytical and numerical groundwater modelling methods and comparing the results.

Numerical and analytical models are both mathematical models and use mathematical equations or algorithms, often similar, to obtain results. Analytical methods are generally used in simple situations whereas numerical methods are used for more complex situations. It is expected that the numerically obtained values will incorporate more accurate results than the analytical solutions. When using analytical methods, assumptions are often made and usually give a broad overview of what can be expected (Dennis, 2008).

Analytical methods for determining groundwater inflow to an opencast pit are especially functional during the planning stages of a mine. It is however more feasible to use numerical methods once mining is approved. (Marinelli & Nicolli, 2000).

This study was conducted to investigate whether analytical methods are in fact a good way of quickly estimating groundwater associated inflows and impacts in an opencast coal mining environment and to determine if it is really necessary to construct a numerical model to obtain the groundwater inflow rates.

1.1 Scope of Study

To ensure safe and dry mining conditions, dewatering of the open pit is conducted if the pit floor is lower than the water table. The dewatering of the pit causes a drop in the water level not only in the pit but also in the close surrounding areas. The area surrounding the pit area to which the groundwater level is affected as a result of dewatering is known as the cone of depression. This total area is also referred to as the area of influence (DWA, 2008). The extent of the cone of depression will be simulated by using the numerical groundwater model that will be constructed for the study area.

To successfully plan for pit dewatering the volume of groundwater inflow needs to be determined before mining starts. The inflow to the mine can be determined by using numerical and analytical methods.

For the study area a numerical groundwater flow model will be constructed and the groundwater inflow will be determined by making use of the so-called water budget function in the software. The analytical approaches to determining the inflow will include three different methods as were investigated in reports done by Aryafar *et al.* (2007) and Marinelli & Nicolli (2000). Furthermore, a self-constructed analytical model will be used. In this method the recharge to the mining strips and the Darcy inflow to the pits will be added together to obtain an answer. A sensitivity analysis will also be performed on the recharge with the numerical and analytical methods.

The aims of the study are therefore to construct a numerical groundwater flow model and using the model to determine the extent to which the mining operation will have an impact on the surrounding water levels. The numerical model will then be used to determine the groundwater inflow rate to the pit. The inflow to the pits will also be determined by making use of analytical methods and the results will be compared with the results obtained from the numerical model.

The results from these two approaches will be compared to investigate whether the analytical approach is in fact a good way of obtaining values that relates with the numerically obtained results. If there is a good correlation between the

analytical and numerical results, the analytical approach can be regarded as a safe and representative way to obtain groundwater related values. Especially during the early stages of mine planning it would be supportive to quickly determine mine related issues as this will assist in decision making and related cost estimates.

Analytical approaches that were best applicable to the study site were selected so that the results could be compared to the numerical results.

As no actual inflow values to the pits are available and no case studies exist for the area, the results of the inflow rates determined in this thesis cannot be compared to actual measured values. It is therefore recommended for further study that actual inflow rates be obtained from the mine to compare with the results in this study. This comparison will then convey the best approach to determining inflow to an opencast mine.

1.2 Methodology

The following procedure will be followed in the study:

- Evaluate the pre-mining groundwater conditions (Baseline conditions).
- Conduct a literature review of studies with contents that are applicable to the study area.
- Collect all information needed to construct a comprehensive and representative conceptual model.
- Use the evaluated baseline information and conceptual model to aid in the analytical groundwater methods.
- Formulate the self-constructed analytical model by adding Darcy inflows and recharge to the opencast strips.
- Construct and calibrate a numerical groundwater model by making use of the same baseline information.
- Determine the groundwater inflow for each year of mining by making use of the water budget package in the modelling software.
- Perform a sensitivity analysis for recharge to determine the changes in groundwater inflow to the mine.
- Determine and present the maximum cone of depression.
- Compare the results from the numerical and analytical solutions.
- Discuss the results and come to a conclusion on the results obtained in the study.
- Make recommendations based on the results and conclusions of the study.

1.3 Data acquisition

Data needed for the purpose of the study was obtained from several different sources. Data obtained from the mine itself included:

- Field measurements of water levels and quality in and around the mine lease area,
- the mining blocks with the life of mine (LOM) plans / progress plots,
- coal floor contours,
- and very importantly, maps of geological structures which included positions of dykes, faults and sills. Geological structures are very important as they influence the groundwater flow in the aquifer.

The mine plans were used to determine an area surrounding the mining areas in which a hydrocensus was performed. During the hydrocensus the following information was collected:

- borehole localities
- groundwater users and uses
- groundwater levels in the boreholes
- sampling of groundwater for quality analysis

Eight new boreholes were drilled in the study area for the main purpose of groundwater monitoring around the mining areas. Blow yields, borehole construction and geological logs were noted and water levels measured and groundwater samples taken in these boreholes. Short duration pumping tests were performed on seven of the newly drilled monitoring boreholes and on four exploration boreholes. Pumping tests were performed to aid in estimating aquifer characteristics including transmissivity and storativity.

All the information that were collected were processed and analysed for the baseline evaluation by the software program WISH (Windows Interpretation

System for the Hydrogeologist) which was developed by Eelco Lukas from the Institute for Groundwater Studies at the University of the Free State.

1.4 Structure of thesis

The thesis consists of 13 chapters which include the references and appendix. Chapter 1 gives a short introduction to the coal mining industry in South Africa and a brief overview of the study area. In this chapter the scope of the study is discussed as well as the methodology that will be followed to come to the results and conclusions. Data that are needed to complete the thesis is obtained from several different sources which are discussed in section 1.3.

Studies conducted by other scientists on the groundwater flow rates to an opencast mine are discussed in Chapter 2- Literature review.

In Chapter 3 the background characteristics of the study area are discussed. This chapter includes a discussion on the locality of the study area, the topography, climate, geology and geohydrology. The aquifer types, groundwater levels and groundwater chemistry are discussed under the subheading of 'Geohydrology'.

Chapter 4 takes a closer look at the field investigations that were performed in the study area. These investigations include geophysical surveys by magnetic and electromagnetic methods to delineate any anomalies, drilling of monitoring boreholes by a percussion drilling rig and aquifer test analysis. The aquifer test analysis includes blow yields and short duration pumping tests.

In Chapter 5 a conceptual model is constructed. The model is constructed by incorporating the background information and the information obtained from the field investigations. The conceptual model is constructed to aid in development of the numerical model.

In Chapter 6 analytical calculations are used to determine the groundwater inflow and recharge to each mining block for each mining year. Three different analytical approaches are used to calculate the groundwater inflow to the pits: the Vandersluis *et al*. (1995) approach, the Krusseman & De Ridder (1985) approach

and the Marinelli & Nicolli (2000) approach. The estimated cumulative recharge to the two mining blocks is also determined analytically in this chapter.

The self-formulated analytical model for determining groundwater inflow to the opencast pits is discussed in Chapter 7. This approach uses the Darcy inflow rates and recharge to the mining strips to determine the total estimated inflow to the pits.

Chapter 8 is used to discuss the construction and results of the numerical groundwater model. In this chapter the modelling software that was selected is discussed together with the model construction and the model calibration. The use of river nodes and general head boundaries are presented together with the recharge distribution. The parameters that eventually give the best calibration and correlation between the calculated and measured water levels are also presented in this chapter. A figure of the cone of depression as simulated numerically as well as graphs of the groundwater inflow rate at different recharge rates is presented in this chapter.

In Chapter 9 the numerical and analytical results are compared. Line graphs of the groundwater inflows during each mining period and the recharge volumes and correlation graphs are presented in this chapter. The total water make according to the different modelling approaches are tabled in Chapter 8.

In Chapter 10 the results of the numerical and analytical calculations are discussed. In Chapter 11 conclusions are drawn from the results of the study and recommendations are made in Chapter 12. The list of references used during the study is listed in Chapter 13 while Chapter 14 consists of the appendices.

2. Literature review

Analytical modelling for determining groundwater inflow to an opencast mine has been performed in several studies in the past. Names that come up most often include Singh and Reed in 1988 who investigated mathematical methods to estimate groundwater inflow to an opencast mine and Marinelli & Nicolli (2000) who more recently investigated simple analytical methods to determine the groundwater inflow. Aryafar *et al.* (2007) also predicted the groundwater inflow to an opencast pit using both numerical and analytical solutions.

Aryafar *et al.* (2007) used two analytical equations to determine the inflow to an open pit. The first was an equation proposed by Vandersluis *et al.* (1995). This equation can typically be applied to mine workings in arid or semi-arid regions where water inflow to a pit from an unconfined aquifer is horizontal.

$$Q = \frac{1.366 \times K \times (2H - \triangle h) \triangle h}{\log (R + r_o) - \log r_o} \qquad (1)$$

The second equation presented in the study by Aryafar *et al.* (2007) was first proposed by Krusseman & De Ridder (1979) and also presented in Singh *et al.* (1985). This equation can be used to determine inflow from an unconfined aquifer at steady state into an open pit. The equation has been derived from the Thiem-Dupuit equation.

$$Q = \frac{\pi K (H^2 - h^2)}{\ln (R/r_p)} \qquad (2)$$

Where:

Q = groundwater inflow (m^3/day)

K = the hydraulic conductivity of the unconfined aquifer (m/d)

H = original height of the water table above the mine level

h = head at point in time

ℓn = natural logarithm

R = effective radius of influence of dewatering well

r_o = reduced radius of open pit by level (m)

r_p = radius of pit at the desired level (m)

$\triangle h$ = drawdown at desired level (m)

The following case study was presented by Aryafar *et al.* (2007):

- An opencast pit, partially penetrating an unconfined aquifer with;

- R = 1750 m
- r_o = 50 m
- K = 4.3 x 10^{-6} (m/s)
- H = 800 m
- h = 250 m
- △h = 250 m
- r_p = 50 m
- T = 2365 x 10^{-6} (m^2/s)

The groundwater inflow as determined by the analytical solutions and the numerical model (SEEP/W) were compared:

- Numerical model = 2.17 m^3/s
- Equation 1 = 2.18 m^3/s
- Equation 2 = 2.19 m^3/s

In the investigation conducted by Singh and Reed (1988) it was suggested that the equivalent radius of the opencast pit in the case where the pit is not round be determined by using the following equation:

$$r = (2/\pi)(Y.W)^{1/2} ;$$

where: Y = length of mine (m)

W = width of mine (m)

The effective radius of influence can be determined in two ways. According to Singh and Reed (1988) the radius of influence is estimated to be three times the drawdown at the pit wall / saturated thickness at the pit wall. This however is a broad generalisation. Radius of influence is dependent on the transmissivity, time and specific yield / storativity of an aquifer. The extent of the cone will also increase with time. Therefore, for the purpose of this study the radius of influence from the pit walls will only be determined by making use of the following equation (Cooper-Jacob):

$$r_e = 1.5 \sqrt{T * t/S}$$

where T = transmissivity,

t = time,

S = specific yield

For the total radius of influence (R) the effective pit radius will be added to the effective radius of influence from the pit wall (r_e).

In 2000, Marinelli & Nicolli investigated simple analytical equations for estimating groundwater inflow to an opencast mine pit. For the investigation some assumptions were made:

- As the water level decreases the saturated thickness surrounding the pit also decreases.
- Groundwater inflow from the pit walls as well as from the pit bottom exists.
- The rock matrix below the pit is semi-infinite and no impermeable boundary exists
- Steady-state flow conditions exist near the mine.

For the Marinelli & Nicolli (2000) study the conceptual model was divided into two zones: zone 1 represents the flow from the pit walls and zone 2 is the flow from below the pit. The assumption is made that no flow occurs between the two zones.

For zone 1 steady state, unconfined, horizontal radial flow with uniformly distributed recharge to the water table is assumed. The radius of influence of the opencast operation will be determined in the same way as was used for the previous two methods.

Assumptions made for the zone 1 solution include:

- Pit wall are a right circular cylinder
- Groundwater flow is horizontal
- Pre-mining water table is horizontal
- Uniform recharge occurs over the entire area
- Groundwater flow to the pits is axially symmetric

Then the pit inflow can be determined by:

$$Q_1 = W\pi (R^2 - r_o^2)$$, where Q_1 is the inflow from the pit walls.

and: W = recharge flux
r_o = effective pit radius
R = radius of influence (maximum extent of the cone of depression)

According to Marinelli & Nicolli (2000) the inflow to the pits are maximised when the seepage face depth at the pit walls are set to 0. This will be the case where mine dewatering is active since mining will be in a dry state. This will also act as a safety net for determining the maximum possible inflow to the mine.

Some of the shortcomings for this approach are that only horizontal flow is considered and it assumes that no vertical flow component exist in the area near the pit wall.

This approach also assumes a horizontal water table for the pre-mining status. A horizontal water table is highly unlikely since groundwater will be stagnant in this scenario. Groundwater flow always exists along a hydraulic gradient, may it be very small or large.

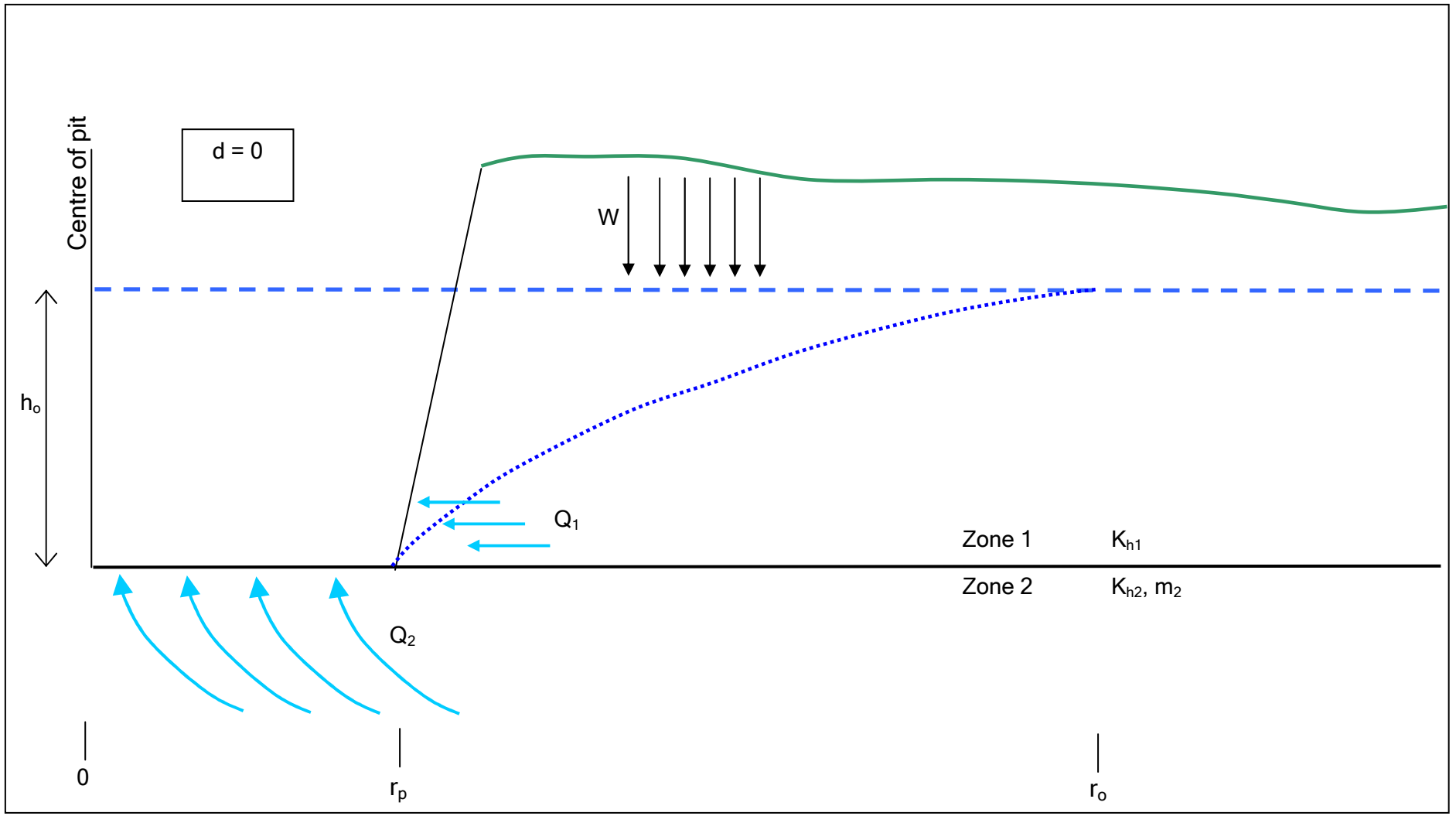

Figure 5: Graphic representation of the analytical approach used by Marinelli & Nicolli (2000).

For the groundwater inflow calculations in zone 2, the pre-mining water table is used as the initial head (h_o). The elevation of the pit bottom is used as the sink head and the flow to the pit are three dimensional and axially symmetric.

The steady state inflow rate from the underlying rock matrix (from zone 2) is determined by using the following equation:

$$Q_2 = 4r_p (K_{h2}/m_2)(h_o\text{-}d)$$

And

$$m_2 = \sqrt{(K_{h2}/K_{v2})2}$$

where: K_{h2} = horizontal hydraulic conductivity
K_{v2} = vertical hydraulic conductivity
m_2 = anisotropy parameter
d = depth of pit lake
h_o – d = drawdown at pit wall

It should be noted that the solutions for groundwater inflow to an opencast pit are based on many assumptions and they assume porous medium over the entire area (zone 1 and 2). One of the constraints in the solutions that is used in the study area is the fact that flow in Karoo rock types predominantly occur in fractures and is therefore known as secondary porosity rock matrix.

Marinelli & Nicolli (2000) represented a case study of a pit lake at a defunct gold mine in northern Nevada, USA. Figure 6 is a graphical representation of the pit. It should be noted that this case study represents an open pit that has been partially filled with water. With active mining no pit lake usually exists and the water level will be drawn down to the pit floor leading to h_p being equal to 0.

The following is applicable to the case study site:

- r_o = 33.5 m
- h_o = 9.1 m
- h_p = 6.4 m
- d = 6.4 m

- $W = 2.4 \times 10^{-9}$ m/s
- $m_2 = 1$
- $K_{h1} = K_{h2} = 5.3 \times 10^{-7}$ m/s
- R = 265 m

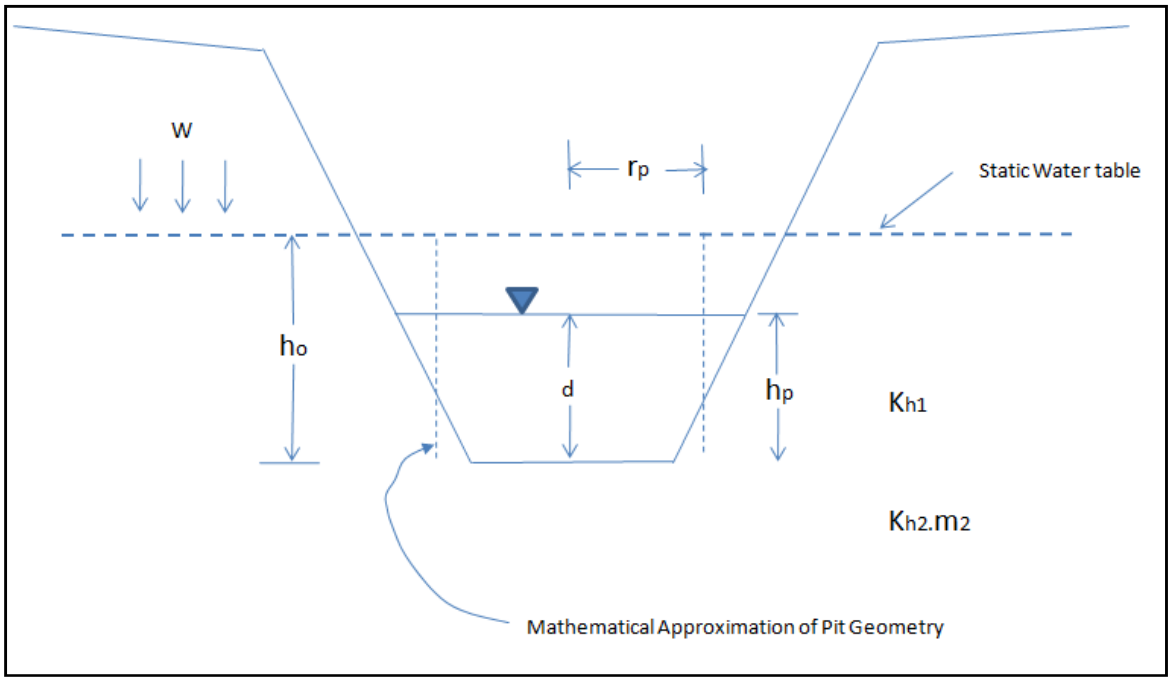

Figure 6: Schematic presentation of the open pit in northern Nevada, USA (Marinelli & Nicolli, 2000)

It was found that the average groundwater inflow to the pit is approximately 2.4 x 10^{-4} m^3/s (21 m^3/day).

Marinelli and Nicolli (2000) concluded that the equations provided in the related study supply the user with a handy tool to estimate groundwater inflows to an opencast mining pit. These equations can be used for pits with or without pit lakes. It is also stipulated that many assumptions are made during the analytical approach. Assumptions should be made relevant to each specific study site. Marinelli and Nicolli (2000) have found in previous studies that the approach used in this specific paper is consistent with water balances and numerical models. It is also stipulated that analytical equations are a handy tool in the early stages of mine planning.

The study conducted by Singh and Reed (1988) proposed three ways of determining groundwater inflow to an opencast pit. These include the equivalent well approach, two-dimensional flow equations and numerical techniques. The

analytical equations provided in their study can be applied for both linear and non-linear flow conditions. These scientists also indicate that analytical methods are handy tools when it comes to the initial planning of the mine. These initial estimations will provide information to successfully plan the design of a pumping system and storage facilities and for the control of water pollution. Singh and Reed (1988) provided three sources of groundwater inflow;

- Mineral beds and underground aquifer
- Geological and structural features
- Abandoned deep mine workings.

At the Belfast study site only the first two are applicable.

For the purpose of this thesis a self-constructed analytical model was also used for determining groundwater inflow to the pits. This analytical model was formulated by adding together the estimated recharge to the opencast strips and the Darcy inflow to the same strips.

Heath R.C. (1983) compiled a handbook describing basic geohydrology. Aquifers function as porous conduits through which water is transported from recharge areas to discharge areas. Henry Darcy (1856) constructed a well known formula considering the factors that control groundwater flow. This formula is known as Darcy's Law and may be considered the first principle of the groundwater science.

$$Q = KAi \ (i = dh/L)$$

Where: Q = quantity of water per unit of time

K = hydraulic conductivity. K is dependent on the size of pores and fractures and on the dynamic characters of the water including density, viscosity and strength of the gravitational field.

i = hydraulic gradient

A = area

The quantity of water that flows through a medium is directly proportional to the hydraulic gradient.

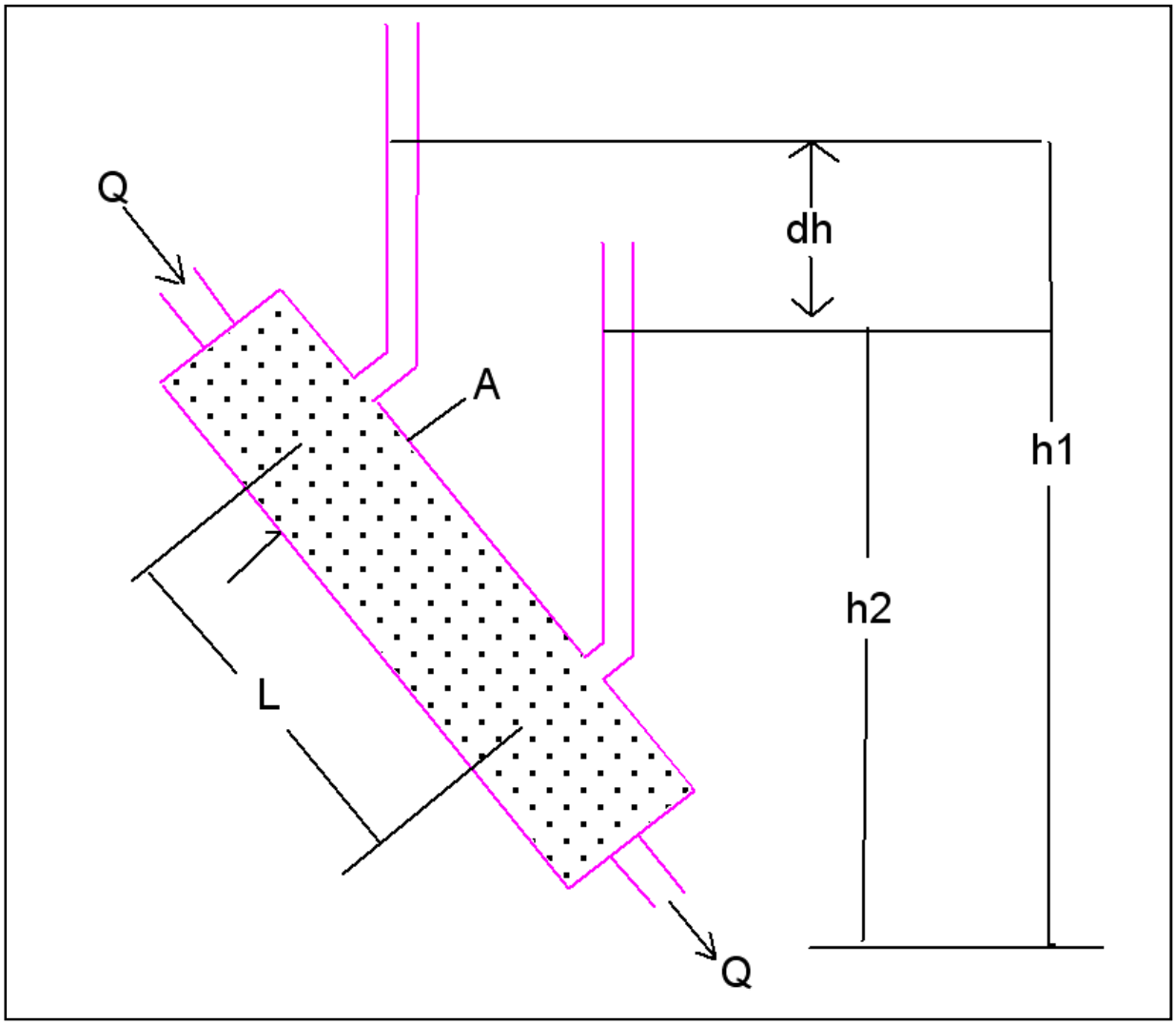

Figure 7: Representation of Darcy Flow through a porous medium (British Columbia Government, 2011).

3. Background information

3.1 Locality of the study area

The study site investigated in the thesis is located in Mpumalanga, South-Africa and is situated south-west of the town Belfast. The study site is located in an area which is known as the Mpumalanga Highveld. The Highveld region of Mpumalanga is extensively covered by coal mining operations. The Mpumalanga region is rich in coal reserves and three of the power stations in the province are the biggest coal-fired power stations in the southern hemisphere. Mining in the Highveld region have been ongoing for several decades. The Belfast region itself has not been disrupted by coal mining operations to such a large extent as the Witbank region for example. In the study site area the closest active mining operation is located directly south of the study area. (South Africa Info, 2010).

The study site consists of two mineable reserves which will be referred to in this document as the West and East blocks. The blocks with their positions are presented in Figure 8 of this document. The West block covers a surface area of approximately 890 hectares (ha) and the East block an area of 1600 ha.

The study site is situated on the boundary between pure and false grassveld type. Some of the country's best agricultural land is situated in Mpumalanga. Mpumalanga is mostly covered by agricultural activities such as sheep farming and also to a large extent crops which is dominated by maize. In the study area this is also the case. (Agis, 2009)

Soils in the study area are mostly reddish- to yellowish-brown. These soils mostly have a low to medium base status. The base status is "a qualitative expression of base saturation" which in turn is "the sum of exchangeable calcium, magnesium, sodium and potassium expressed as a percentage of cation exchange capacity measured at a specified pH value", (Soil Classification Working Group, 1991).

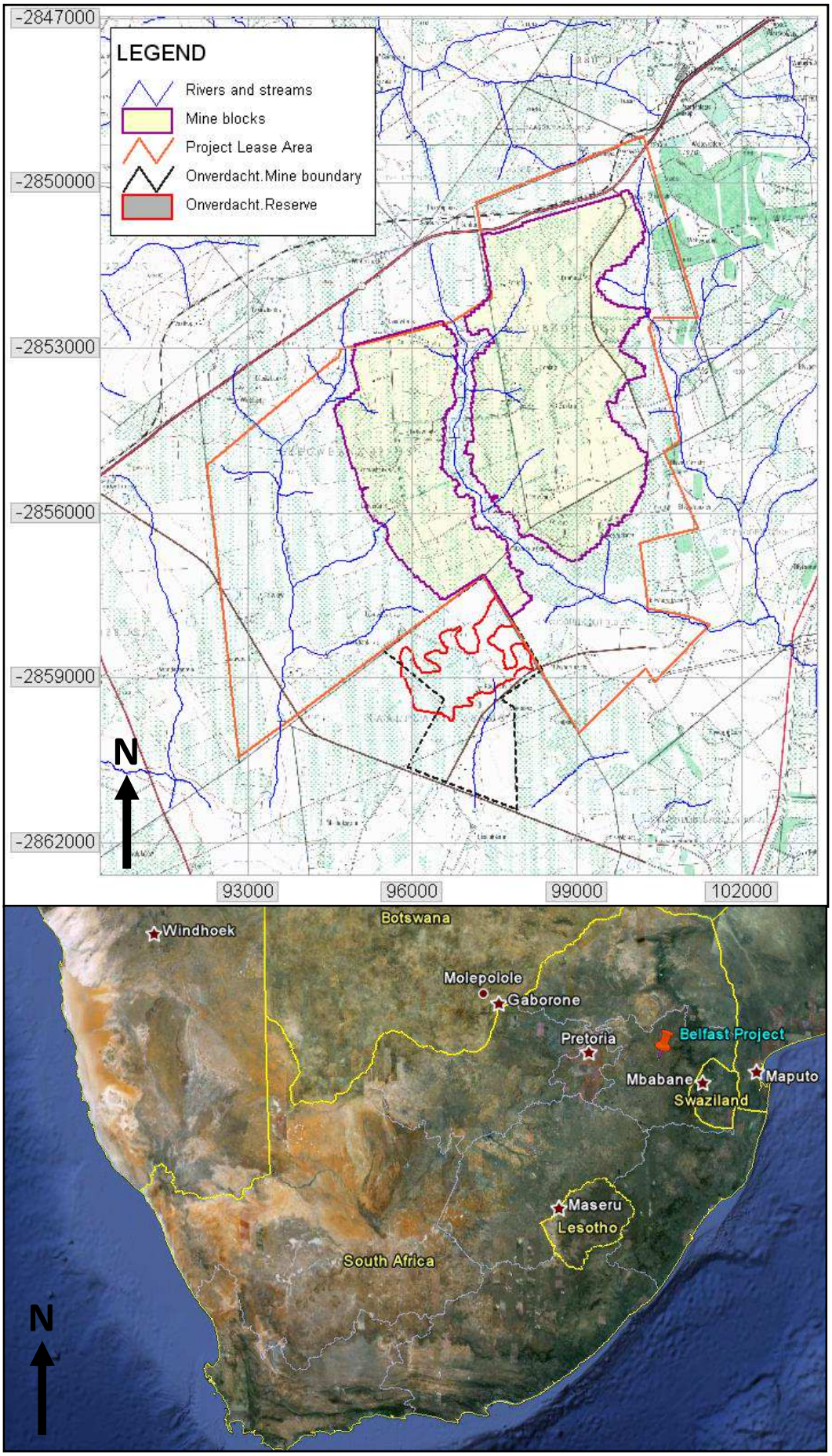

Figure 8: Locality of the study area (Google Earth, 2009).

3.2 Topography

The study area is situated in a mostly slightly sloping area and hills or ridges are also likely to occur. The two mine blocks are located on gently sloping hillocks, which in some cases have steeper gradients. A surface topography map of the study area has been constructed with the aid of the software program Surfer. The topographical contours were digitised from topographical maps after which the data was used for contouring.

The highest topography is approximately 1960 meters above mean sea level (mamsl) and is located towards the north-east of the proposed mining blocks. The lowest topography is approximately 1620 mamsl and is located towards the south-west of the mine blocks. The topography generally dips towards the south and the surface drainage direction will therefore also be from the north to the south in the study area. A difference in elevation over the area is approximately 340 meters.

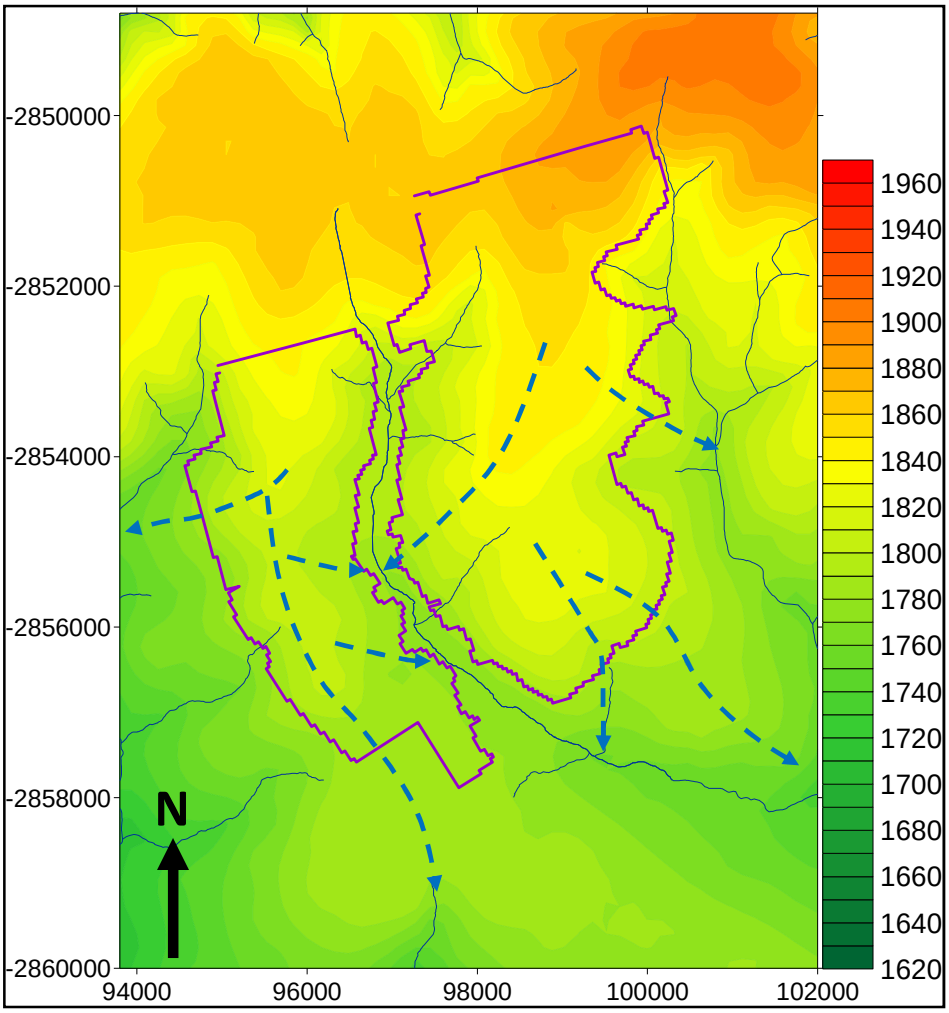

Figure 9: Surface contours in the study area with surface drainage lines and patterns.

3.3 Climate

The study site is located in a summer rainfall region. Average rainfall values for the town of Belfast can vary between 650 and 700 mm/annum. The most intense rainfall events occur during thunderstorms where a large volume of rain falls within a short period of time. The maximum average rainfall usually occurs in the summer month of January while the lowest is in the winter months of June and July. In the winter months an average maximum daily temperature of approximately 14.7°C can be expected while the average maximum temperatures in the summer months are approximately 22.5°C. Average minimum daily temperatures in the winter months are approximately 1.3°C. (SA Explorer, 2010).

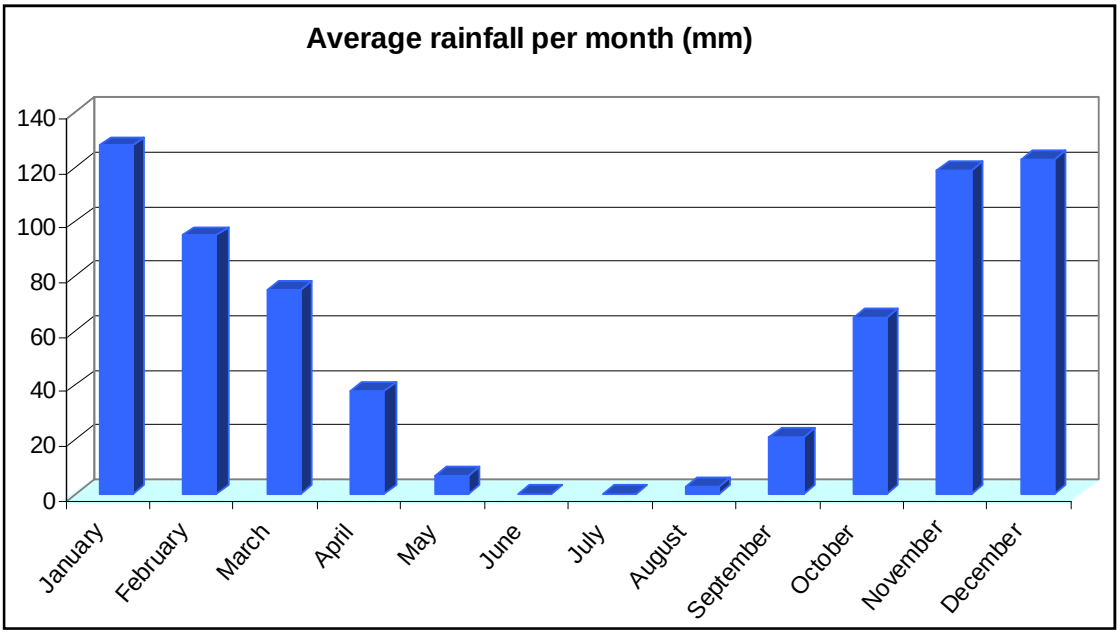

Figure 10: Average rainfall for the Belfast region, (SA Explorer, 2010) .

3.4 Geology

The study site is underlain by rocks of the Karoo Supergroup. This group mainly consists of sedimentary succession of sandstones, shales and coal. The sedimentary succession is underlain by the Dwyka formation consisting of diamictites and tillites. (Exxaro Coal, 2009).

Some dolerite dykes and faults have been mapped in the proposed mining area and will be included in the numerical model. Dolerite dykes usually have a lower transmissivity than the surrounding rock matrix, therefore acting as a horizontal

groundwater flow barrier. Faults on the other hand are more permeable and water in a fault will move at a higher rate than in the surrounding rock matrix. The dykes that were interpreted with the aid of aeromagnetic surveys mostly trend north-east to south-west. The faults strike in random directions. Some dolerite sills were also mapped in the geophysical investigation. Sills will also act as barriers but since these are horizontal structures they will act as barriers for vertical groundwater flow.

The number 2 and 3 seams will mainly be mined in the proposed area (bituminous coal). In areas where the number 4 seam is present it will also be mined. In some areas the number 4 seam has been eroded away especially in valley bottoms. The coal seams were preserved in the Vryheid formation (AGIS, 2009).

The coal floor contours for the number 2 seam was constructed with the Surfer software package. The elevation of the seam floor in the West Block varies between 1765 mamsl and 1825 mamsl. The coal floor elevation in the East Block varies between 1760 and 1870 mamsl. The seam floor dips towards the south at approximately 0.5 to 1%.

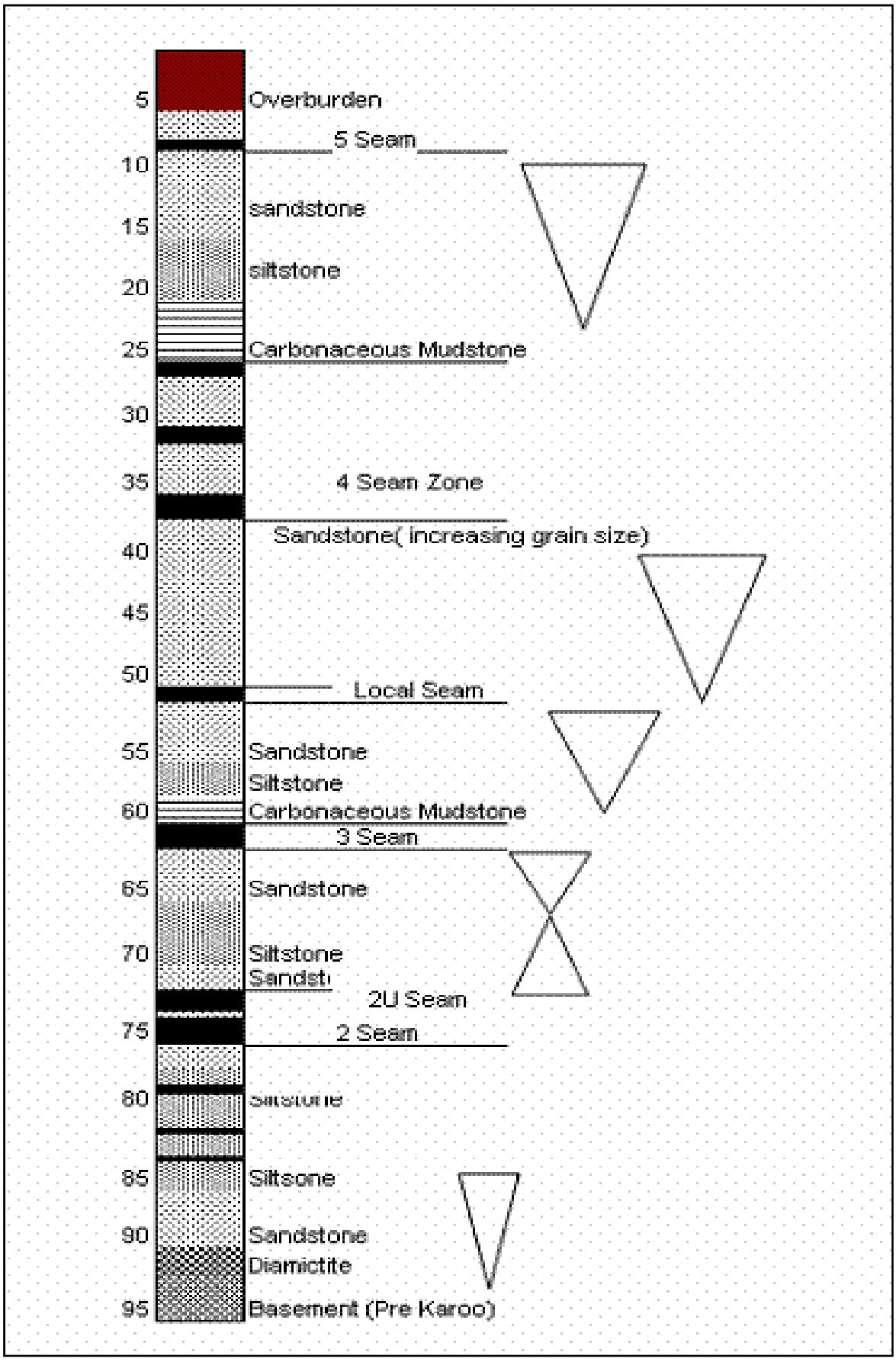

Figure 11: Stratigraphic Column of study area (Exxaro Coal, 2009)

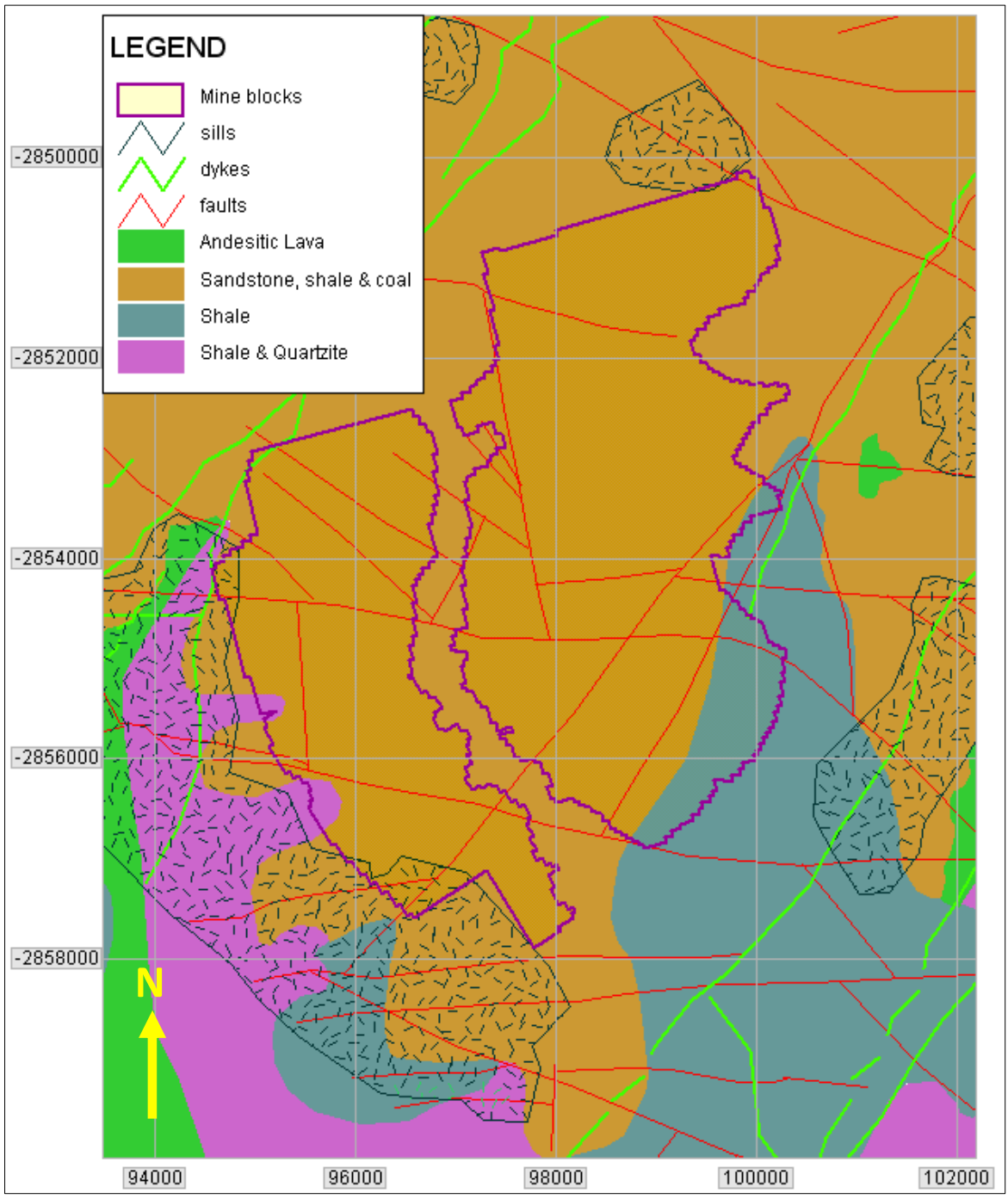

Figure 12: Simplified geology of the study area (AGIS, 2009).

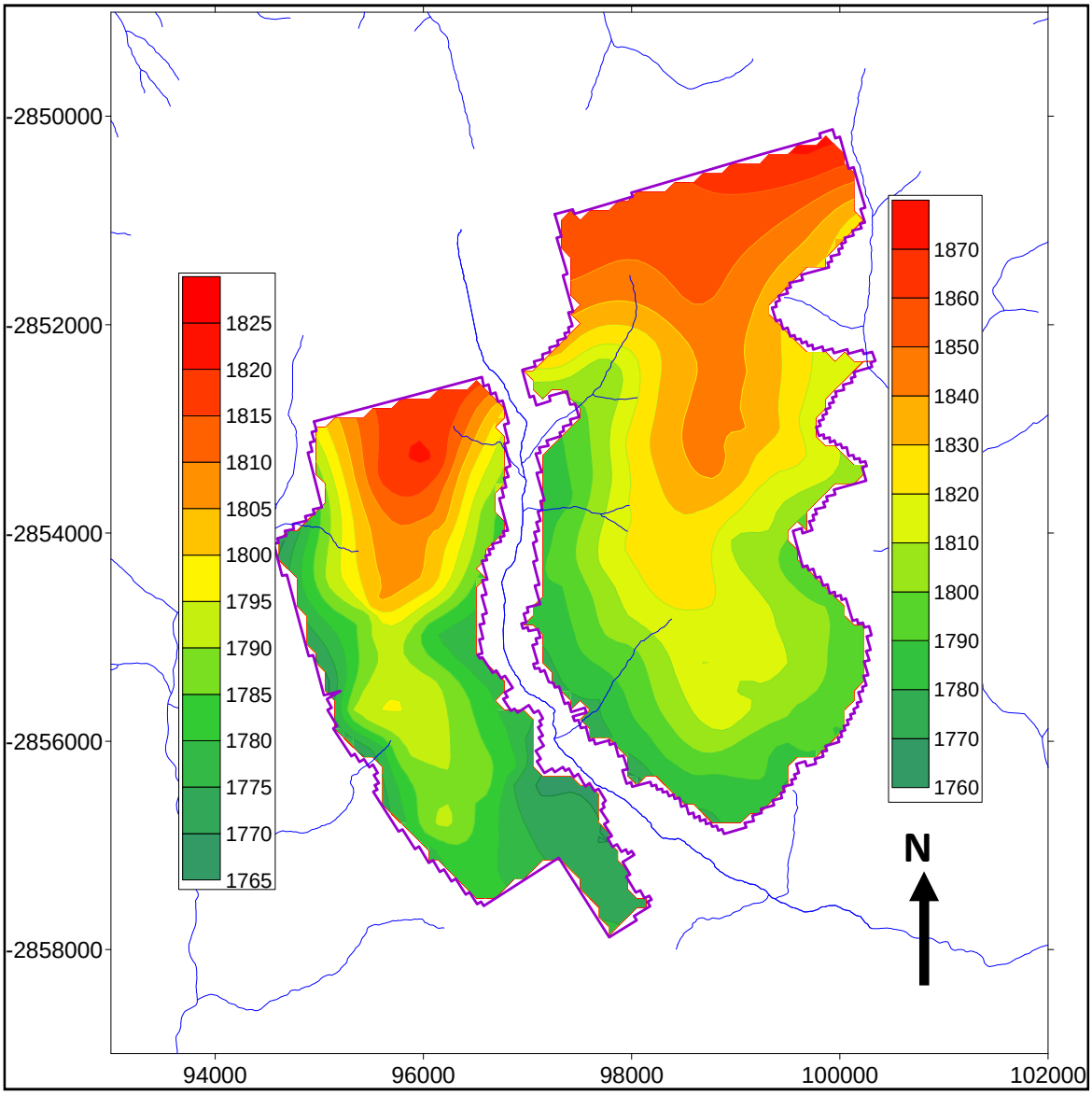

Figure 13: Coal floor contours for the number 2 Seam.

3.5 Geohydrology

3.5.1 Aquifer types

The area under investigation falls within the Mpumalanga Coalfields which consists mainly of two aquifer systems. An aquifer is defined as a geological formation that can yield groundwater in economically viable quantities, (DWA, 2008).

The first is the shallow, weathered aquifer and generally occur at depths of 5 to 12 mbs, (Grobbelaar *et al.*, 2004). From drilling results in the study area it can be concluded that the weathered aquifer occur at depth between 5 and 13 mbs (Please refer to borehole logs in Appendix A). The shallow weathered aquifer will

generally become more prominent during times of high rainfall and is therefore recharged by rainfall. Average recharge to the shallow aquifer can vary between 1 and 3 % but higher recharge values can be present in isolated cases. Recharge can typically vary where the composition of the weathered material varies. Weathered aquifers consisting of fine, compacted material will typically have lower recharge rates than coarse, loose material. Yields in this aquifer are generally low and are normally less than 0.5 l/s. The low yields together with the fact that this aquifer is only recharged directly by rainfall, leads to this aquifer to be unsuitable for sustainable groundwater abstraction and can therefore be classified as a minor aquifer (Environmental-Agency, 2010), (Grobbelaar *et al.*, 2004).

The second aquifer is the deeper, fractured rock aquifer. This aquifer is developed in the fresh, fractured rock material of the Ecca Group, (Grobbelaar *et al.*, 2004). The secondary, fractured aquifer is the most prominent in South-Africa. Since the rock material itself generally has very low transmissivities, groundwater flow in the fractures which form in the solid bedrock. The yields in these aquifers are generally higher, but are still too low to yield economically viable quantities. From pump testing of newly drilled monitoring boreholes as well as information gathered during the hydrocensus yields of this aquifer in the study area can vary between 0 and 2 l/s. Higher yields can also occur and although not very high, this aquifer can be classified as a major aquifer, (Environmental-Agency, 2010). Groundwater in the area is generally pumped from this aquifer. The fractured rock aquifer is usually confined by a less permeable layer making it a confined aquifer.

A third aquifer can occur below the Ecca sediments but will not be discussed in this document since the opencast pits are not deep enough to cut through this aquifer and will therefore not have any significant impacts on this aquifer, (Grobbelaar *et al.*, 2004).

Eight new monitoring boreholes were drilled in the study area for site specific monitoring purposes. All of these boreholes were drilled to depths of 31 meters. Since the boreholes are solely for the purpose of monitoring, all were drilled to the same depth. At this depth both the weathered and fractured aquifers are intersected and some characteristics of the aquifers can be identified. The drilling intersected soil and sandstone in all the boreholes. Coal, shale and interlaminated shale and sandstone were also intersected in a few of the boreholes. The

geological logs of the monitoring boreholes are presented in **Appendix A** of this document.

3.5.2 Groundwater levels

Groundwater levels were measured during the hydrocensus and in the newly drilled monitoring boreholes. The water levels that are not affected by impacts such as pumping vary between 0.5 and 16 mbs. The water level elevations roughly follow the topographical trend (Figure 14). The deepest water levels are mostly found in the higher topographic regions and the shallowest at lower elevations. At low lying areas such as valley bottoms and close to streams and rivers the groundwater can even flow out on surface which is known as springs or fountains. In these low lying areas discharge from the groundwater aquifer rather than recharge to the aquifer can occur. The water level elevations were used in the calibration of the steady state model (Figure 41).

Groundwater naturally flows from higher elevations to lower elevations perpendicular to the groundwater contours. The groundwater generally follows the surface topography and levels are usually deeper in the higher topographical regions and shallow at or near valley bottoms. At low areas in the surface topography the groundwater can even discharge on surface, which is known as springs. The two mining blocks are situated on ridges; therefore groundwater flow is towards the south, south-west and south-east for both blocks. The predominant flow direction at the West block is towards the south-west and at the East Block towards the south. A groundwater divide area is present to the north of the mine blocks.

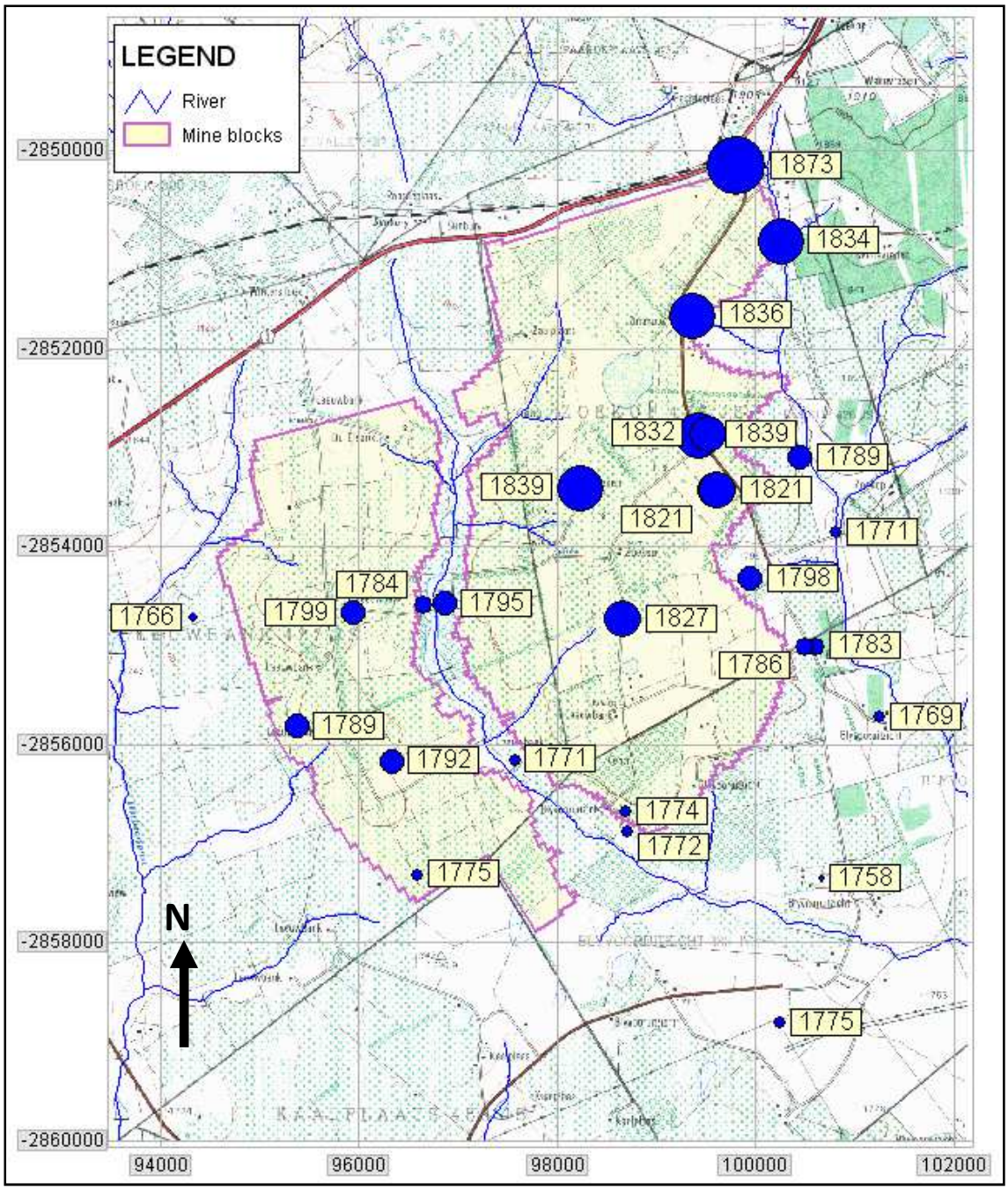

Figure 14: Thematic map representing the groundwater levels of the boreholes used in the numerical model calibration

The highest groundwater elevation in the modelling area is approximately 1900 mamsl and the lowest 1690 mamsl. The groundwater gradient was determined by using the following equation:

$$i = \frac{h_1 - h_2}{L},$$

where i = groundwater flow gradient

h_1 = highest groundwater elevation

h_2 = lowest groundwater elevation

L = distance between the highest and lowest elevations.

The estimated groundwater flow gradient in the project area is approximately 1 to 1.2 %.

Faults, dykes and sills will have an effect on the groundwater flow regime. A dyke and sill generally have a low permeability and can act as a groundwater flow barrier. Dykes are vertical structures and will therefore affect the lateral flow of groundwater while sills are horizontal structures which can have an effect on the vertical flow of groundwater. Faults on the other hand have higher permeability and flow occur much faster along these structures. Faults are unfavourable at or near an area where groundwater contamination can occur and dykes on the other hand can be beneficial since they can act as flow boundaries.

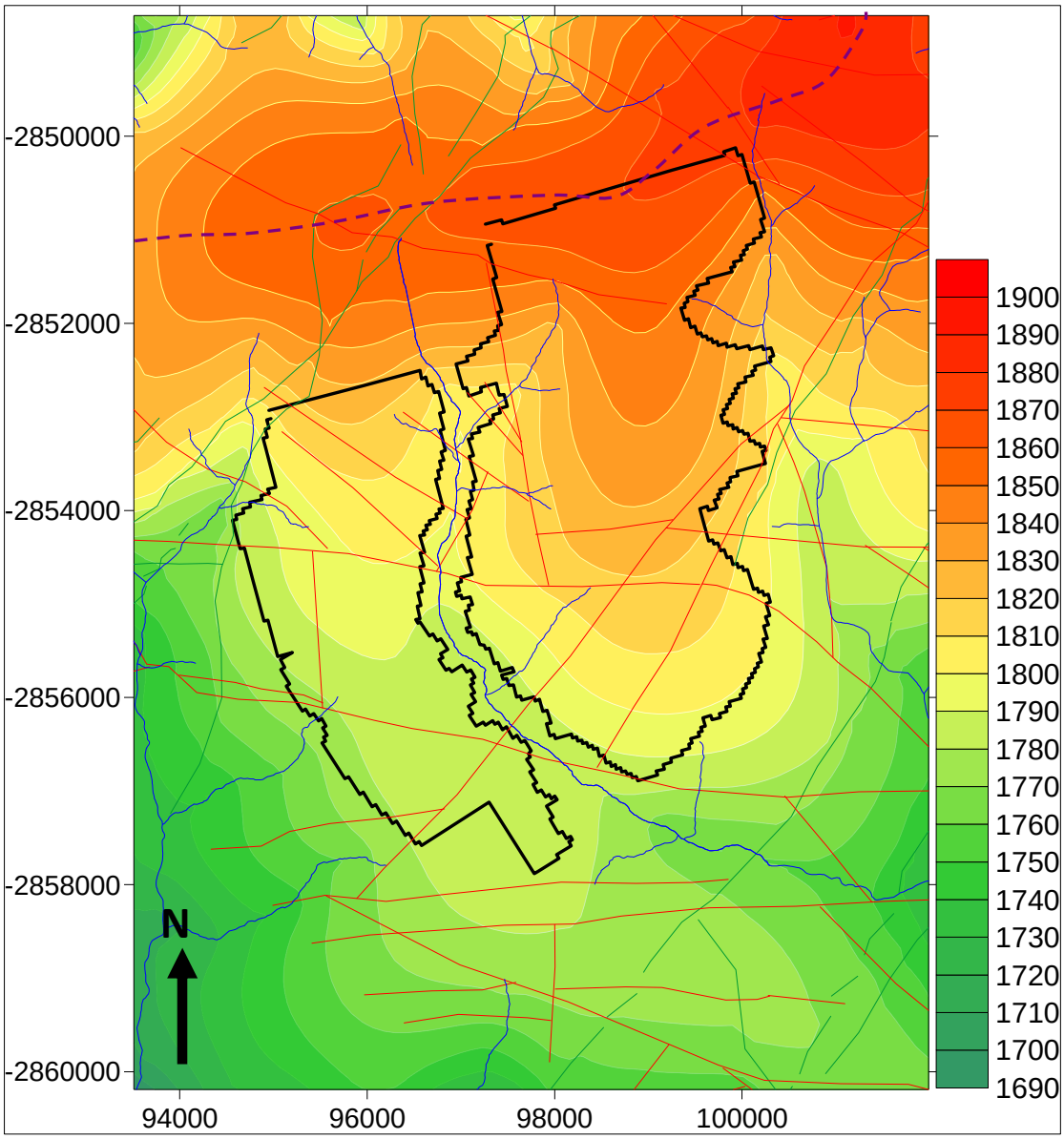

Figure 15: Steady state water levels for the study area

3.5.3 Groundwater chemistry

Although not the focus of this study, the pre-mining groundwater quality for the proposed project will be discussed. Coal mining operations in almost all cases have a negative impact on the groundwater quality. The most common impact from coal mining operations is known as acid mine drainage. Sulphate and pH is generally the indicator parameters used in the industry.

The closest active mining operation is situated on the southern boundary of the West Block of the proposed project. According to the local farmers some old coal

outcrops and surface excavations are present in the area. The potential for acid mine drainage reactions to occur are therefore present in these areas.

Groundwater samples for quality analysis were collected in boreholes and springs during the hydrocensus and in the newly drilled monitoring boreholes. Total dissolved solid concentrations in all the boreholes are within ideal limits for drinking water. The exception is groundwater from one spring south of the proposed project area where the concentrations exceed ideal permissible limits but still remain within maximum permissible limits. The sulphate concentration exceeds the maximum permissible limits for drinking water in the same spring. Iron concentrations in several springs and boreholes exceed the ideal limits or the maximum permissible limits for drinking water.

One of the most appropriate ways to represent the chemical composition of the sampled groundwater is by means of an expended Durov diagram. The groundwater qualities are dominated by either magnesium or by sodium + potassium on the cation side. On the anion side the qualities are mostly dominated by bicarbonate alkalinity. These qualities plot in fields 2 and 3 of the diagram and are representative of clean, fresh and recently recharged groundwater. The qualities plotting in fields 5 and 6 are dominated by sulphate on the anion side and ion exchange has started to occur. Some qualities plot in fields 8 and 9 and is dominated by chloride + nitrate on the anion side. Although these fields usually represent old and stagnant groundwater, the quality of this groundwater is still very good and fresh.

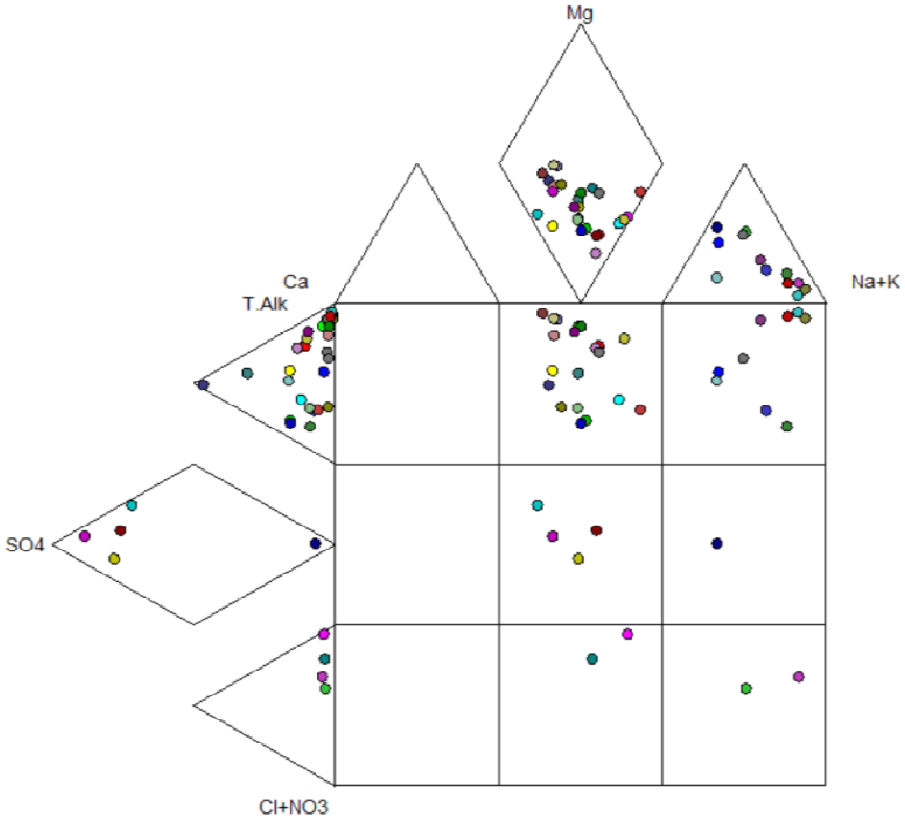

Figure 16: Expanded Durov diagram for the water qualities in the study area.

3.6 Life of mine layout

Mining will start at the East Block in 2011 and will end in 2049, while mining at the West Block start in 2016 and end in 2037. Mining in both blocks will occur in a northerly direction. The total surface area mined per annum is presented in Table 2. The size of the mining strips at the East Block decreases when mining in the West Block commences.

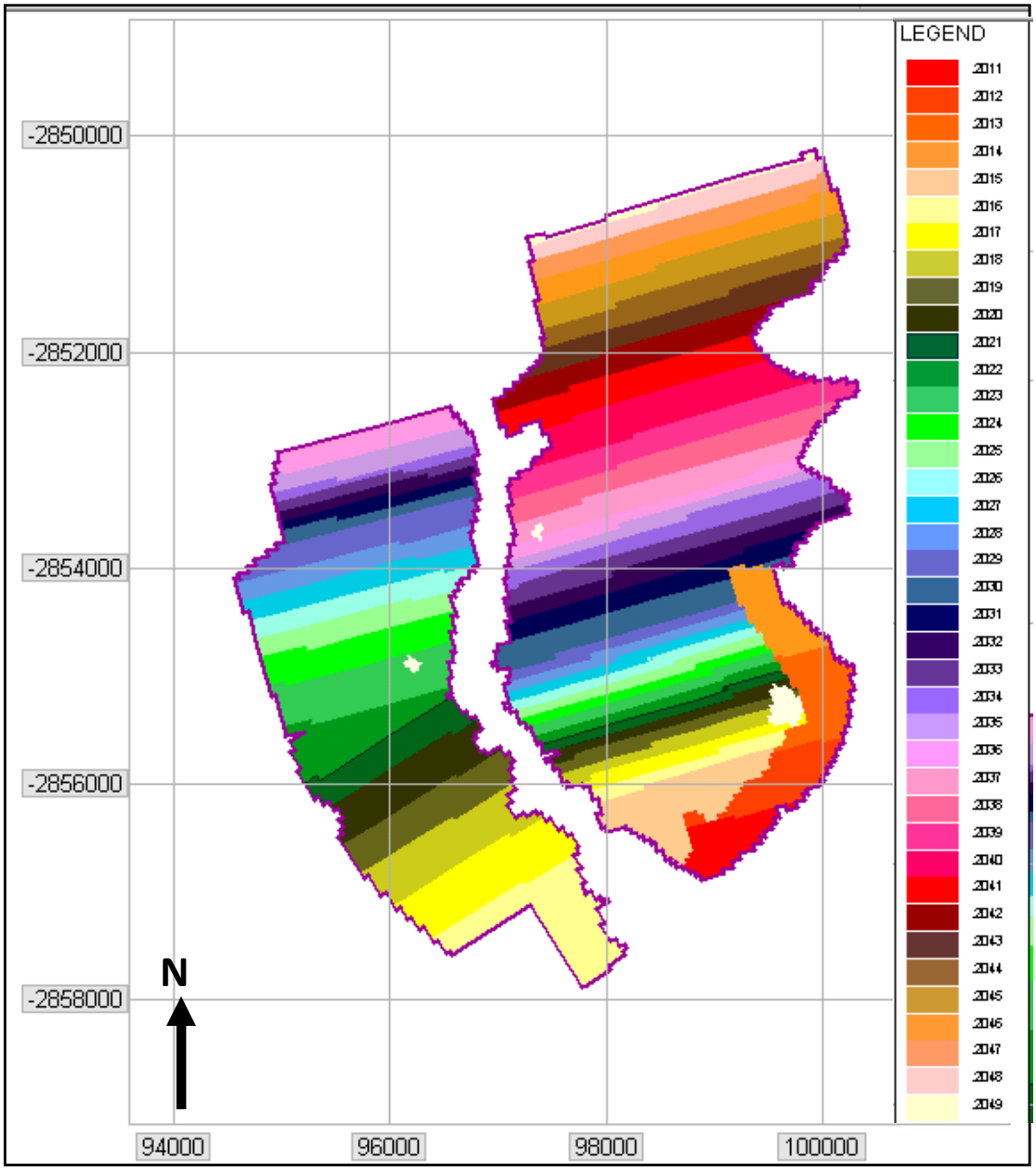

Figure 17: Life of mine layout.

Table 2: Annual surface area mined for each mining block.

	Total Area (m^2)	
Year	East Block	West Block
2011	315920	
2012	406100	
2013	430000	
2014	387000	
2015	690000	
2016	214000	756000
2017	230010	732000
2018	238000	595000
2019	218970	542000
2020	221240	554000
2021	216000	438000
2022	212000	493000
2023	212000	637000
2024	219000	495000
2025	220000	382000
2026	226000	375000
2027	225000	381000
2028	220000	393000
2029	215000	514000
2030	554400	192000
2031	490000	187000
2032	482000	187000
2033	477000	158000
2034	488000	147000
2035	295000	318000
2036	319000	312000
2037	560000	72500
2038	664000	
2039	725000	
2040	775000	
2041	644000	
2042	564000	
2043	559000	
2044	563000	
2045	646000	
2046	586000	
2047	513000	
2048	448000	
2049	159000	

4. Field data collection

In order to obtain site specific data for the study area, several field investigations have been conducted. These investigations include a geophysical survey, drilling of monitoring boreholes and pump testing of the monitoring boreholes. These investigations are done to obtain a better overview of the aquifer conditions in the study area.

4.1 Geophysical investigations

The geophysical survey was conducted by using magnetic and electro-magnetic methods.

4.1.1 The magnetic method

Electrical currents that move in the outer core of the earth are responsible for the earth's magnetic field, (Macmillan, 2004). In some rock formations, magnetic minerals are present. Minerals that are most commonly associated with magnetism include magnetite, ilmenite and pyrrhotite. These minerals with their own magnetic field cause variations in the earth's magnetic field. The magnetic method is used to detect these changes in the magnetic field of the earth (IGS Geophysics class notes, 2008).

For the magnetic survey conducted in the study site a Proton Precession Magnetometer was used. This apparatus is the most commonly used for magnetic surveys.

Traverses for the geophysical survey were positioned around the two pits over delineated geological structures such as faults and dykes. The main aim of the geophysical survey was to determine the positions, dip and strikes of the geological structures. The results have been used to position the boreholes that have been purposely drilled for groundwater monitoring.

The initial planning was to do the survey along 11 traverses (lines). These lines have been indicated in Figure 18. Due to several reasons such as no access and boreholes that are already drilled on the course of the lines, no survey was performed at lines 3, 7 and 10. The results of the geophysical survey have been included in **Appendix B** of this document. The results are presented on line graphs with the best position to drill monitoring boreholes.

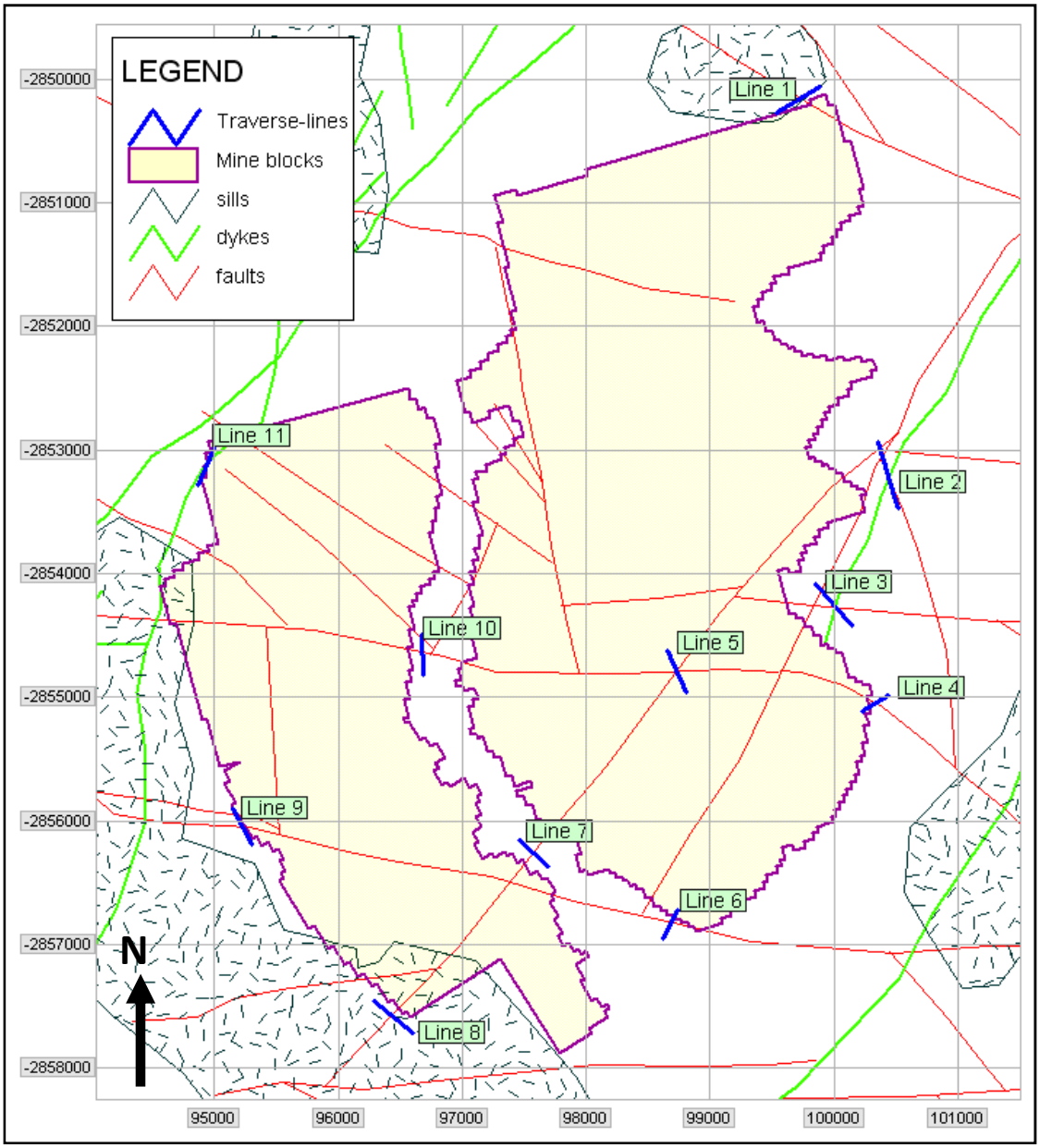

Figure 18: Positions of the proposed traverses to be followed in the geophysical survey.

4.1.2 Electromagnetic survey

The main aim of an electromagnetic survey is to detect any conductive zones in the subsurface. The principles of the electromagnetic method have been obtained from the Field Manual for Technicians No. 3 edited by van Zijl and Köstlin.

- An AC current is passed through a coil to establish an alternating magnetic field which consists of magnetic field lines.
- The magnetic field lines penetrates the earths subsurface

- If the magnetic field lines move through conductive zones, induced currents start to flow.
- These currents generate secondary magnetic fields that can be detected and measured by the receiver.
- If the actual measured field is compared to the calculated field that is received in the absence of a conductive zone, the presence of a conductive zone can be confirmed.

The electromagnetic survey has been performed along the same traverses as those of the magnetic survey. The results have been presented on the same graphs as the magnetic results in **Appendix B**. The positions with the best probability to intersect water during drilling were proposed by the geophysicist and are indicated on the line graphs in Appendix B.

4.2 Drilling of monitoring boreholes.

Eight new monitoring boreholes were drilled in the project area at the positions that were obtained from the geophysical survey that was performed at the study site. The new monitoring boreholes were mostly situated at or near geological structures such as dykes and faults. The positions of these boreholes are indicated in Figure 19. Details of borehole construction are presented in Table 3 below. Geological logs of the new monitoring boreholes are included in Appendix A of this document.

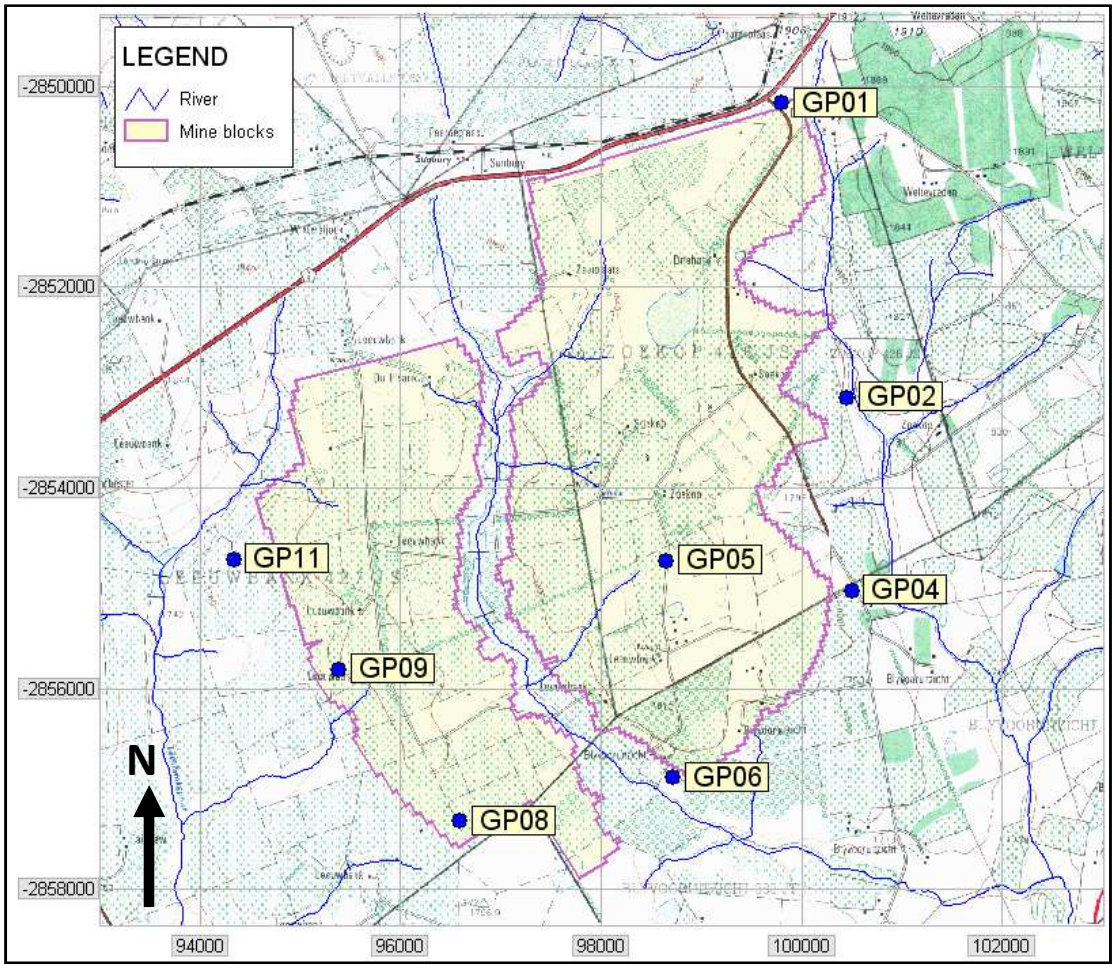

Figure 19: Positions of the monitoring boreholes drilled in the study area.

The monitoring boreholes were drilled by a conventional percussion drilling rig. All the boreholes were drilled to a depth of 31 meters.

Table 3: Drilling detail for the monitoring boreholes

BH	Depth	Lithology*	X-Coord	Y-Coord	WL	Casing
GP01	31	Samples lost before logging	99802	-2850160	7.6	11
GP02	31	SOIL, SNDS	100452	-2853109	6.7	5
GP04	31	SOIL, SNDS	100494	-2855021	6.9	11
GP05	31	SOIL, SNDS, SHLE, COAL, SDSL	98656	-2854725	3.1	13
GP06	31	SOIL, SNDS	98721	-2856886	7.4	11
GP08	31	SOIL, SHLE	96591	-2857316	8.2	7
GP09	31	SOIL, SNDS, SHLE, COAL, SDSL	95380	-2855815	1.2	12
GP11	31	SOIL, SHLE, SNDS	94338	-2854716	4.6	11

* *SHLE - Shale*

SNDS - Sandstone

SDSL - Sandstone and Shale – interlaminated

WL – Water Level (meters below surface)

Casing - casing depth (m)

Co-ordinate system – Cape LO29

4.3 Aquifer tests analysis

4.3.1 Blow yields

Fractures were intersected in six boreholes during drilling. The results of the blow yields together with the fracture depth are presented in Table 4.

Table 4: Blow yields of the drilled boreholes.

Borehole	Fracture depth (mbs)	Blow yield (l/hr)	Blow yield (l/s)
GP1	11	20	0.006
GP2	11	1000	0.28
GP4	22	1500	0.4
GP5	25	600	0.17
GP9	20	20	0.006
GP11	16	750	0.2

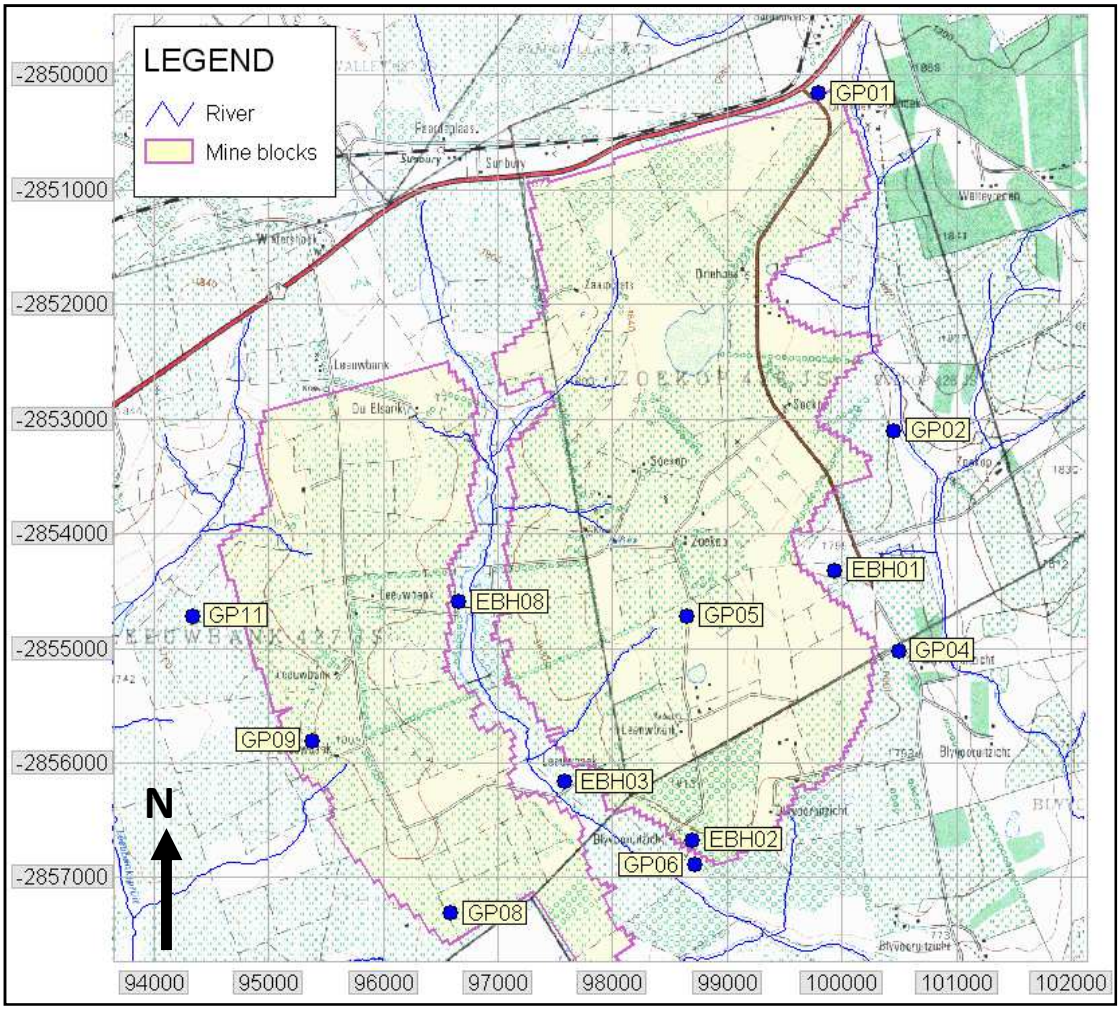

Figure 20: Distribution of pumping test boreholes

Short duration constant rate pumping tests were performed on seven of the newly drilled monitoring boreholes and on four exploration boreholes drilled by the mine. The purpose of the pumping tests was to get an indication on aquifer parameter values. The pumping duration in all the boreholes was 30 minutes. Some of the boreholes were dry at drilling or had very low blow yields. Since the boreholes are purposely drilled for monitoring and not water supply, pumping tests were performed on all boreholes with water even if no distinct fractures were encountered. Due to the low yields it is not possible to perform long duration pumping tests. The Aquitest software package was used to evaluate the pump test results.

Table 5: Aquifer parameters of monitoring boreholes

Borehole	Tf	Tm	Sf	Sm
Unit	m^2/d	m^2/d		
EBH01	1.7	0.2	0.005	NA
EBH02	1.9	0.2	0.004	NA
EBH03	59	14	0.005	0.1
EBH08	1.7	0.5	0.004	0.007
GP01	1.1	0.2	0.002	NA
GP02	29	7.7	NA	0.005
GP04	29	8.8	NA	0.007
GP05	13.6	5.5	0.006	0.04
GP08	1.6	0.2	0.004	0.005
GP09	1.5	0.4	0.003	0.01
GP11	10.3	4.8	0.001	0.007
Harmonic Mean	2.6	0.4	0.003	0.01
Geometric Mean	5.3	1.2	0.004	0.015
Har + Geo Mean Average	**4.0**	**0.8**	**0.003**	**0.012**

***Note**:*

Tf – Transmissivityof the fracture.
Tm – Transmissivityof the matrix.
Sf – Storativityof the fracture.
Sm – Storativityof the matrix.
NA – not accurately determinable by the specific method or test or unrealistic result.

5. Conceptual model

A conceptual model is constructed to aid in predicting the behaviour of groundwater in the sub-surface. To construct a high-quality numerical model for the prediction of the mine impacts on the groundwater regime, one needs a good conceptual model. A conceptual model includes the evaluation of aquifer types, aquifer boundaries, groundwater flow behaviour and many more.

The mining area is situated in the Mpumalanga Coalfields area and is underlain by rocks of the Karoo Supergroup. Two aquifer systems are present in the Karoo Supergroup; the upper weathered aquifer and the secondary, fractured rock aquifer. A third aquifer can exist in the area. This aquifer is situated below the Ecca sediments. The third aquifer will however not be incorporated into this study since the mining operation will have no impact on it in terms of quantity. The aquifer types and characteristics have also been discussed in Chapter 2 of this document. (Grobbelaar *et al.*, 2004)

Recharge is that part/percentage of the total precipitation that reaches the aquifer after all factors including runoff, evaporation and evapo-transpiration have taken place. Factors that influence the recharge to an aquifer include: soil type and its permeability, ground slope, vegetation, rainfall and the intensity thereof, geology and man's influence, (Cogho and van Niekerk, 2009).

Van Tonder and Kirchner (1990) conducted a three year long study on Karoo type aquifers. During this study the SVF (saturated volume fluctuations) method was used to estimate the groundwater recharge to the aquifers. The results of the study showed that the recharge to the Karoo aquifers can vary between 2 and 5 % of the annual precipitation. If the soil cover is very thick the recharge can decrease to less than 3%.

Boundaries can include features such as surface water bodies and groundwater divide areas. In the model developed for the proposed project area, rivers and pans were defined as constant head boundaries. The rivers and pans were inserted as river nodes in the model and the head in the river were fixed at 2 meters below the ground surface. On the edge of the model area, general head boundaries were inserted. The general head boundaries are also known as Cauchy boundary conditions which mean that the heads can vary with time.

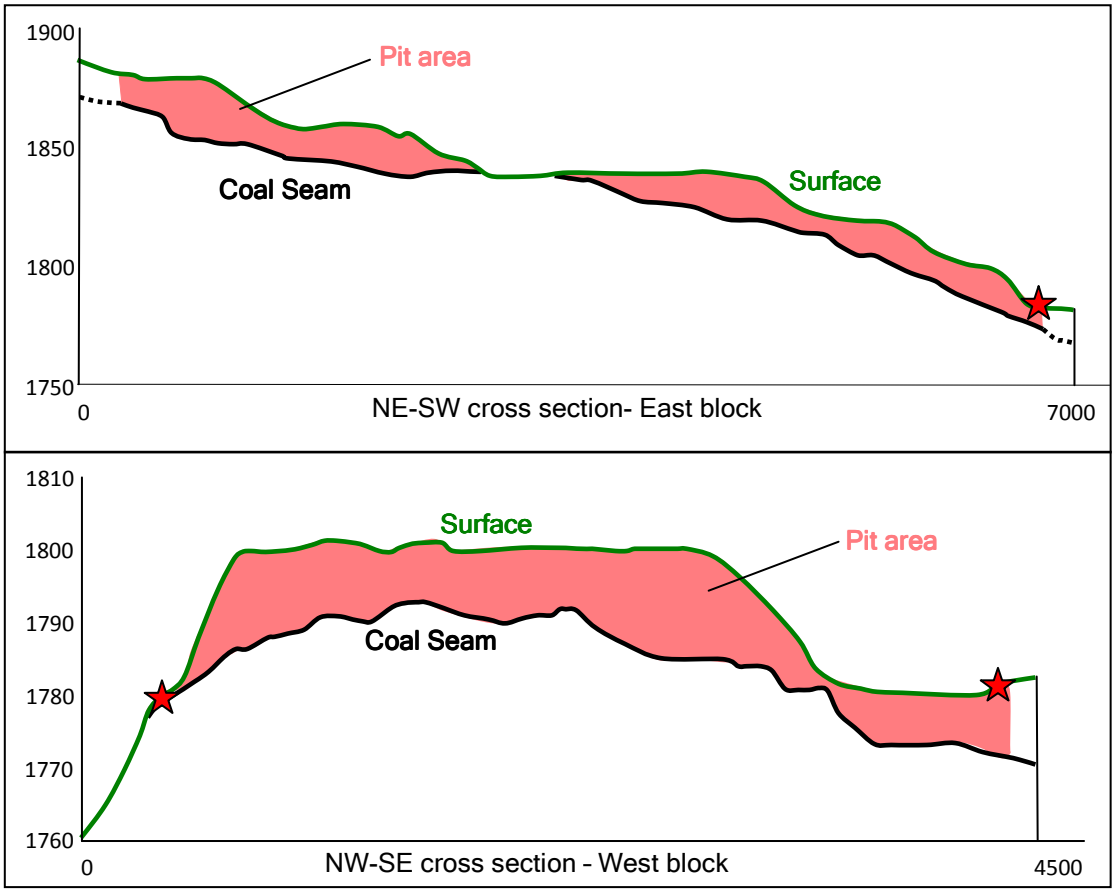

Figure 21: Cross sectional cuts through the mining blocks to indicate the coal floor and surface geometry.

From the cross section through the East block and the West block it is clear that the decant elevation is lower than the majority of the opencast pit. This means that the pit will not completely fill with water before decanting starts. The major problem with this scenario is that the carbonaceous backfill material will be exposed to oxygen, which will lead to the formation of acid mine drainage (AMD). It is custom in the coal mining industry that the carbonaceous material is placed at the bottom of the pit so that it can be covered by water as soon as possible (reducing conditions). Since a large part of the carbonaceous material will not be covered by water in this case, oxidising conditions will prevail leading to the formation of acid mine drainage.

Another problem in the West block is the fact that there is a ridge separating the eastern and the western portion of the mine block from each other. The ridge leads to the West block having two decanting points; one on the western boundary and one on the eastern boundary.

Below is a figure indicating which part of the backfilled pit areas will be covered by water at the decanting elevation.

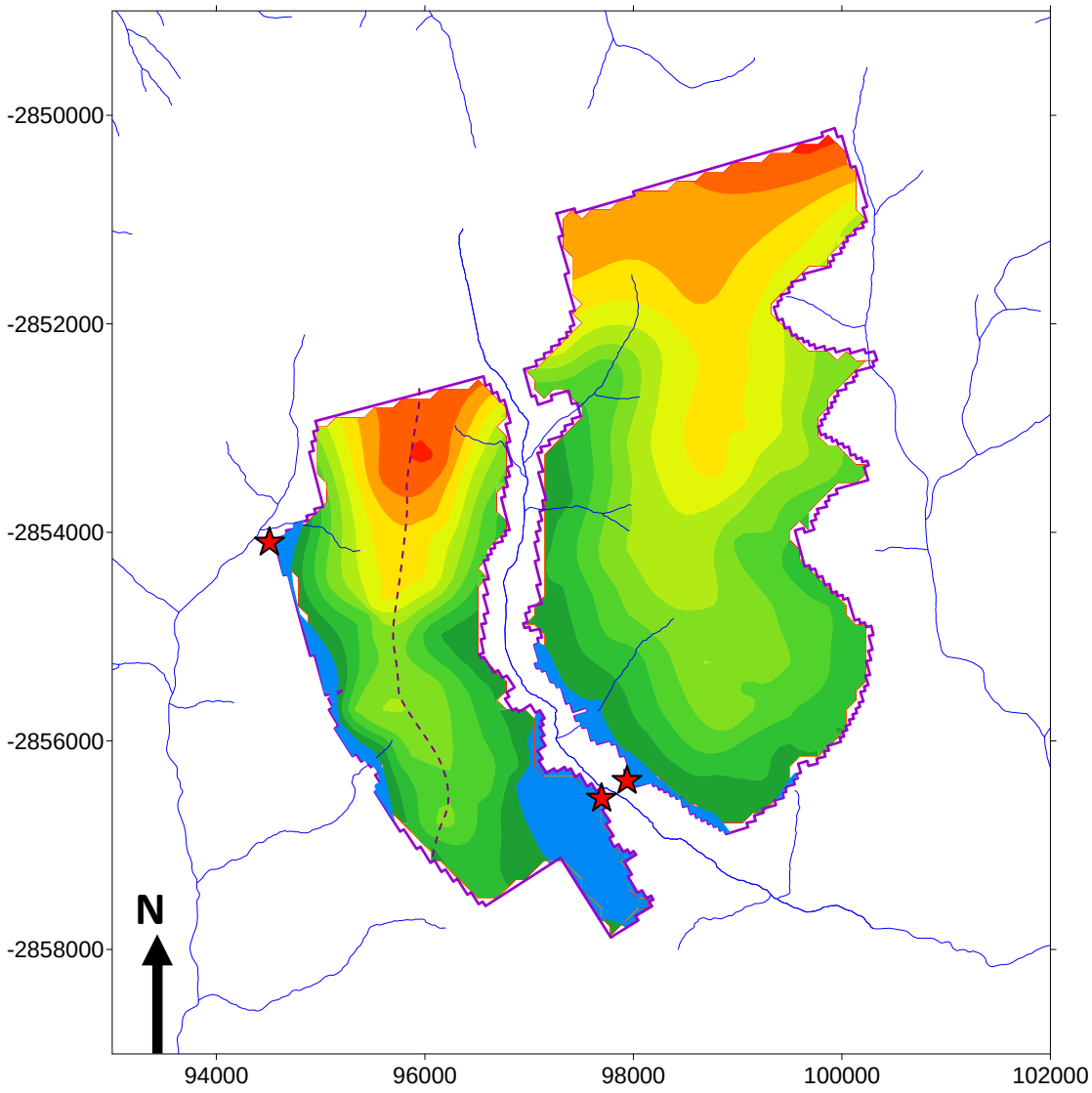

Figure 22: Indication of the area of the mining blocks that will be filled with water at the decant elevation.

The lowest coal floor elevations in the East block are approximately 1760 mamsl and at the West block 1765 mamsl. The highest coal floor elevations in the East block are approximately 1870 mamsl and at the West block 1825 mamsl. The coal floor gradients at the two blocks are approximately 0.5 to 1% and the general dip direction is to the south. The coal floor geometry is very similar to that of the topography. It should be noted that the assumption is made that the pits can start backfilling as they progress. This can occur since mining will start at lower elevations and progress up-gradient.

The thickness of the unsaturated zone is equal to the water level depth. From water level information obtained from the hydrocensus boreholes and the new monitoring boreholes, the unsaturated zone in the area generally varies between 0.5 and 16 mbs.

The thickness of the aquifer in the project area was determined by subtracting the depth of the water level from the depth of the main water strike in the borehole. The aquifer thickness in the area can vary between 3 and 22 metres.

Table 6: The water levels, main water strike depth and aquifer thickness for the drilled monitoring boreholes

Borehole	Water Level depth (m)	Main Water strike depth (m)	Aquifer thickness (m)
GP01	7.6	11	3.4
GP02	6.7	11	4.3
GP04	6.9	22	15.1
GP05	3.1	25	21.9
GP06	7.4	dry at drilling	-
GP08	8.2	dry at drilling	-
GP09	1.2	20	18.8
GP11	4.6	16	11.4

Blow yields in the monitoring boreholes as determined during drilling varied between approximately 20 l/hr and 1500 l/hr.

The steel casing in the new monitoring boreholes have been inserted to depths where the rock material changed from weathered to fresh. These depths vary between 5 and 13 meters and therefore also present the depth of the weathered zone.

Geological structures influence the groundwater flow regime. The impacts of structures such as dykes, faults and sills have been discussed in Chapter 2.4 of this document and the positions are indicated in Figure 18.

6. Analytical calculations

Analytical methods are usually a fast way of getting a good first order estimate of the required results. Analytical methods do however have some undeniable constraints and it is impossible to incorporate all factors that can have an effect on the groundwater flow.

The scope of this study is to determine the groundwater inflow to and opencast pit by using analytical and numerical methods and comparing these results. The total volume of groundwater inflow to the opencast pits has been determined by analytical methods. The results were compared with values obtained in the numerical groundwater flow model. The water that will flow into the pit during the life of mine will consist of water from two main sources (Hanna *et al*., 1994):

1. Groundwater seepage
2. Recharge from precipitation

Four approaches will be used to analytically estimate the groundwater inflow to the opencast pits. These include the Vandersluis *et al*. (1995) and Krusseman & De Ridder (1979) methods as investigated by Aryafar *et al.* (2007), the one by Marinelli and Nicolli (2000) and a self-constructed analytical model with recharge and the Darcy method. These methods have been discussed in Chapter 1 of this document under the subheading 'Literature Review'.

6.1 Vandersluis et al. approach

The equivalent radius first needs to be estimated to account for the rectangular geometry of the mine strips as opposed to the theoretical round pit of the equation. The equation for the equivalent radius is provided below and the calculated equivalent radii per year are provided in Table 7.

Equivalent radius: $r = (2/\pi)(Y.W)^{1/2}$

Table 7: Length, Width and Equivalent Radius of the mining strips during each year

Year	East Block			West Block		
	Length (Y)	Width (W)	Equivalent radius (r)	Length (Y)	Width (W)	Equivalent radius (r)
2011	770	320	316	-	-	-
2012	950	480	430	-	-	-
2013	840	500	413	-	-	-
2014	880	400	378	-	-	-
2015	1700	360	498	-	-	-
2016	1870	80	246	1490	500	550
2017	1940	110	294	1620	450	544
2018	1980	110	297	1440	400	483
2019	2070	110	304	1720	310	465
2020	2370	90	294	1440	370	465
2021	2380	90	295	1540	270	411
2022	2380	90	295	1570	240	391
2023	2340	100	308	1660	400	519
2024	2400	100	312	1800	260	436
2025	2390	90	295	1840	190	377
2026	2480	100	317	2070	180	389
2027	2380	90	295	2200	170	390
2028	2340	90	292	2200	190	412
2029	2240	90	286	2120	240	454
2030	2300	200	432	1850	110	287
2031	2800	160	426	1850	100	274
2032	3300	130	417	1890	120	303
2033	3300	150	448	1900	80	248
2034	3100	140	420	1940	80	251
2035	2990	100	348	1930	150	343
2036	2800	110	353	1760	180	359
2037	2800	150	413	1590	50	180
2038	3060	220	523	-	-	-
2039	3380	200	524	-	-	-
2040	2300	310	538	-	-	-
2041	2480	220	470	-	-	-
2042	2520	230	485	-	-	-
2043	2640	170	427	-	-	-
2044	2870	210	494	-	-	-
2045	2970	220	515	-	-	-
2046	2930	190	475	-	-	-
2047	2880	180	459	-	-	-
2048	2840	150	416	-	-	-
2049	2780	50	237	-	-	-

Flow by Vandersluis *et al*. equation:

$$Q = \frac{1.366 \times K(2H - h)\ h}{\log(R+r_o) - \log(r_o)}$$

h = 0; no head above the base of the pit.

K = Transmissivity / thickness of aquifer = 1.2 / 20 = 0.06 m/day.

R = radius of influence from the pit centre (m)

r_o = effective pit radius

A constant radius of influence will be used for the Vandersluis *et al*. approach. The radius of influence for this approach will be determined as follows (Cooper-Jacob):

$$R = 1.5\sqrt{T*t/S}$$
$$= 1.5\sqrt{1.2*365/0.1}$$
$$= 100 \text{ meter}$$

The hydraulic conductivity was determined by taking the transmissivity of the matrix as used in the model namely 1.2 m^2/day and dividing this value by the thickness of the aquifer. For the weathered aquifer the K-value is equal to 1.2 divided by 20 meters. A constant K-value of 0.06 m/day was used for the entire area. Since the Vandersluis *et al*. approach do not take into account any recharge, recharge as determined in Section 6.4 of this document have been added to the Q.

A specific yield of 0.1 has been used for the weathered, unconfined aquifer.

In the analytical calculations the radius of influence will be determined by adding a constant of 100 meters to the pit radius.

The groundwater inflow into an opencast pit for steady state flow in an unconfined aquifer has been determined for each year of mining in the figures below.

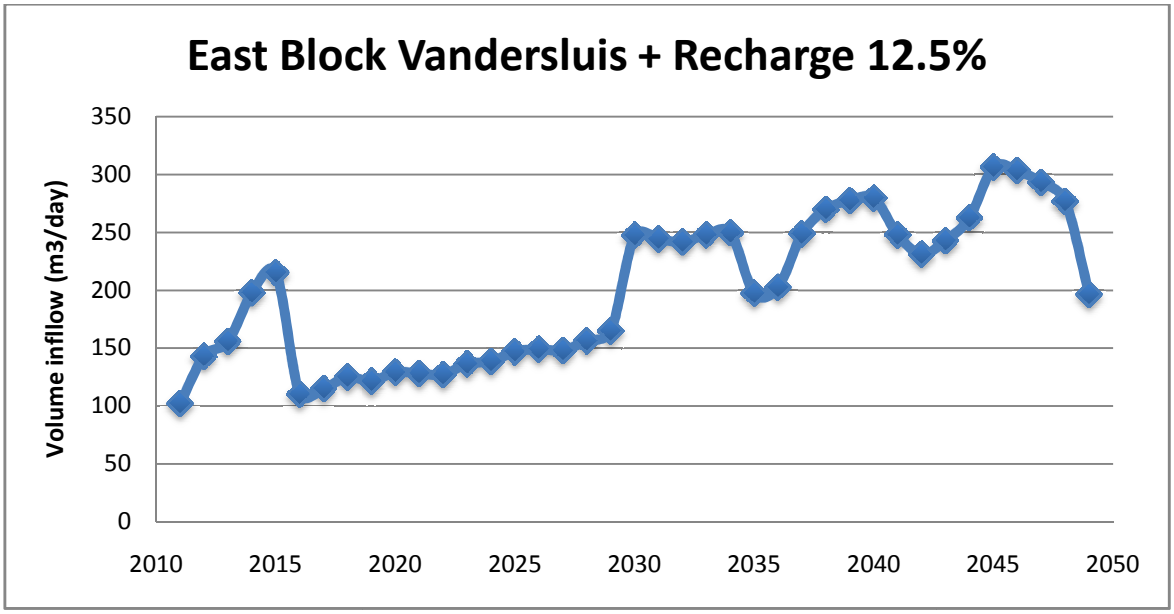

Figure 23: Groundwater inflow to the East Block as determined by the Vandersluis *et al*. method.

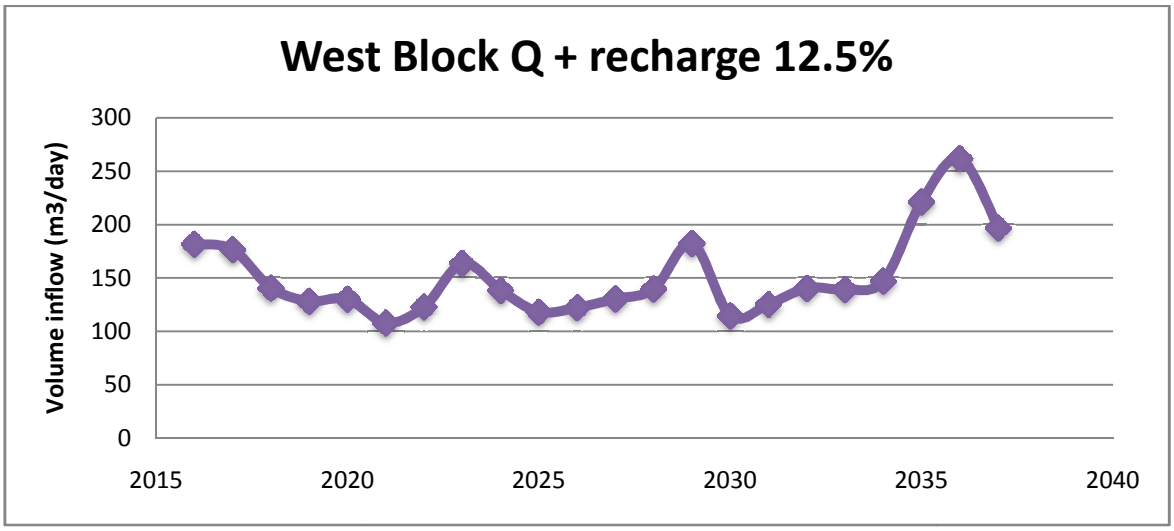

Figure 24: Groundwater inflow to the West Block as determined by the Vandersluis *et al*. equation.

6.2 Krusseman and De Ridder approach

Krusseman and De Ridder's approach is used for determining steady state inflow to an opencast pit from an unconfined aquifer. The inflow (Q) has been determined by making use of the following equation and the results are presented in Figures 25 and 26.

$$Q = \frac{\pi K (H^2 - h^2)}{\text{Ln}\,(R/r_p)}$$

The radius of influence was determined in the same way as for the Vandersluis *et al*. approach; the Cooper-Jacob equation. Similar as with the Vandersluis *et al*. method, recharge is not considered in the Krusseman & De Ridder approach. Once again the recharge as determined in Section 6.4 of this document was added to the Q determined from the equation above.

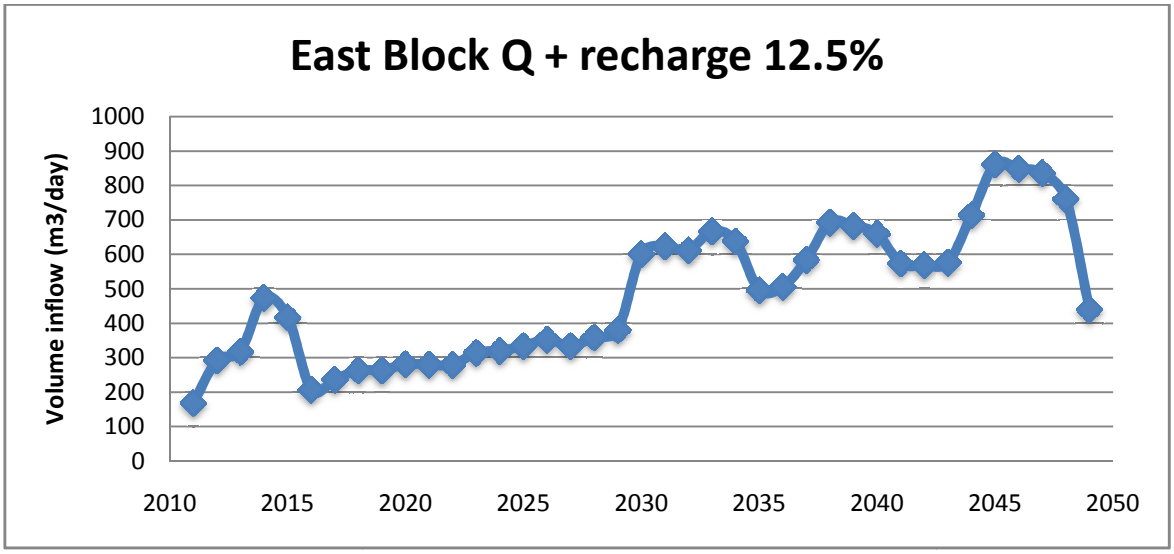

Figure 25: Groundwater inflow to the East Block as determined by the Krusseman & De Ridder approach.

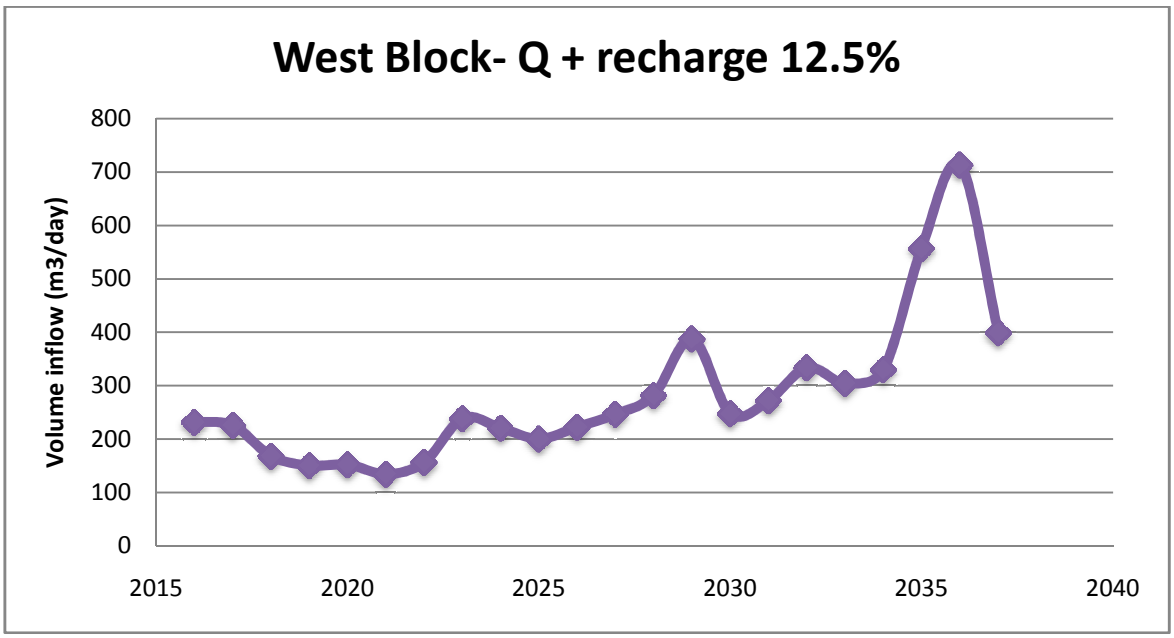

Figure 26: Groundwater inflow to the West Block as determined by the Krusseman& De Ridder approach

6.3 Marinelli and Nicolli approach

According to the Marinelli and Nicolli approach the inflow from the pit floor is significantly larger than that from the pit wall. Only the inflow from the pit wall is determined with the use of the radius of influence. The flow from the pit floor will be the same even if the radius of influence differs.

$Q_1 = W\pi (R^2 - r_o^2)$, where Q_1 is the inflow from the pit walls.

and: W = recharge flux
r_o = effective pit radius
R = radius of influence (maximum extent of the cone of depression)

$Q_2 = 4r_p (K_{h2}/m_2)(h_o-d)$

And

$$m_2 = \sqrt{(K_{h2}/K_{v2})2}$$

where: K_{h2} = horizontal hydraulic conductivity
K_{v2} = vertical hydraulic conductivity
m_2 = anisotropy parameter
d = depth of pit lake
$h_o - d$ = drawdown at pit wall

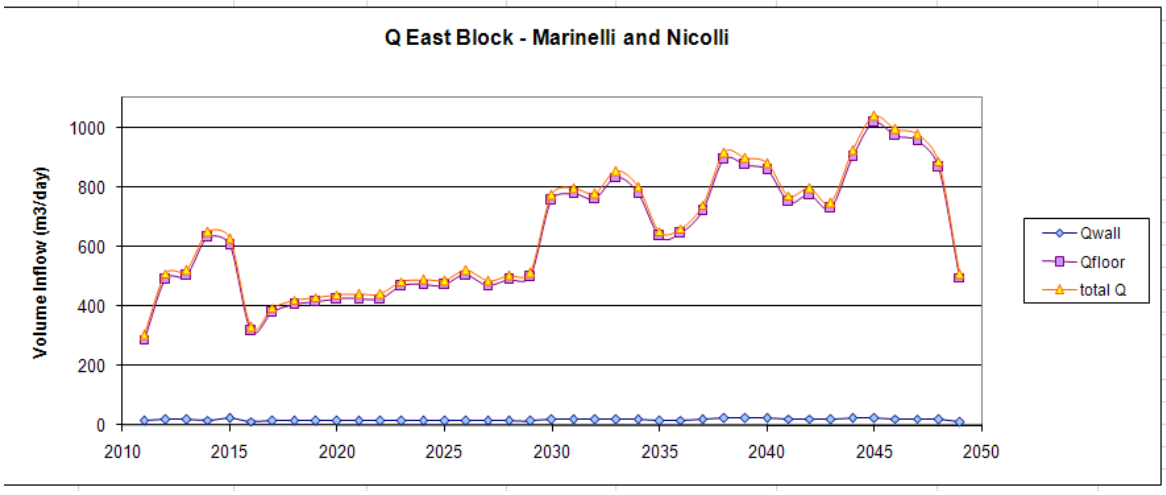

Figure 27: Groundwater inflow to the East Block as determined by the Marinelli and Nicolli approach

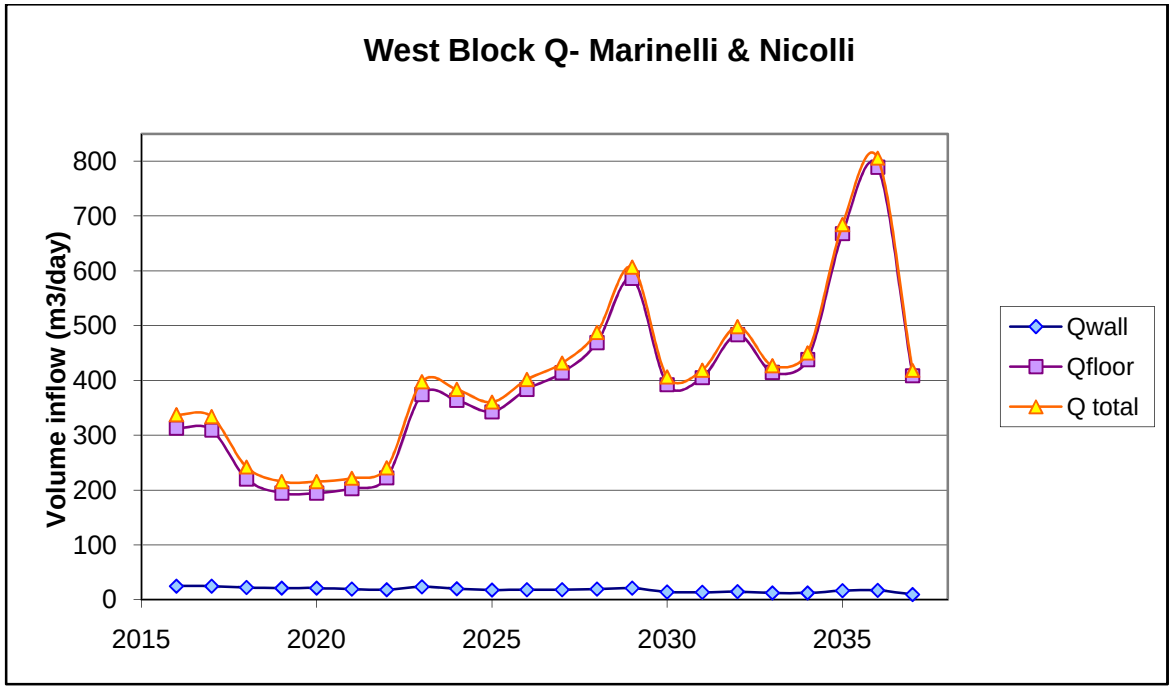

Figure 28: Groundwater inflow to the West Block as determined by the Marinelli and Nicolli approach

6.4 Analytical approach to recharge determination

Recharge to the Karoo type aquifers have been estimated in a previous study by van Tonder and Kirchner (1990). According to the study recharge to the aquifers can vary between 2 and 5% of the annual precipitation. However, when opencast mining is active, the recharge can increase significantly to up 20% of the annual precipitation (Grobbelaar *et al.* 2004). For the analytical recharge volume estimations, a sensitivity analysis with recharge of 10, 12.5 and 20% were performed. The aim is to compare these results with those obtained by the numerical model. The results are indicated in Table 8. The recharge rate to the mining strips is determined as follows:

Recharge per day = area * (MAP/365days) * % recharge

Where: MAP = mean annual precipitation (650 mm/annum)

Table 8: Estimated aquifer recharge over the LOM (m^3/day)

Year	East Block			West Block		
	RCH (10%)	RCH (12.5%)	RCH (20%)	RCH (10%)	RCH (12.5%)	RCH (20%)
2011	56	70	113			
2012	72	90	145			
2013	77	96	153			
2014	69	86	138			
2015	123	154	246			
2016	38	48	76	135	168	269
2017	41	51	82	130	163	261
2018	42	53	85	106	132	212
2019	39	49	78	97	121	193
2020	39	49	79	99	123	197
2021	38	48	77	78	98	156
2022	38	47	76	88	110	176
2023	38	47	76	113	142	227
2024	39	49	78	88	110	176
2025	39	49	78	68	85	136
2026	40	50	80	67	83	134
2027	40	50	80	68	85	136
2028	39	49	78	70	87	140
2029	38	48	77	92	114	183

2030	99	123	197	34	43	68
2031	87	109	175	33	42	67
2032	86	107	172	33	42	67
2033	85	106	170	28	35	56
2034	87	109	174	26	33	52
2035	53	66	105	57	71	113
2036	57	71	114	56	69	111
2037	100	125	199	13	16	26
2038	118	148	236			
2039	129	161	258			
2040	138	173	276			
2041	115	143	229			
2042	100	126	201			
2043	100	124	199			
2044	100	125	201			
2045	115	144	230			
2046	104	130	209			
2047	91	114	183			
2048	80	100	160			
2049	28	35	57			

Cumulative recharge over the LOM

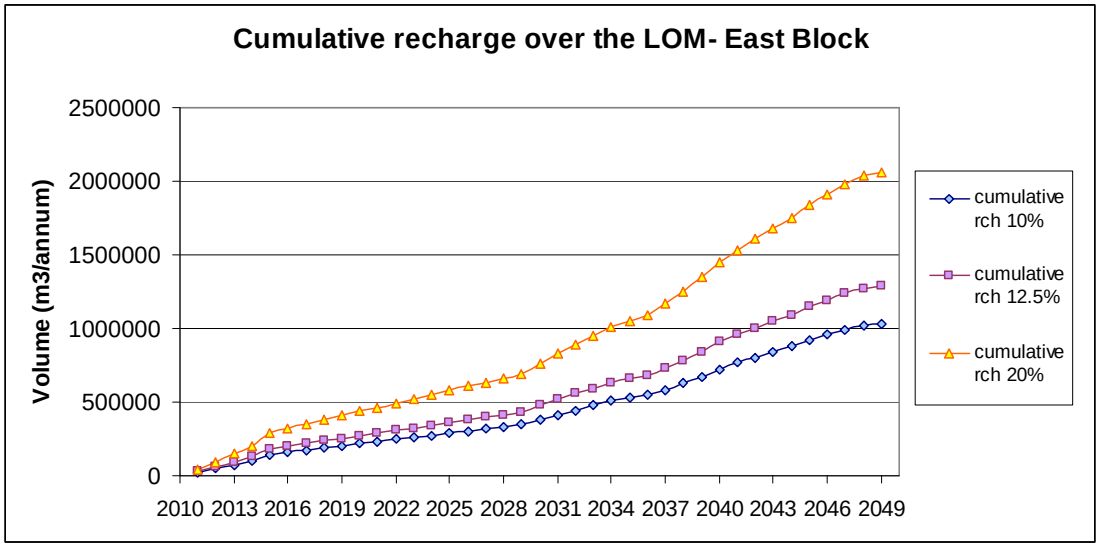

Figure 29: Cumulative recharge for the East Block

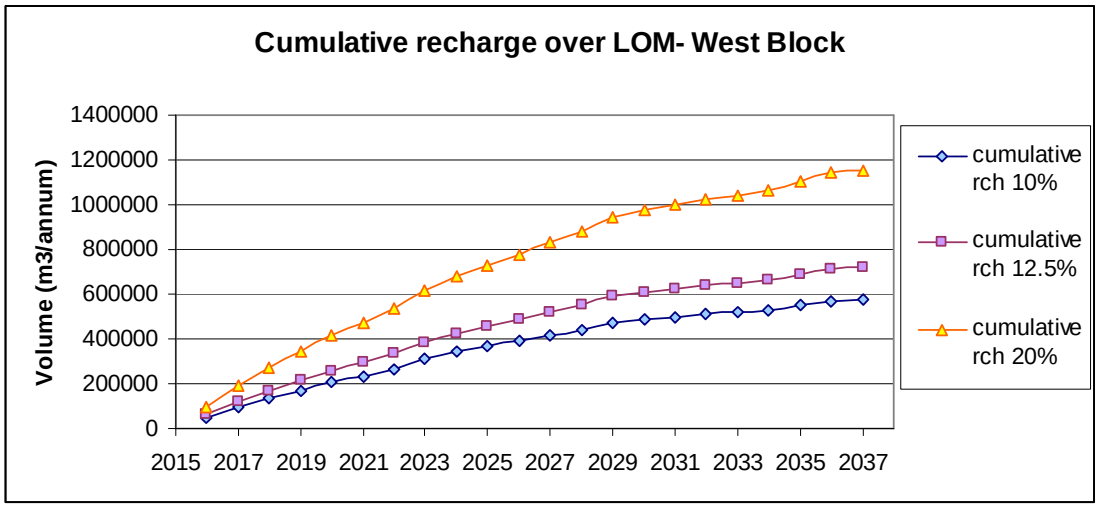

Figure 30: Cumulative recharge for the West Block

6.5 Analytical model incorporating Darcy equation and recharge

For this approach the recharge water to the pit as determined in Section 6.4 of this document is added to the inflow from the pit walls as determined by the Darcy equation.

Darcy states that: Q = KiA

The inflow to the pit during the operational phase will therefore be determined as follows:

Q = Darcy Q + estimated recharge at 12.5%

The area (A) that is used for determining the inflow to the pit is determined by multiplying the depth of the pit by the length of the walls through which groundwater can flow. At the first cut (year 1) the inflow will be from all four walls of the mine strip. The following years will exclude the wall that is mined during the previous year (back wall). Therefore groundwater will flow only from the side wall and the front wall.

This concept is conceptualized in Figure 31. The red lines indicate the walls through which groundwater flows during the operational phase. The dashed line in year 3 was mined in year 2 and therefore flow from the back wall will not occur since it isn't there anymore.

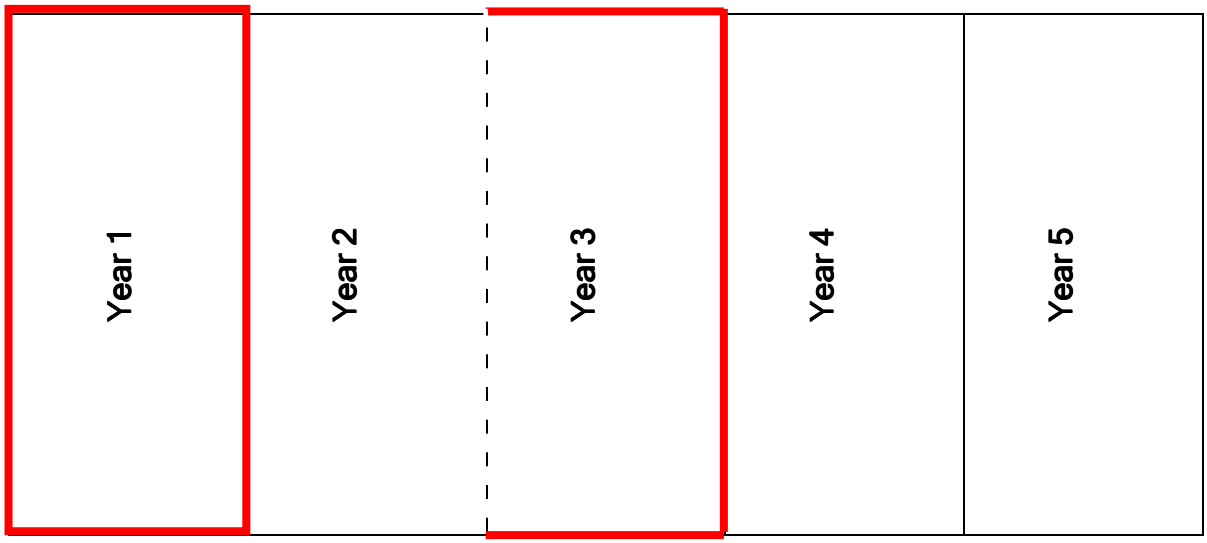

Figure 31: Conceptual presentation of walls through which groundwater flows into the pit during the operational phase.

The groundwater gradient is determined as follows:

$$i = (dh - dl) / L$$

Where: **(dh - dl)** is the difference in height between two points. **dh** will be the water level elevation **L** meters from the pit and **dl** will be the pit floor elevation. **L** is the radius of influence of the mining activity. **L** is referred to as **R** (radius of influence).

Two different scenarios were used for determining the radius of influence, somewhat of a sensitivity analysis. Firstly, the radius of influence was determined by using the S=0.1 value. The second approach was to lessen the storativity to 0.01. Therefore a simple equation:

$$R = 1.5 * \sqrt{T * t/S}$$

$$= 1.5 * \sqrt{1.2 * 365/0.1}$$

$$= 100 \text{ meters}$$

And where S=0.01 the radius of influence is 314m.

Darcy				
T (m2/day)	1.2			
S	0.01			
ho (m)	7.5			
K (m/day)	0.06			
outline	5800			
A (m2)	43500			
	days	Re	i	Q
t	365	314	0.02	62

Recharge (m3/day)		
MAP (m/annum)	0.6	
MAP (m/day)	0.0016	
Area (m2)	312000	
Recharge 10%	51	m3/day
Recharge 12.5%	64	m3/day
Recharge 20%	103	m3/day

Recharge + Darcy	m3/day
10% RCH	114
12.5% RCH	126
20% RCH	165

Figure 32: Representation of the excel spreadsheet for determining the groundwater inflow with Darcy.

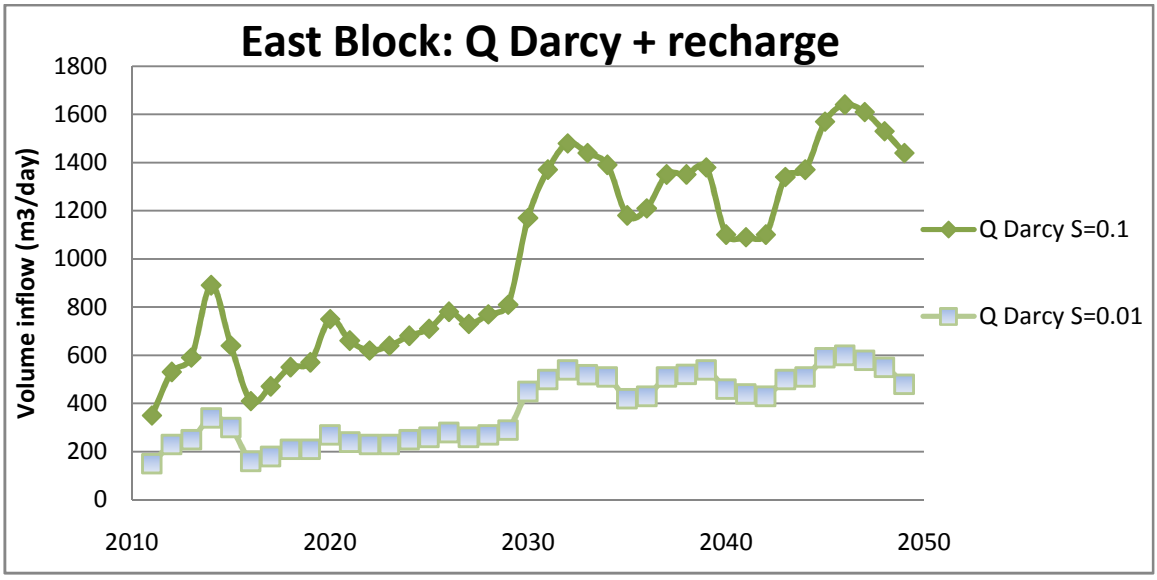

Figure 33: Comparing the two different scenarios for groundwater inflow to the East Block.

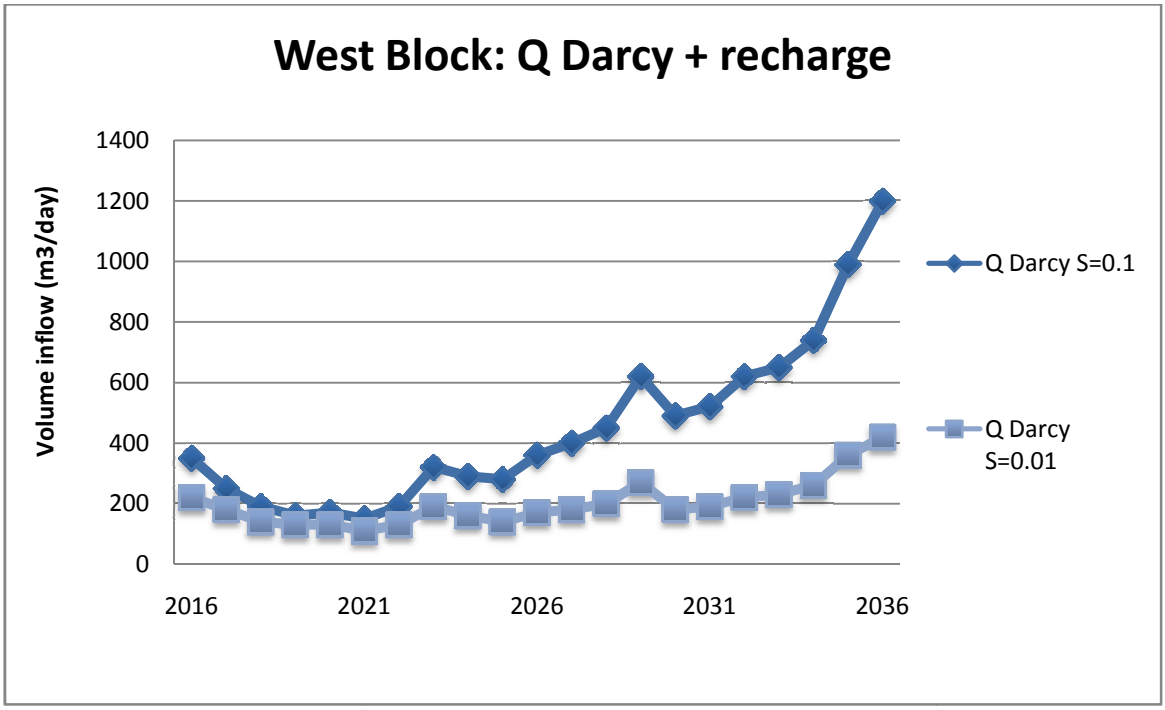

Figure 34: Comparing the two different scenarios for groundwater inflow to the West Block.

6.6 Comparing analytical approaches

The analytical approaches were chosen as they were best applicable to the study area. The Vandersluis et al. approach is typically used in semi-arid environments. South Africa is known as a semi-arid environment. The Marinelli and Nicolli approach together with the Krusseman and De Ridder approach is typically used to determine inflow from an unconfined aquifer. In the study area flow is expected to be mainly from the unconfined aquifer. The Darcy equation is typically used for a porous medium aquifer, but has been applied to the Belfast study area underlain by double porosity and fractured rock aquifers.

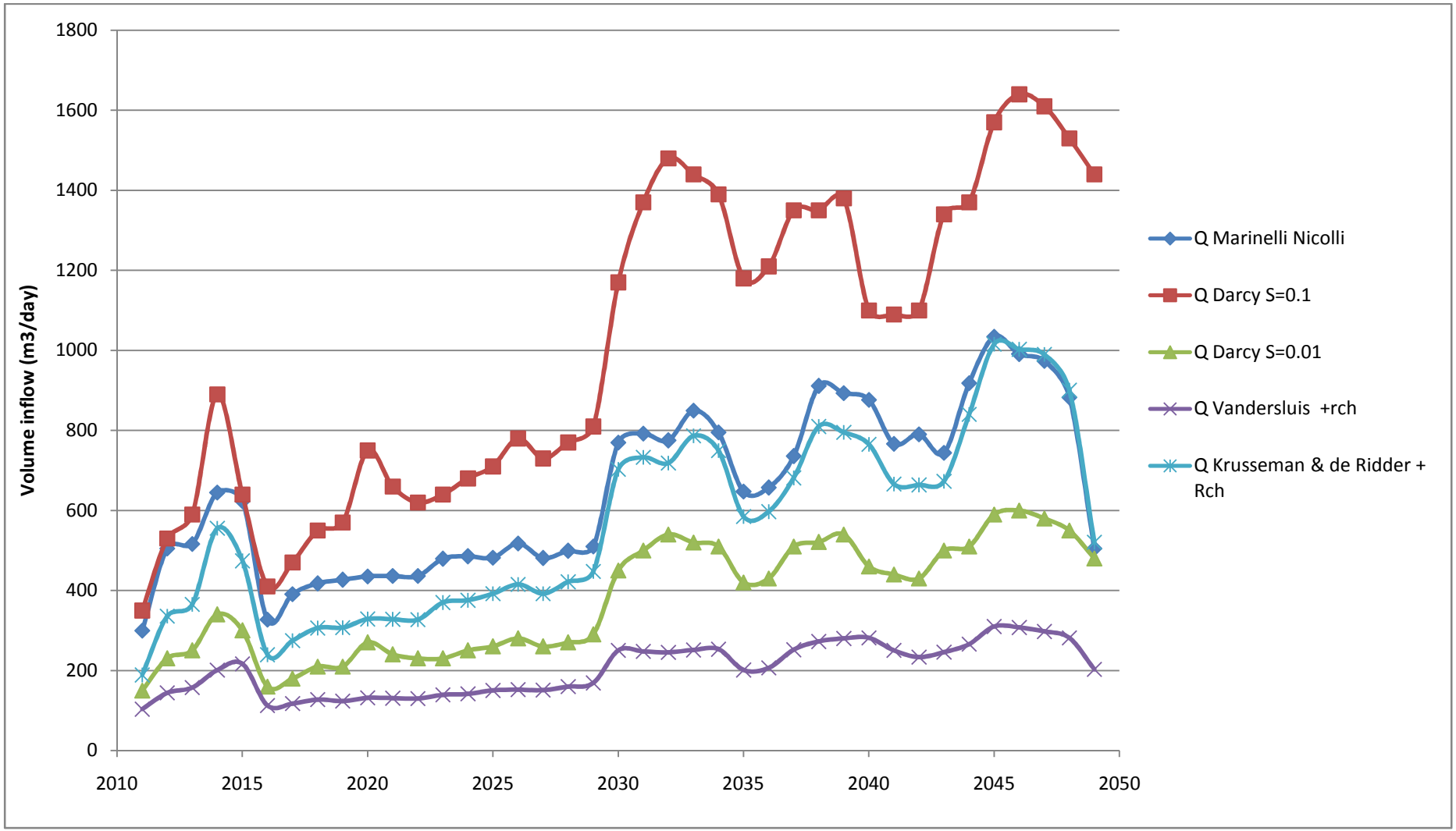

Figure 35: Comparing analytical inflow rates for the East Pit

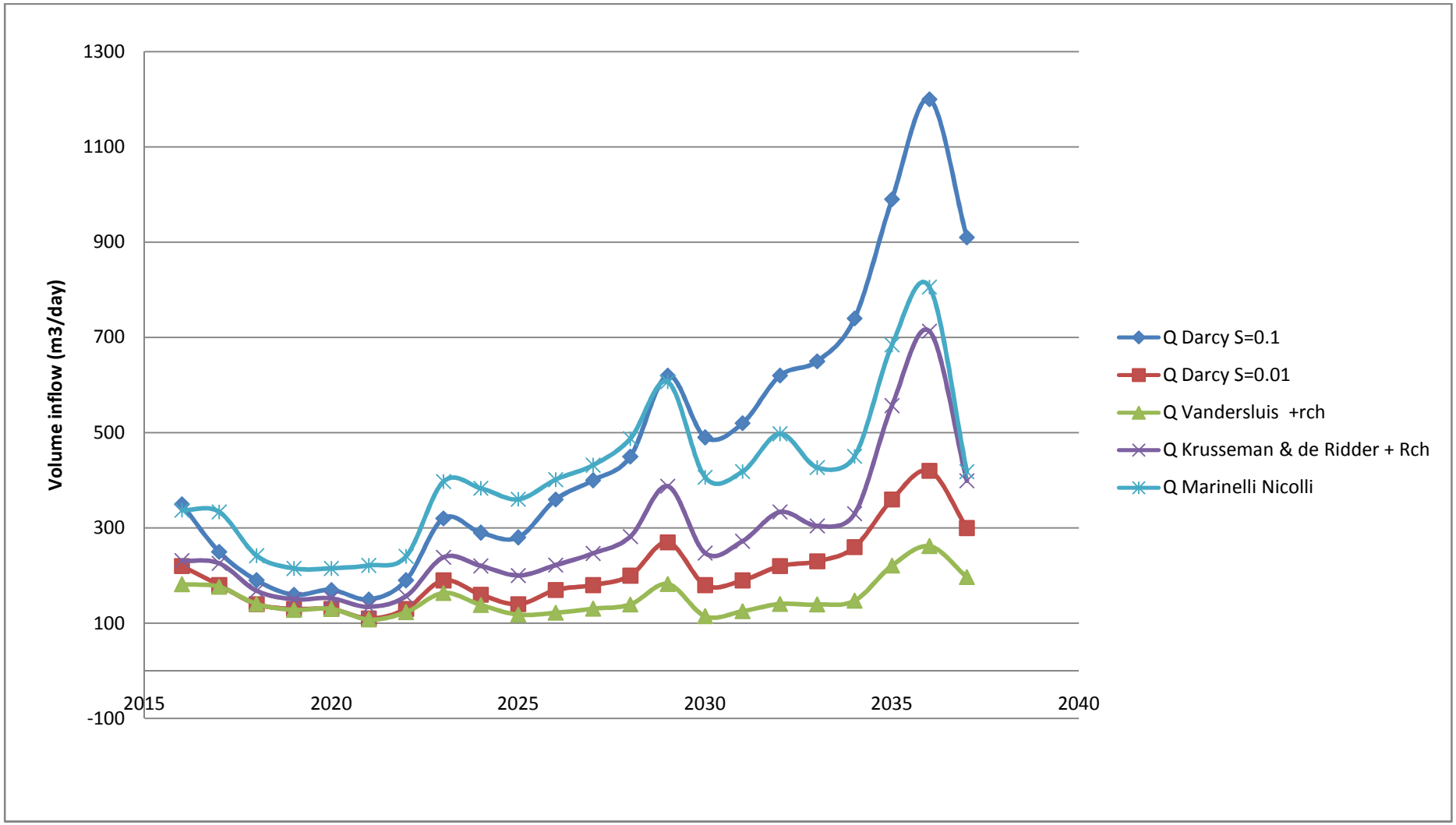

Figure 36: Comparing analytical inflow rates for the West Pit

7. Numerical modelling

7.1 Modelling software

The modelling software Processing Modflow for Windows was used in the modelling process. This software uses the finite difference method in its calculations. The finite difference method is a solution method that uses the Taylor series expansion to estimate the derivatives in the flow equation. Data input and programming changes to the model is easy but the model does require regular grids (Dennis I., 2008).

7.2 Model Construction and Calibration

The model size for the study area is 8.5km (East) by 11.5km (North). The cell size for the entire model is the same at 20 X 20 metres. The model consists of two layers. The upper layer represents the upper, weathered aquifer and is defined as a confined/unconfined aquifer type in the model with the transmissivity constant (Type 2). The second layer represents the fresh, secondary fractured rock aquifer and is defined in the model as a confined aquifer (Type 0). The thickness of the upper layer is 20 metres for the entire model area and the thickness of the second layer is 100 metres.

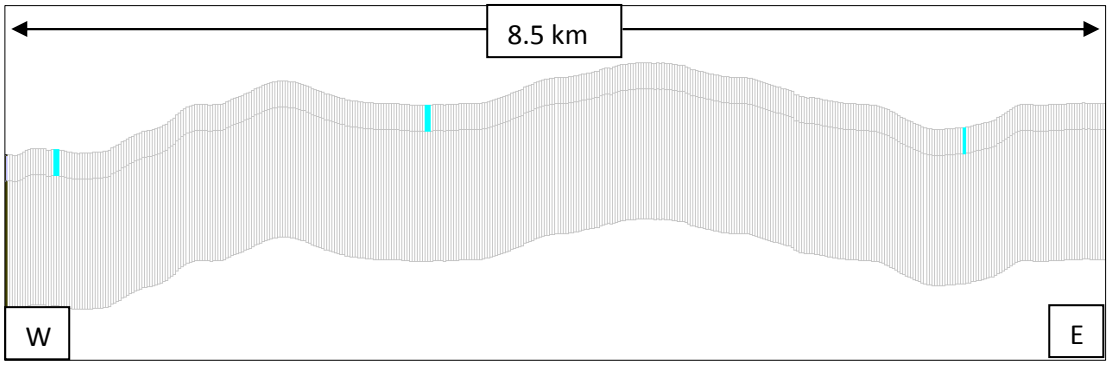

Figure 37: Cross sectional presentation of the numerical model extent.

7.2.1 Rivers and streams

River nodes were inserted where natural rivers and streams occur in the study area. The head of the rivers was placed 2 metres below the ground surface and the bottom of the river 3 metres below surface.

Two model scenarios were included for the process of determining groundwater inflow to the pits. Firstly a general head boundary was assigned to the edge of the model area. A general head boundary is a boundary where the flux is proportional to the difference in heads. A general head boundary can also be referred to as a Cauchy Boundary. The head at the general head boundary were assigned the same elevation than the steady state elevations. The second scenario does not include any general head boundaries. These two scenarios were included to determine what the effect of the general head boundary will be on the groundwater inflow to the pits.

A model grid which indicates the position of the river nodes and general head boundaries (as in Scenario 1) is presented in Figure 38. Also included on this figure are the positions of the interpreted dykes and faults as obtained from the mine.

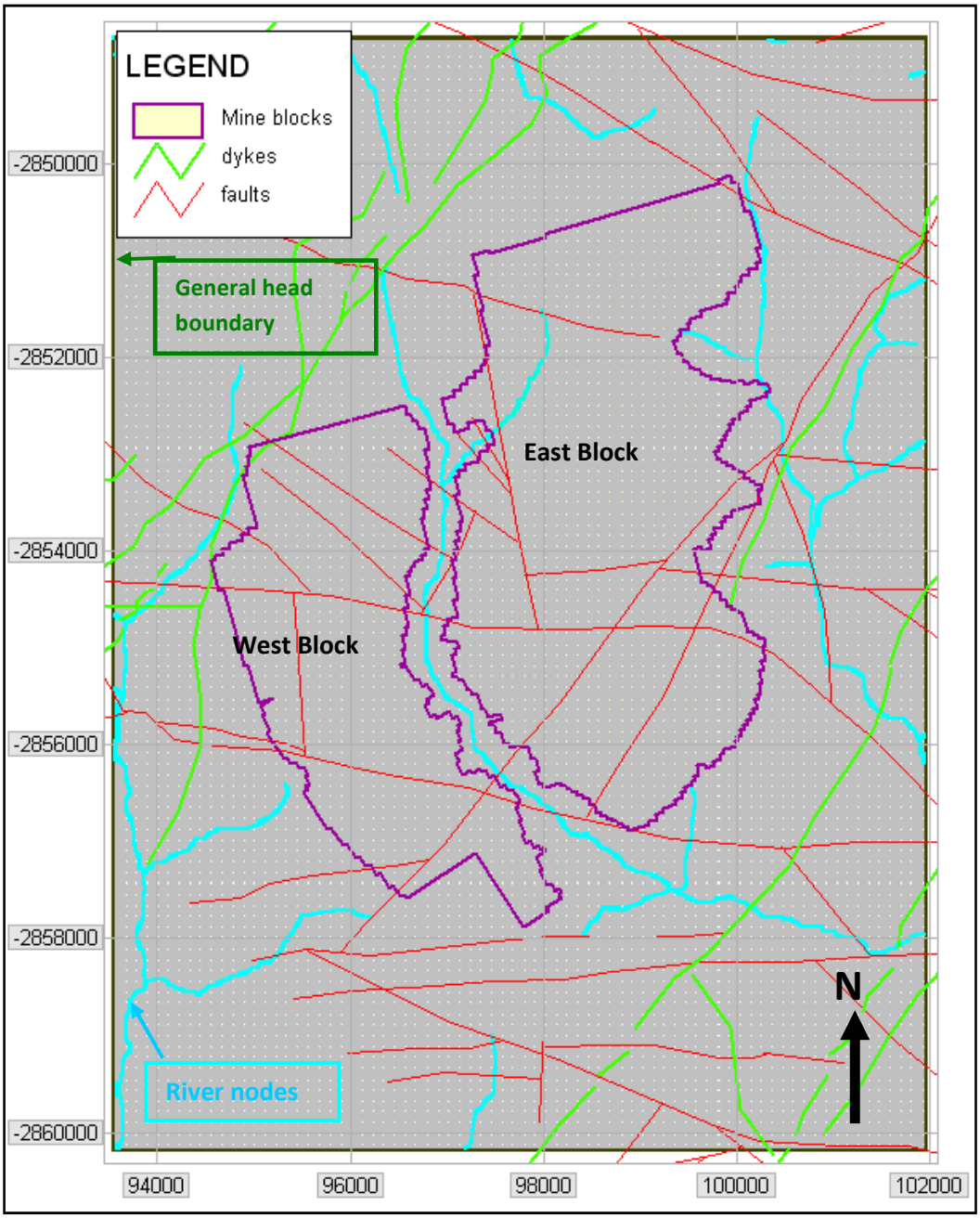

Figure 38: presentation of the model grid with river nodes and general head boundaries.

7.2.2 Recharge distribution

Different recharge rates have been applied to the model grid area. The distribution of the recharge is indicated in Figure 39. A recharge of 3% was assigned to the higher topographical regions in the model area. Normally in the higher lying areas the soil cover is thinned by erosion as the soil particles are transported from the higher areas to the lower regions via surface runoff, gravity and wind. More recharge can therefore reach the aquifer since less water is held back in the soil profile and less evaporation will occur before the water reaches the aquifer, (van Tonder and Kirchner, 1990).

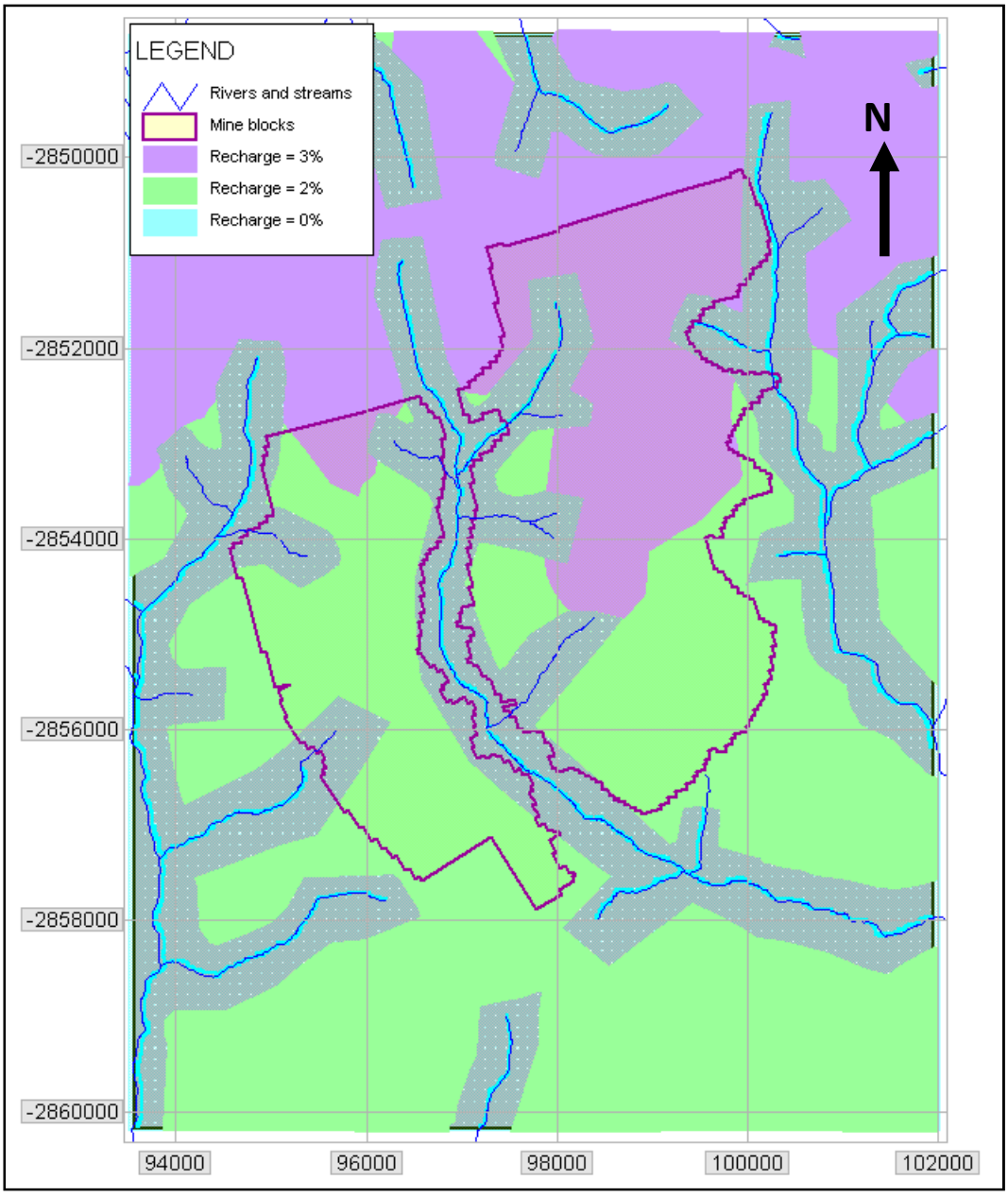

Figure 39: Recharge distribution over the study area

In the lower topographical regions recharge are usually less because of a thicker soil cover. The soil particles that were eroded from the higher regions accumulate in the lower areas increasing the soil cover depth. The natural catena formation processes also cause the clay content of the higher topography soils to reduce (better infiltration) and to accumulate in the valley bottom soils. A recharge of 2% was assigned to these lower regions of the model grid. (van Tonder and Kirchner, 1990)

At or near surface drainage areas such as streams and rivers no recharge was assigned. In these areas discharge rather than recharge will occur. A schematic representation of the soil profile thickness as well as the discharge areas have been indicated in Figure 40.

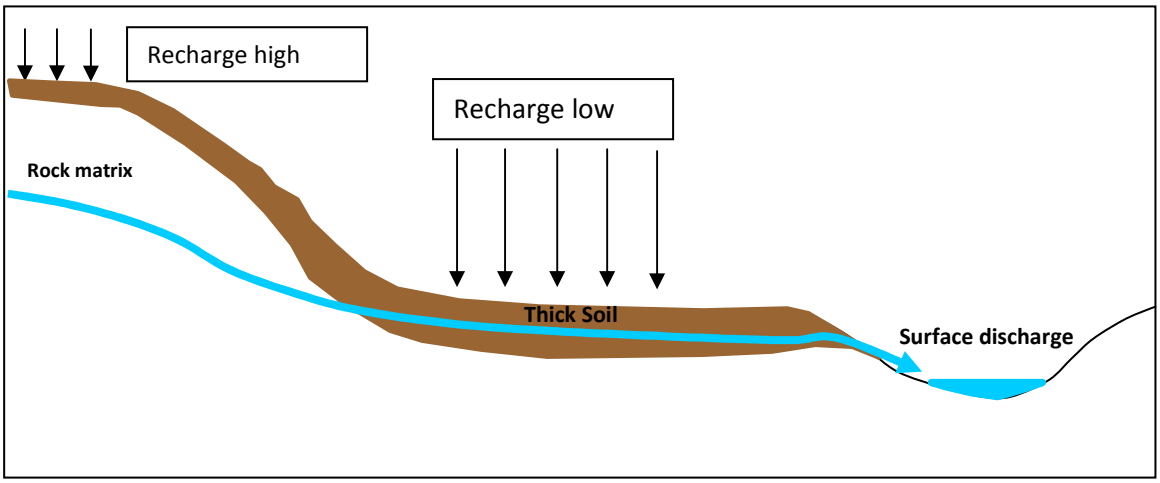

Figure 40: Schematic representation of soil profile thickness and discharge areas.

Model input parameters are changed during the calibration step to obtain results that mimics reality as closely as possible. The main parameters that can be varied to have an impact on the groundwater levels include the transmissivity and recharge rate.

Head observations that were obtained during the hydrocensus and from the NGDB and new monitoring boreholes, were used as input levels for steady state model calibration. The position and water level elevation for every applicable borehole was inserted.

The model was run in steady state during which period all parameters remain the same. After the model was run in steady state the scattered diagram function is used to compare the model calculated and observed (actual) water level elevations. The higher the correlation between the calculated and observed levels the better the model calibration. If the difference between an observed and calculated water level elevation is less than 10 meters the calibration is good.

The best calibration was obtained when the parameters were inserted as follow:

Table 9: Parameters used in the numerical groundwater model for best calibration

Parameter		Layer 1	Layer 2
Transmissivity (m^2/day)	Matrix	1.2	0.5
	Dykes	0.05	0.05
	Faults	10	10
Recharge (m/day)	High topography	0.000065 (3.6%)	-
	Lower topography	0.000042 (2.3%)	-
	Valley bottoms and rivers	0	-

At these parameter values the correlation between the calculated and observed water level elevations is 94%.

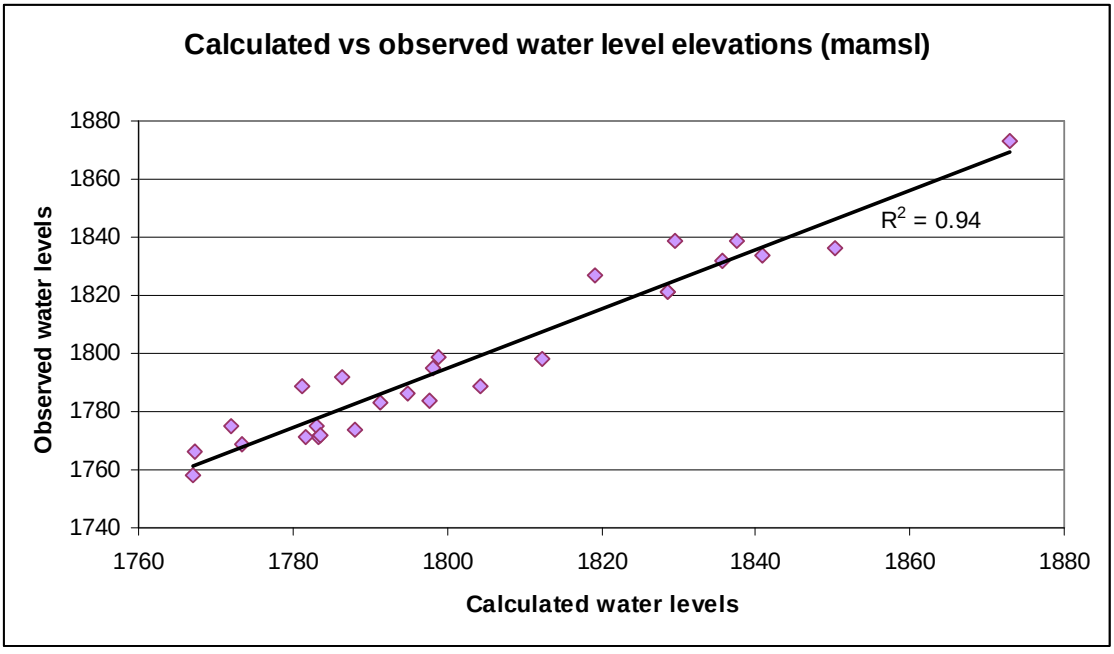

Figure 41: Correlation graph of calculated vs observed water levels.

Table 10: Boreholes used in the numerical model calibration with positions, water levels, observed and calculated water levels.

Borehole	X-coord	Y-coord	Surface elevation (mamsl)	Water level (mbs)	observed water level elevation (mamsl)	calculated water level elevations (mamsl)
G03	99369	-2851672	1839	3.4	1836	1850
ZK3	96877	-2854575	1797	2	1795	1798
VILG01	100267	-2850919	1835	0.5	1834	1841
COETZ01	100603	-2855020	1786	2.7	1783	1791
LB7	96334	-2856175	1799	7	1792	1786
Z5	99435	-2852874	1840	1.4	1839	1837
Z8	99612	-2853427	1822	0.7	1821	1829
EBH01	99940	-2854327	1805	7.3	1798	1812
EBH02	98692	-2856672	1787	13	1774	1788
EBH03	97581	-2856161	1774	2.7	1771	1783
EBH08	96660	-2854594	1787	3.1	1784	1798
GP01	99802	-2850160	1881	7.5	1873	1873
GP02	100452	-2853109	1796	6.7	1789	1804
GP04	100494	-2855021	1793	7.3	1786	1795
GP05	98656	-2854725	1830	3.4	1827	1819
GP08	96591	-2857316	1783	8.2	1775	1783
GP09	95380	-2855815	1790	1.2	1789	1781
GP11	94338	-2854716	1771	4.6	1766	1767
ZK2	98240	-2853410	1840	0.8	1839	1830
JOUG01	100665	-2857351	1774	16	1758	1767
KOTZE01	100805	-2853847	1779	8.3	1771	1782
Z11	101250	-2855718	1779	10	1769	1774
Z4	99529	-2852869	1842	9.5	1832	1836
Z7	99609	-2853432	1831	9.8	1821	1829
ZK7	95951	-2854664	1804	4.7	1799	1799
ZOEKOP04	100239	-2858815	1778	3.4	1775	1772
GP06	98715	-2856877	1779	7.4	1772	1784

After the steady state levels were obtained they were used as initial hydraulic heads for the transient model. The transient model exists of different stress periods which can vary in time length. Parameters such as recharge and the river package can be changed during the different time steps but transmissivity and storativity remains unchanged. The regional model for the study region consisted of 39 stress periods.

Table 11: Breakdown of the stress periods in the numerical groundwater model.

Stress Period	Conditions
1 – 5	Opencast mining at the East block begins.
6 – 27	Mining of the West block begins at the beginning of stress period 6. Mining of the East block continuous. Mining in the West Block ceases at the end of stress period 27.
28-39	Mining at the East block ceases at the end of stress period 39 according to the mine schedule.

Each stress period represents one mining year and mining at the study area will continue for 39 years. The opencast pits were simulated by making use of drain nodes. Drain nodes removes water from the model and is therefore representative of dewatering in the opencast pits. The elevation of the drains will be the same as the elevation of the pit floor. Drain nodes were inserted for every year to simulate the progressive mining of the pits year by year.

7.3 Flow model results

A sensitivity analysis on the effect of recharge on the flow rates into the opencast pits was done. The range of the recharge for the sensitivity analysis is 10, 12.5 and 20%.

The flow rates were rounded to the nearest 10 unit. The graphs indicate that at a recharge rate of 10 and 12.5% the recharge volume to the pits are very similar. At a recharge rate of 20% the inflow to the East block is slightly higher with a maximum difference of 100 m^3/day. The recharge volume to the West block is similar with a maximum difference in volume of 100 m^3/day.

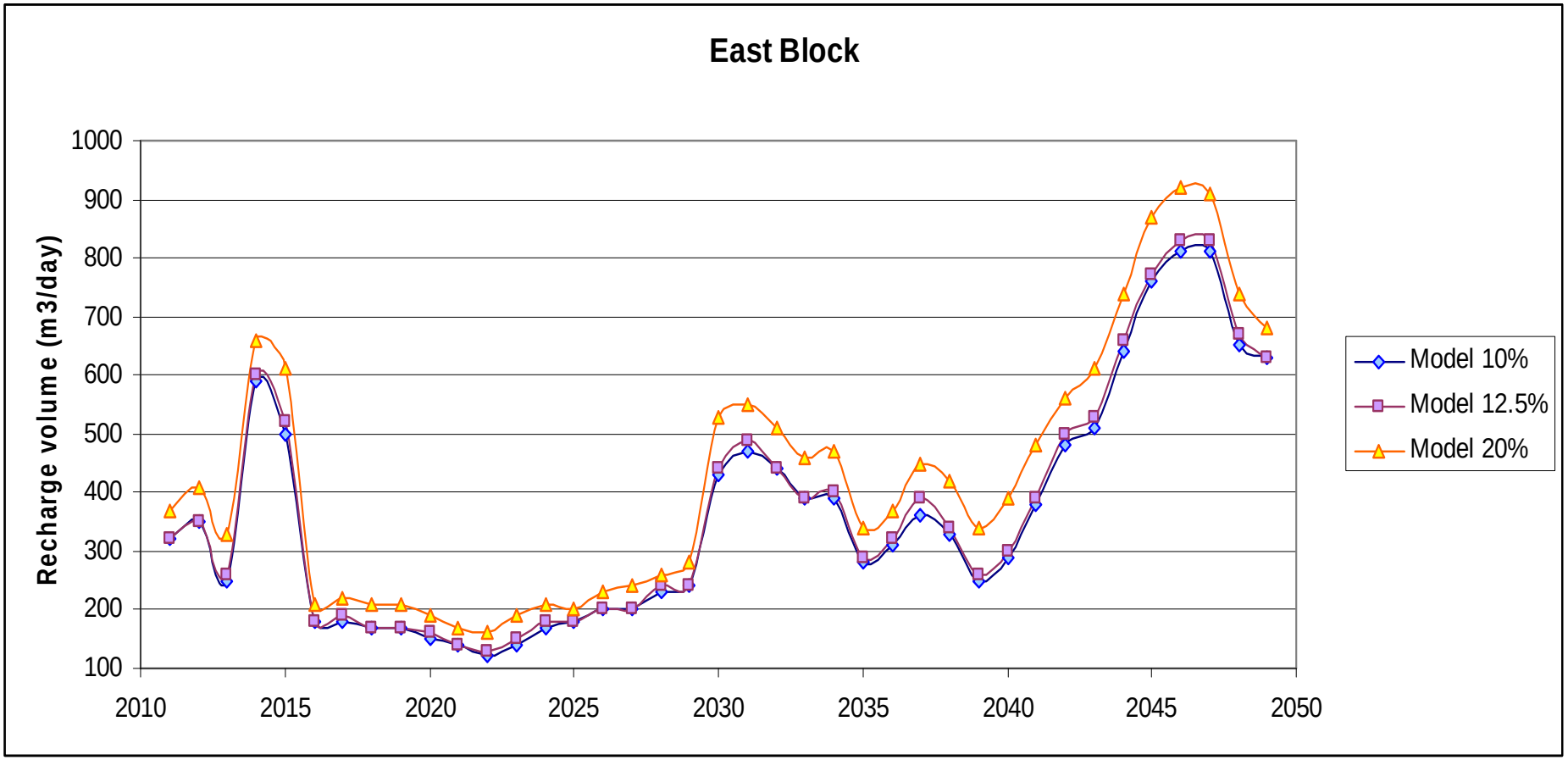

Figure 42: Sensitivity analysis results for recharge in terms of groundwater inflow to the East Block.

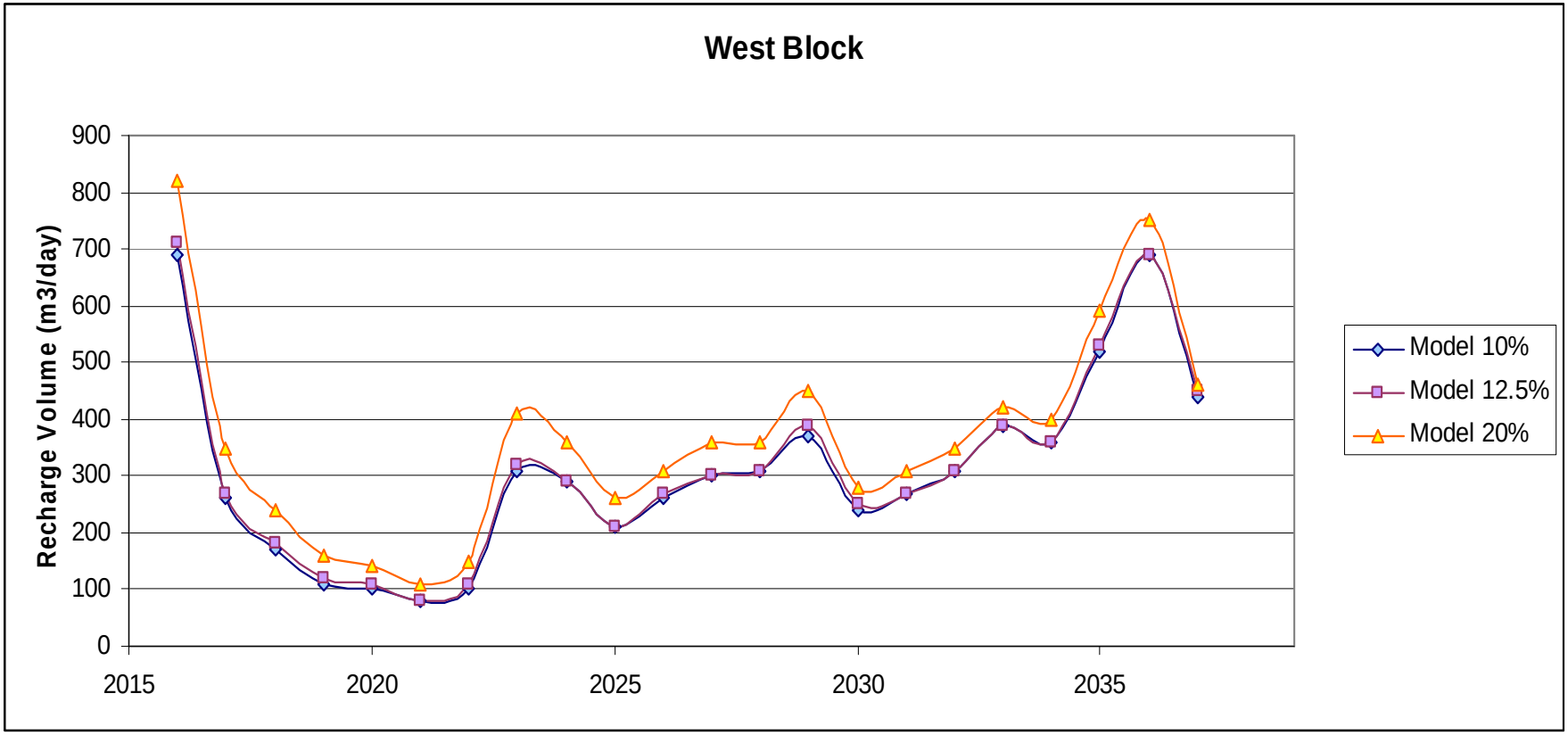

Figure 43: Sensitivity analysis results for recharge in terms of groundwater inflow to the West Block.

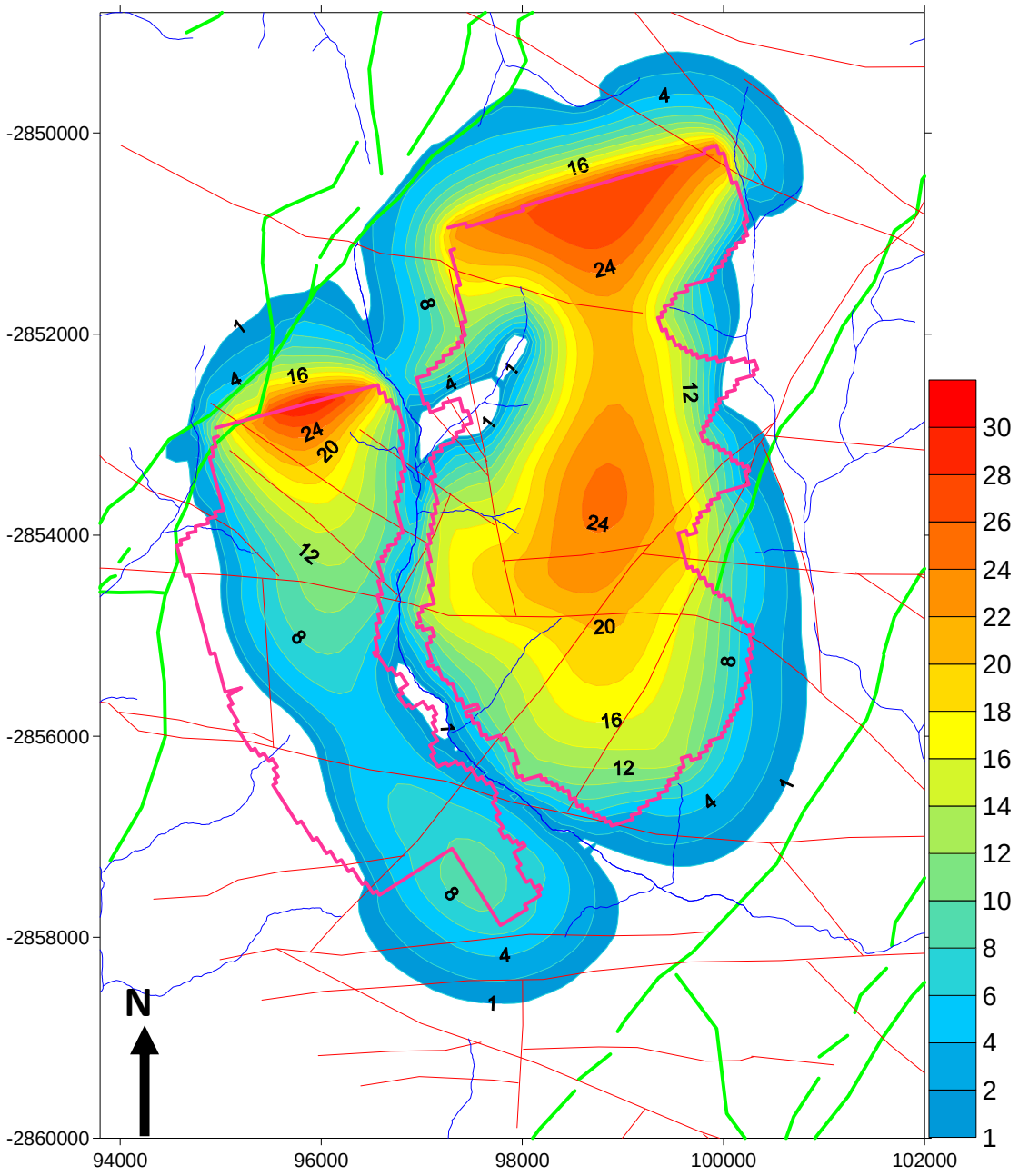

Figure 44: Maximum extent of the cone of depression at mine closure.

The results from the two scenarios where general heads on the edge of the model was included and excluded to determine what effect the boundary will have on the inflow to the pits is presented Figures 45 and 46.

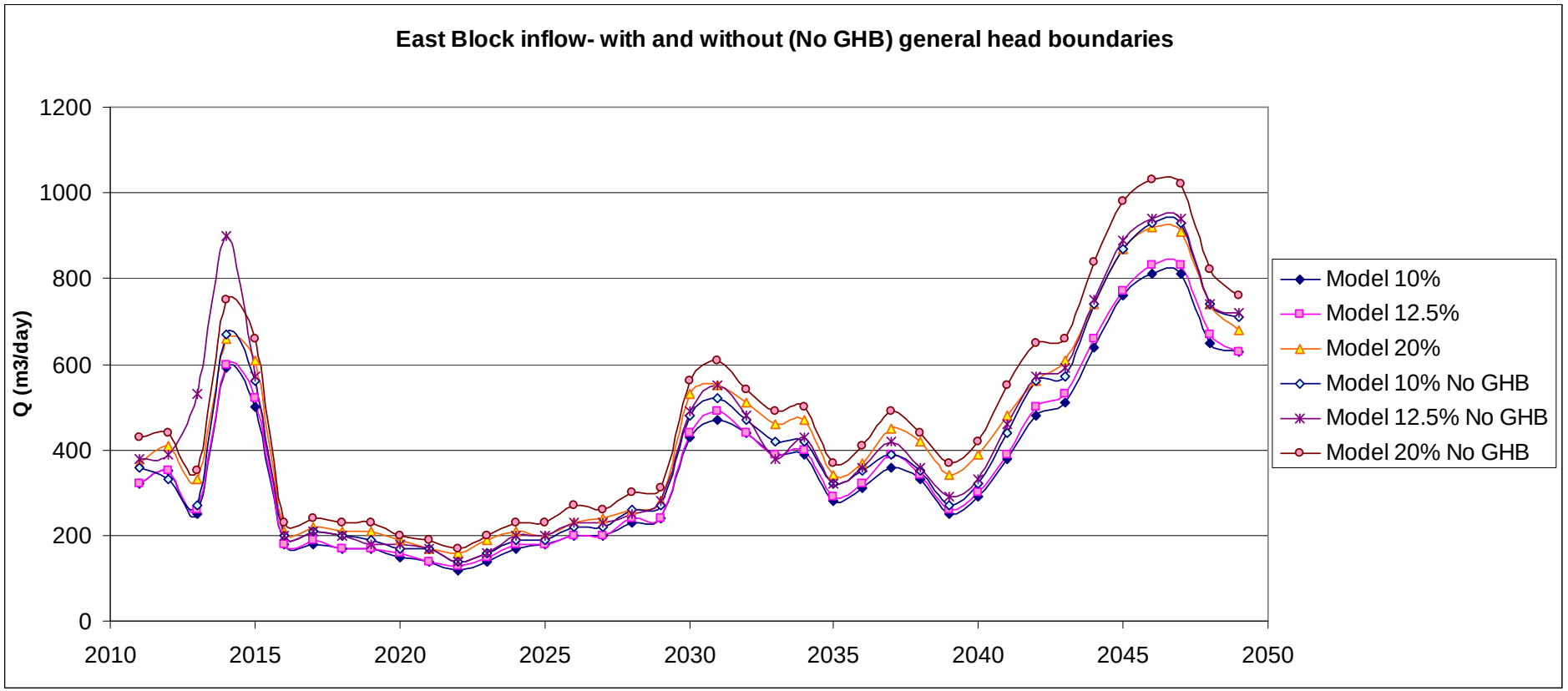

Figure 45: Inflow to the East pit as determined with and without general head boundaries on the edge of the model.

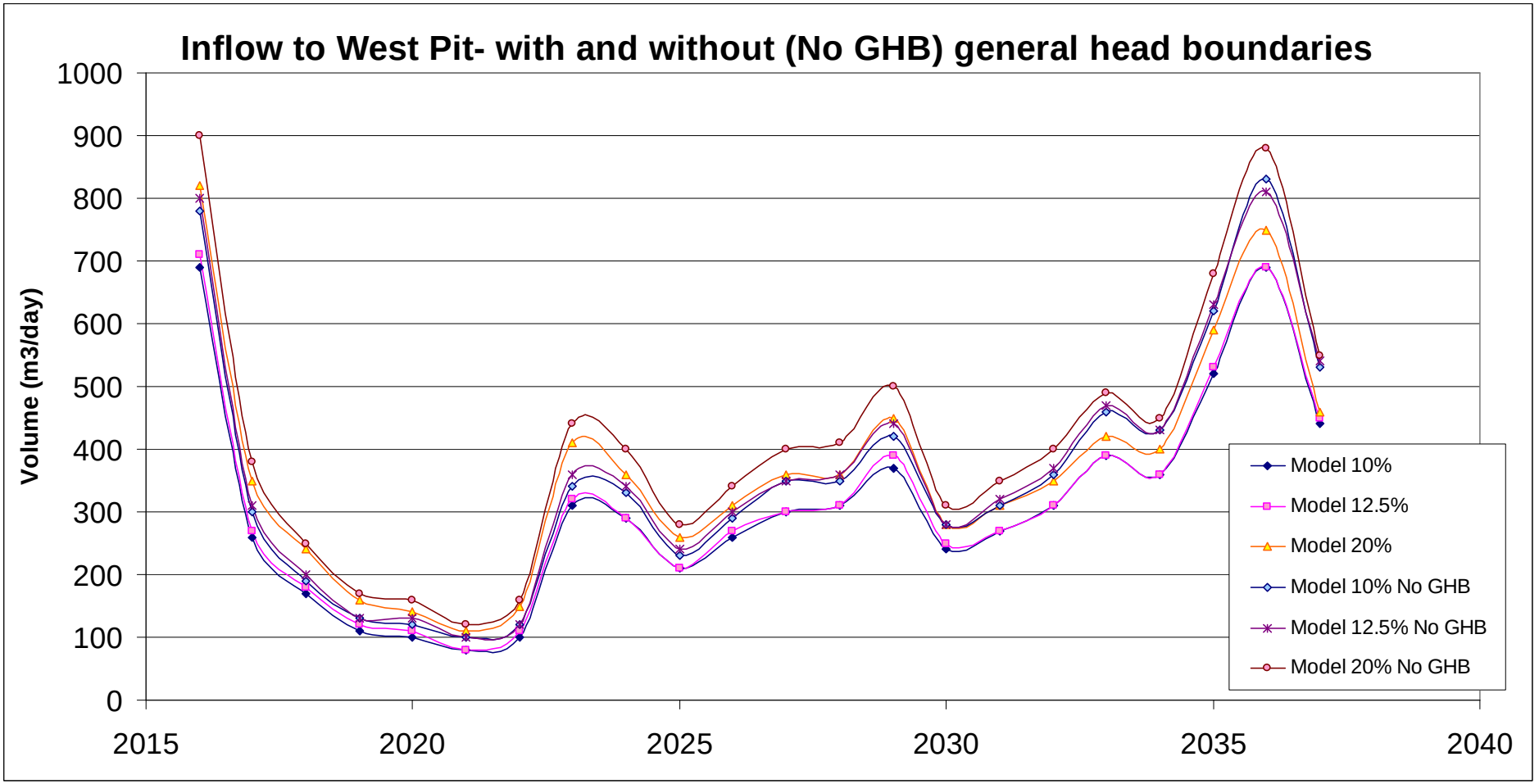

Figure 46: Inflow to the West pit as determined with and without general head boundaries on the edge of the model.

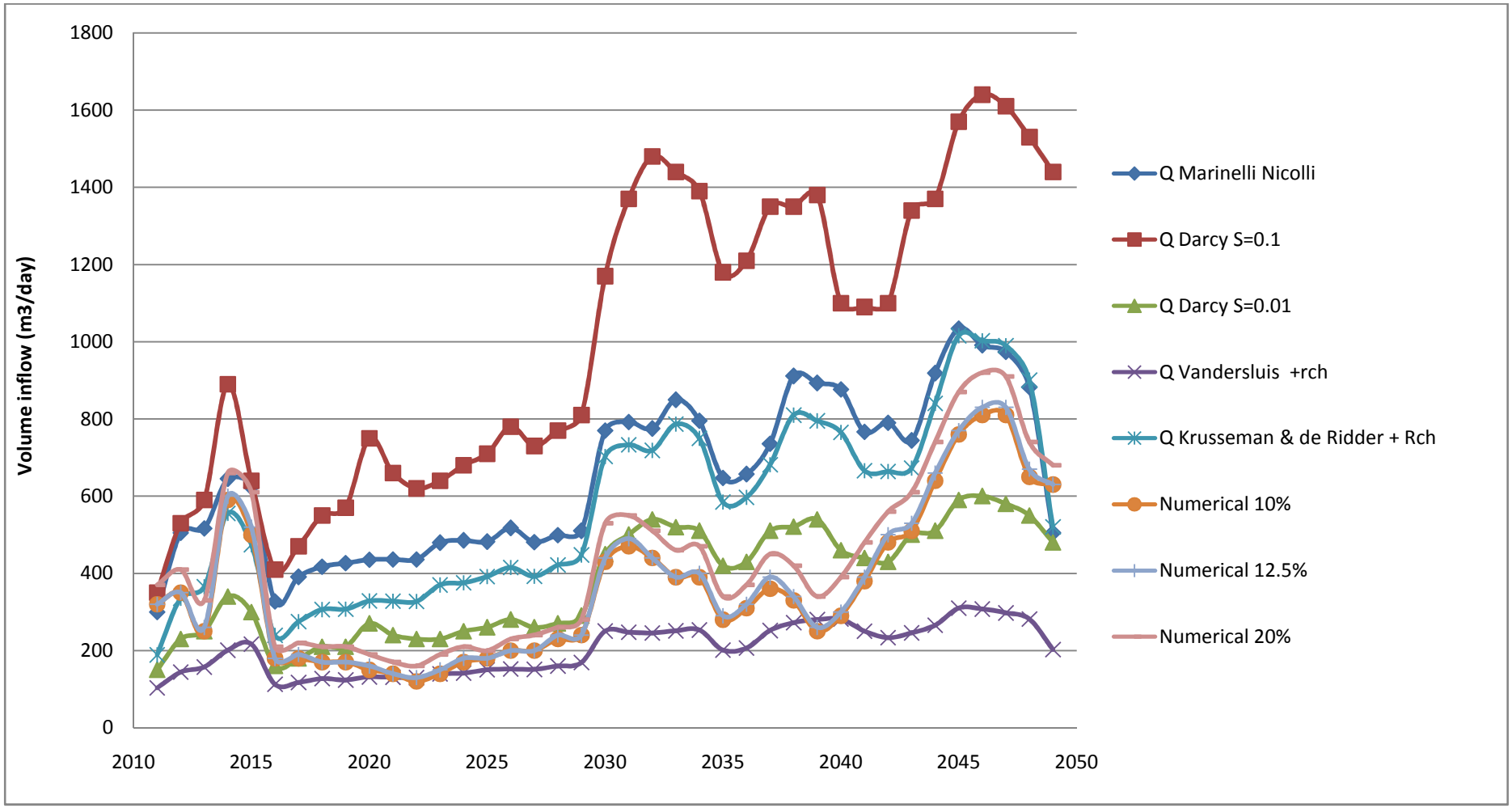

Figure 47: Numerical vs. analytical inflow rates for the East Block

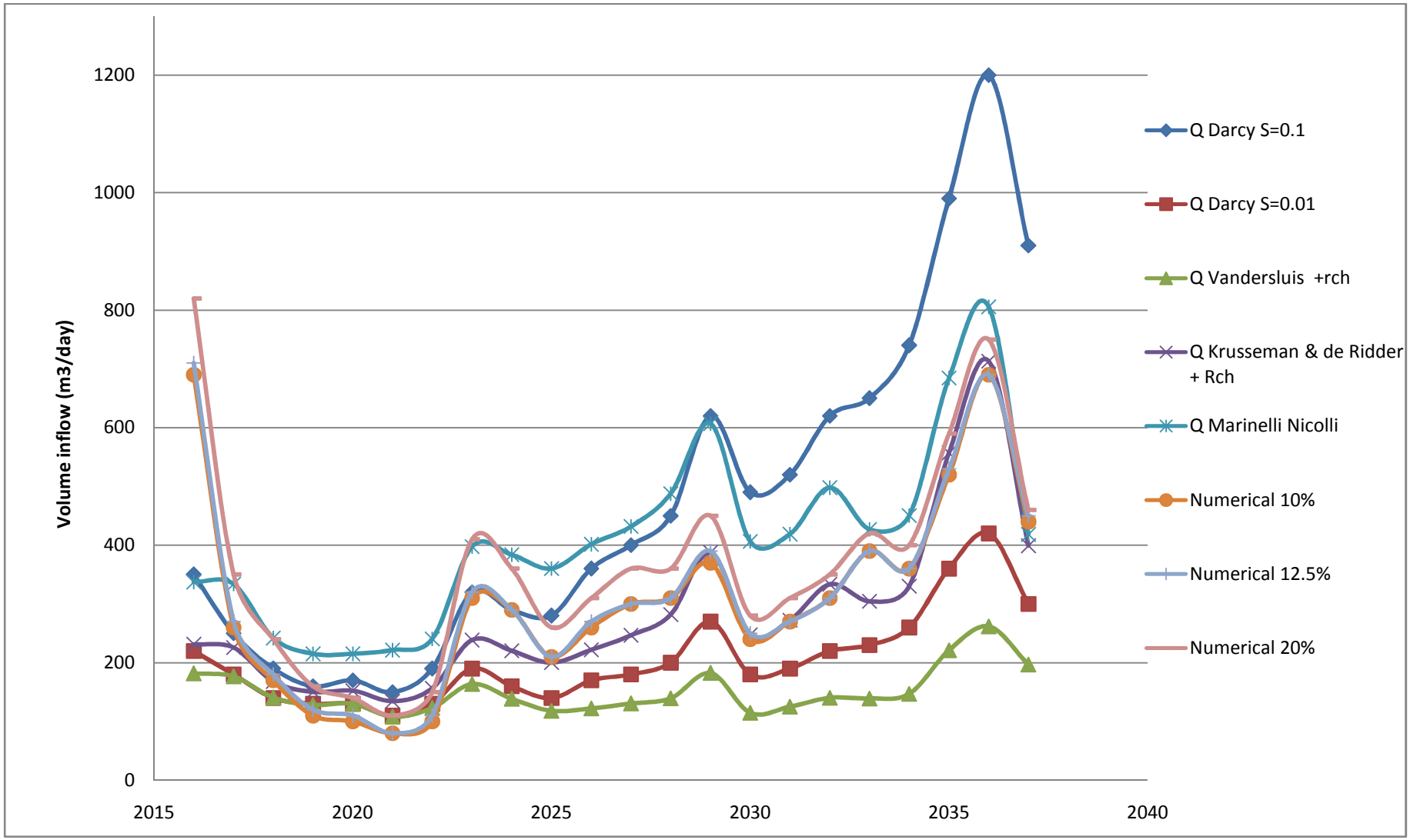

Figure 48: Numerical vs. analytical inflow rates for the West Block

To determine the volume of groundwater that is originating from recharge in the numerical model, the model was run for four different recharge rates: 20% of annual precipitation, 12.5%, 10% and 0%. With this approach the difference of inflow to the pits between the 0% recharge and the 10, 12.5 or 20% can be determined and this difference in volume is then the recharge volume.

Table 12: Recharge volume contributing to the total groundwater inflow to the East Block according to the numerical model.

	Total inflow				Recharge volume contributing to groundwater inflow		
	Numerical 0%	Numerical 10%	Numerical 12.5%	Numerical 20%	10% RCH	12.5 % RCH	20% RCH
2011	260	320	320	370	60	60	110
2012	290	350	350	410	60	60	120
2013	190	250	260	330	60	70	140
2014	530	590	600	660	60	70	130
2015	420	500	520	610	80	100	190
2016	140	180	180	210	40	40	70
2017	160	180	190	220	20	30	60
2018	140	170	170	210	30	30	70
2019	110	170	170	210	60	60	100
2020	130	150	160	190	20	30	60
2021	120	140	140	170	20	20	50
2022	100	120	130	160	20	30	60
2023	110	140	150	190	30	40	80
2024	130	170	180	210	40	50	80
2025	140	180	180	200	40	40	60
2026	160	200	200	230	40	40	70
2027	170	200	200	240	30	30	70
2028	200	230	240	260	30	40	60
2029	200	240	240	280	40	40	80
2030	360	430	440	530	70	80	170
2031	410	470	490	550	60	80	140
2032	370	440	440	510	70	70	140
2033	330	390	390	460	60	60	130
2034	310	390	400	470	80	90	160
2035	230	280	290	340	50	60	110
2036	260	310	320	370	50	60	110
2037	300	360	390	450	60	90	150
2038	260	330	340	420	70	80	160
2039	180	250	260	340	70	80	160
2040	220	290	300	390	70	80	170
2041	300	380	390	480	80	90	180
2042	410	480	500	560	70	90	150
2043	440	510	530	610	70	90	170
2044	560	640	660	740	80	100	180

2045	680	760	770	870	80	90	190
2046	720	810	830	920	90	110	200
2047	730	810	830	910	80	100	180
2048	600	650	670	740	50	70	140
2049	580	630	630	680	50	50	100

Table 13: Recharge volume contributing to the total groundwater inflow to the West Block according to the numerical model.

	Total inflow				Recharge volume contributing to groundwater inflow		
	Numerical 0%	Numerical 10%	Numerical 12.5%	Numerical 20%	10% RCH	12.5% RCH	20% RCH
2016	580	690	710	820	110	130	240
2017	190	260	270	350	70	80	160
2018	130	170	180	240	40	50	110
2019	70	110	120	160	40	50	90
2020	70	100	110	140	30	40	70
2021	60	80	80	110	20	20	50
2022	80	100	110	150	20	30	70
2023	230	310	320	410	80	90	180
2024	240	290	290	360	50	50	120
2025	160	210	210	260	50	50	100
2026	220	260	270	310	40	50	90
2027	250	300	300	360	50	50	110
2028	260	310	310	360	50	50	100
2029	310	370	390	450	60	80	140
2030	210	240	250	280	30	40	70
2031	240	270	270	310	30	30	70
2032	280	310	310	350	30	30	70
2033	350	390	390	420	40	40	70
2034	330	360	360	400	30	30	70
2035	480	520	530	590	40	50	110
2036	630	690	690	750	60	60	120
2037	420	440	450	460	20	30	40

8.1 Recharge: numerical vs analytical

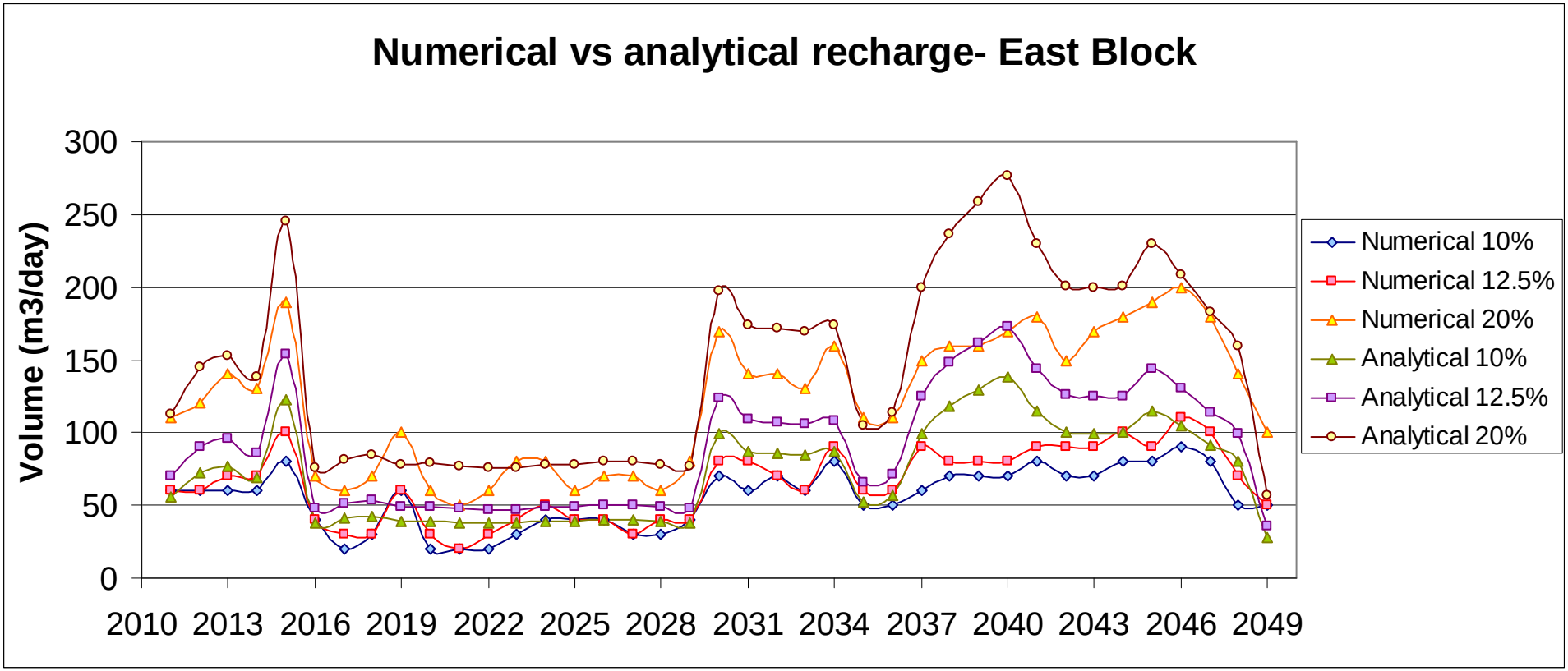

Figure 49: Numerical vs analytical recharge at the East Block.

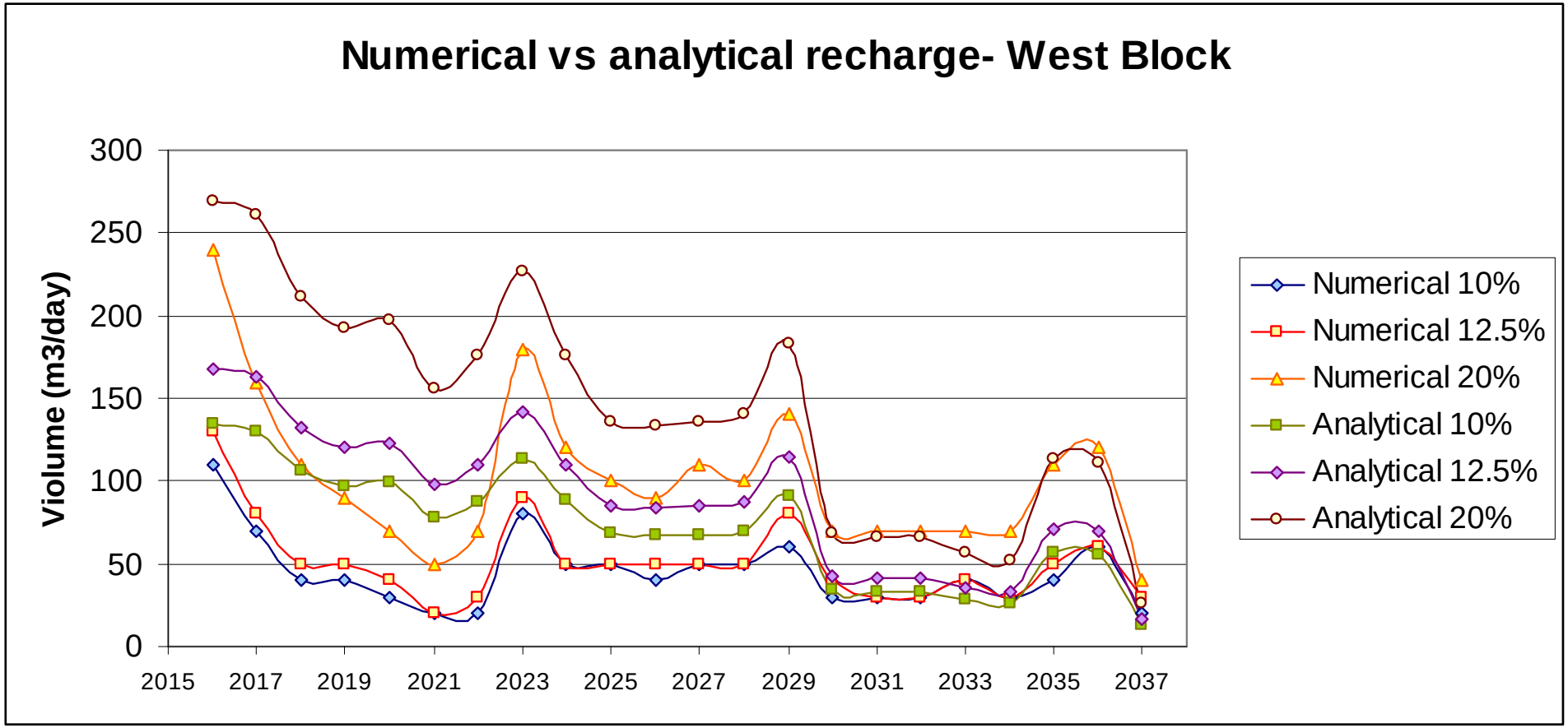

Figure 50:Numerical vs analytical recharge at the West Block.

8.2 Correlation between analytical and numerical approaches for groundwater inflow

The groundwater inflow to the mining strips as determined by the various analytical approaches and the numerical approach will be compared by plotting the inflow on a correlation graph. Note that the numerical inflow at 12.5% recharge will be used for correlation purposes.

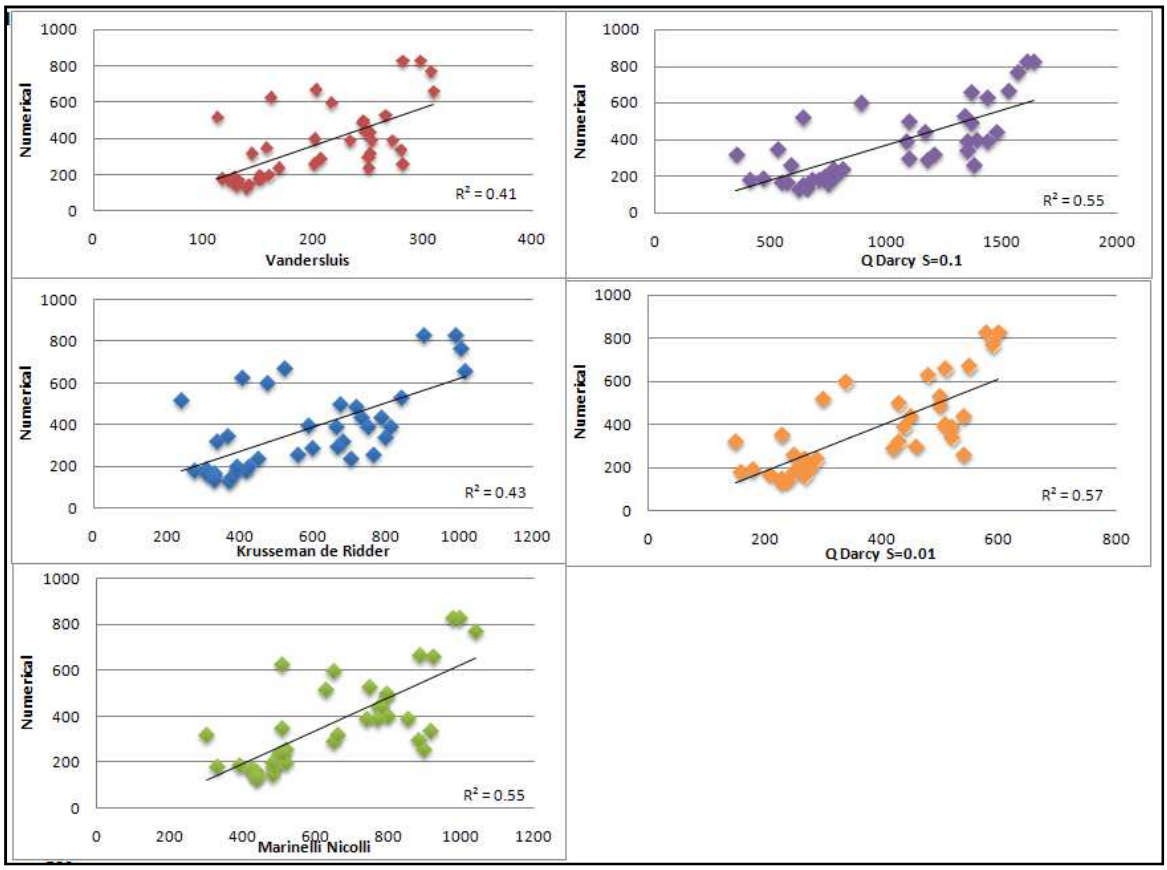

Figure 51: Correlation graphs for the analytical vs numerical approaches for inflow determination at the East Block

Table 14: Correlation between the numerical groundwater inflows and the different analytical inflows for the East Block.

Analytical Model	Correlation Percentage (%)
Krusseman& De Ridder	43
Marinelli & Nicolli	55
Q Darcy S=0.1	55
Q Darcy S=0.01	57
Vandersluis *et al*.	41

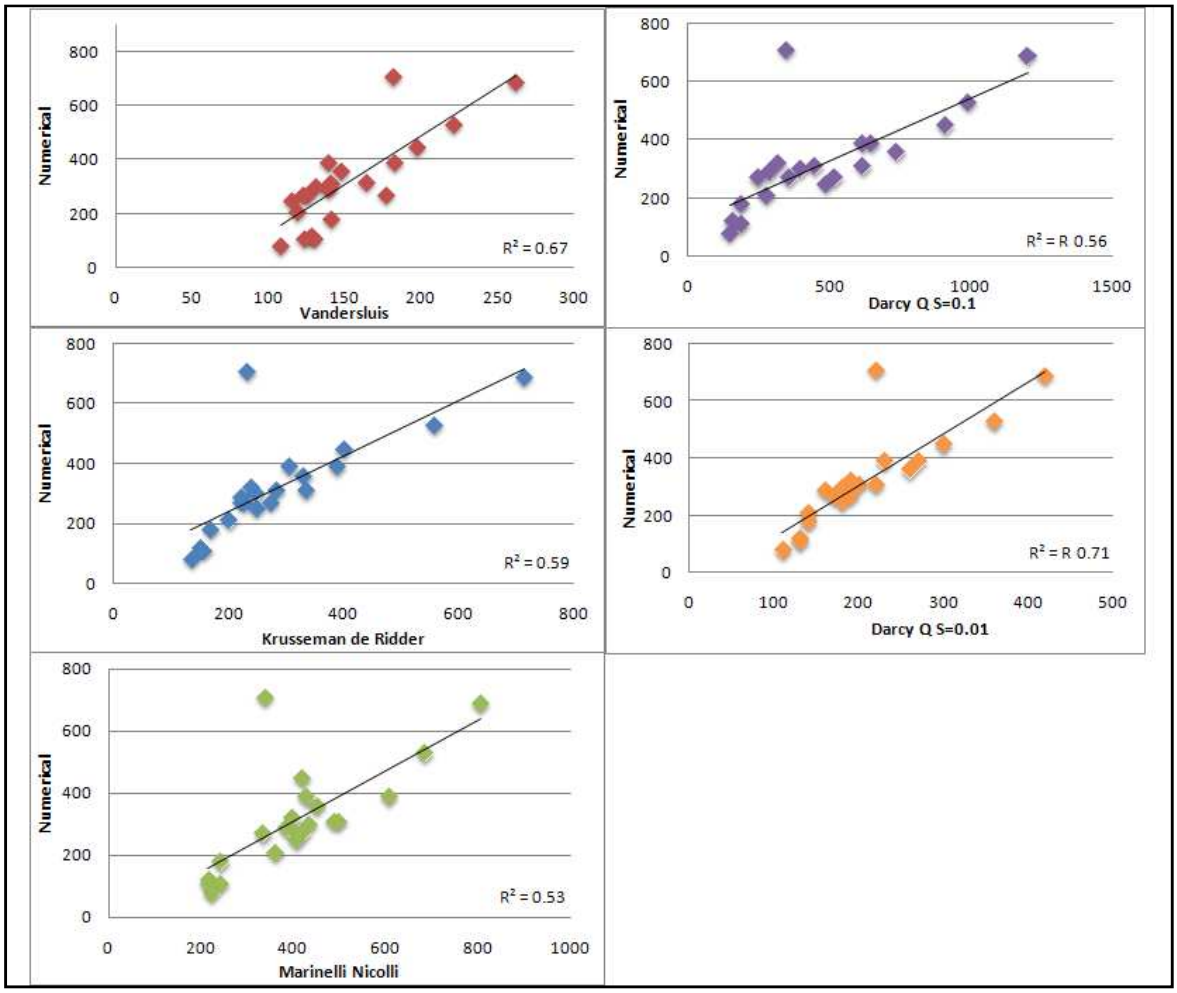

Figure 52: Correlation graphs for the analytical vs numerical approaches for inflow determination at the West Block

Table 15: Correlation between the numerical groundwater inflows and the different analytical inflows for the West Block.

Analytical Model	Correlation Percentage (%)
Marinelli & Nicolli	53
Krusseman& De Ridder	59
Q Darcy S=0.1	56
Q Darcy S=0.01	71
Vandersluis *et al*.	67

Table 16: Total water make at the end of mining according to each analytical and numerical approach (m3)

Method	East	West
Q Vandersluis *et al*. +rch	2882000	1215000
Q Krusseman & De Ridder + Rch	8045000	2253000
Q Marinelli & Nicolli	9258000	3279000
Q Darcy S=0.1	14330000	3760000
Q Darcy S=0.01	5362000	1646000
Numerical 10%	5143000	2475000
Numerical 12.5%	5274000	2526000
Numerical 20%	6096000	2935000

9. Discussion

The results of the numerical and analytical estimates will be discussed in this part of the thesis.

In the numerical modelling approach the inflows to the opencast pits were determined. To determine the impact of recharge on the groundwater inflow to the pits, a sensitivity analysis for recharge was performed. Recharge percentages of 10, 12.5 and 20% was applied to the active mining strips and the inflows obtained from these recharge values were compared for the East Block and West Block.

The following observations can be made for inflow to the East Block as determined by the numerical model:

- The groundwater inflow in 2011 varies between 300 and 400 m^3/day after which it decreases slightly in 2013.
- In 2014 and 2015 the inflows increase significantly to volumes of more than 500 m^3day.
- In 2016 the inflows decrease significantly and remain below 300 m^3/day up to 2029.
- An increase in inflow is again observed in 2030.
- The most significant increase in groundwater inflow to the mining pits occurs in 2039 to 2047 and 2046/2047.
- In 2046 and 2047 the inflow volume is estimated to be more than 800 m^3/day.
- After 2047 the inflow rates decrease again to just over 600 m^3/day.
- The groundwater inflows to the pits are therefore very dependent on the pit radius and the depth of the saturated zone.
- With increasing drawdown depth an increase in groundwater flow gradient is observed.

The following observations can be made for inflow to the West Block as determined by the numerical model:

- Numerically simulated groundwater inflow to the West Block starts off very high in 2016 with inflow of approximately 700 m^3/day.
- The inflow decreases to ± 300 m^3/day in 2017 and continues to decrease up to 2021 when the inflow is expected to be ± 100 m^3/day.
- From 2023 to 2034 the inflow volume to the mining strips varies between 200 and 400 m^3/day.
- The groundwater inflow increases again in 2036 to approximately 700 m^3/day.
- In 2037 the inflow to the last mining strip is expected to be approximately 450 m^3/day.

In the analytical modelling part of the thesis, four different approaches were used to determine the groundwater inflow to the mining strips. These approaches include the Vandersluis *et al*. (1995), the Krusseman and De Ridder (1979), the Marinelli and Nicolli (2000) and the Darcy + recharge (S=0.1) approach. In all four these approaches the radius of influence (R) of the mine dewatering was determined by the Cooper-Jacob method where the

$$R = 1.5 \sqrt{T * t/S}$$

$$= 100 \text{ meters}$$

Another approach was also used to determine the inflow with Darcy. The storativity (S) was lessened to 0.01 after which the radius of influence was determined once again. At this storativity value the radius of influence increase to 314 meters. This radius of influence was only used with the Darcy method and acts as a sensitivity analysis to determine the impact of the storativity value on the groundwater inflow volume.

The following observations can be made for the analytical determined inflows to the East Block:

- The Vandersluis *et al*. method + recharge (12.5%)
    - The inflows as determined by the Vandersluis *et al*. approach vary between 103 and 310 m^3/day.
    - As the drawdown or size of the mining strips increases the inflows also increases.
    - Over the mining period a increasing inflow trend can be observed, which is a result of increase of size of the strips and/or the increase in mining depth.
- Krusseman and De Ridder + recharge (12.5%) method
    - The groundwater inflows fluctuate over the LOM.
    - The inflows in 2016 increases from 189 m^3/day to a maximum of 1016 m^3/day in 2045.
    - Drawdown thickness and strip size play a significant role in the groundwater inflow.
- Marinelli and Nicolli method
    - The groundwater inflow from the pit wall is significantly less than from the pit floor.
    - It is clear that the groundwater inflow from the pit contributes more to the total water make. This is also the case in the case study presented by Marinelli and Nicolli.
    - The total groundwater inflow to the pit increases from 330 m^3/day in 2011 to 1039 m^3/day in 2045.
    - Between 2016 and 2049 the groundwater inflow increases uniformly as this is the period when the West pit is also active and the strip size of the East Block remain relatively constant over this period.

- Darcy + recharge method
  - Q was determined by using two approaches for this method.
  - Firstly the radius of influence was determined by using a storativity value of 0.1. The Q was then determined by using the radius of influence of 100m.
    - This approach is referred to in the graphs as Q Darcy S=0.1.
    - The groundwater inflow volumes display very similar trends than the inflow determined with the other three analytical methods.
    - The groundwater inflow with this method increases from 350 m^3/day in 2016 to 1 640 m^3/day in 2046.
  - Secondly the radius of influence was determined by using a storativity value of 0.01.
    - This approach is referred to in the graphs as Q Darcy S=0.01.
    - Once again the groundwater inflow volumes display very similar trends than the inflow determined with the other three analytical methods.
    - The inflows as determined by this approach are much lower than determined by the first approach as discussed above (Q Darcy S=0.1).
    - The difference in groundwater inflows between these two approaches varies from 200 to 1040 m^3/day.
    - The groundwater inflow with this method increases from 150 m^3/day in 2016 to 600 m^3/day in 2046.

The following observations can be made for the analytical determined inflows to the West Block:

- The Vandersluis *et al*. method
  - The groundwater inflow as determined by this method varies over the monitoring period, but display similar trends than the other four analytical methods.
  - Groundwater inflow varies from a minimum of 108 m^3/day in 2021 to 262 m^3/day in 2036.
  - The inflows of this method compared with the Q Darcy S=0.01 is very close from 2016 to 2025 after which the differences increase.
- Krusseman and De Ridder method
  - An overall increasing trend in the groundwater inflow is observed.
  - The inflows in 2021 increases from 135 m^3/day to a maximum of 713 m^3/day in 2036.
- Marinelli and Nicolli method
  - The groundwater inflow from the pit wall is significantly less than from the pit floor.
  - The total groundwater inflow to the pit increases from 215 m^3/day in 2020 to 806 m^3/day in 2036.
  - A sharp increase in groundwater inflow is observed between 2034 and 2036.
- Darcy approach
  - The first approach, referred to as Q Darcy S=0.1, displays similar trends than the inflow determined with the other four analytical methods, but the inflows are higher from 2030 onwards.

        - The groundwater inflow with this method increases from 150 m^3/day in 2021 to 1 200 m^3/day in 2036.

- The second approach, referred to as Q Darcy S=0.01, once again has very similar trends than the inflow determined with the other four analytical methods.
    - The inflows as determined by this approach are much lower than determined by the first approach as discussed above (Q Darcy S=0.1).
    - The difference in groundwater inflows between these two approaches varies from 30 to 780 m^3/day.
    - The groundwater inflow with this method increases from 110 m^3/day in 2021 to 420 m^3/day in 2036.

The following observations can be made in terms of the comparison between analytical approaches:

- East Block:
    - The groundwater inflow as determined with all of the approaches display similar trends.
    - Results from the Krusseman & De Ridder and the Marinelli & Nicolli approaches display the closest values to each other and varies between only 12 m^3/day to a maximum of 170 m^3/day.
    - The Vandersluis *et al*. method displays the lowest inflow rates while the Darcy method where S=0.1 display the highest inflows.
- West Block:
    - Once again similar trends are observed in all the approaches in terms of groundwater inflows.
    - Vandersluis *et al*. once again display the lowest inflows over the mining period.

- Between 2016 and 2028 the Marinelli and Nicolli approach results in the highest inflows. Thereafter the Darcy S=0.1 approach display the highest inflow rates.

- Between 2016 and 2022 the Vandersluis *et al*. , Darcy S=0.01 and the Krusseman & De Ridder approaches results in inflows very close to exh other. Thereafter although still close, the differences in inflows between these methods increase somewhat.

It should be noted that this mining project is a greenfields project indicating that mining has not yet occurred. Estimated inflow rates as determined by analytical and numerical methods can thus not be compared to actual measured inflow rates. It is therefore one of the main recommendations that the actual rates be compared to rates determined in this document once these rates become available. Since the numerical model approach incorporates all factors that might not be considered in the analytical methods, one can expect the numerical results to be closest to reality. Therefore, for the purpose of this study the figures as obtained from the numerical model will be used as indicative figures and the analytical results will be compared to the numerical figures.

In the aim of determining of any of the analytical approaches correlates well with the numerical approach, all the analytical approaches have been compared to the inflow to the pits at 12.5% recharge as determined by the numerical model.

The following discussion on the results of the correlation at the East Block:

- The numerical model simulated inflows display similar trends than the analytical approaches.

- The correlation between the analytical and numerical methods is very poor at the East block.

- The correlation varies between 41 and 57 %.

- The lowest correlation is between the numerical method and the Vandersluis *et al*. approach.

- Highest correlation, although not good, is between the numerical and Darcy S=0.01 approach.

The following discussion on the results of the correlation at the West Block:

- The correlation between the analytical approaches and the numerical approach is also poor and varies between 53 and 71%.
- The least correlation is between the numerical and Marinelli & Nicolli approaches.
- Highest correlation at 71% is between the numerical and also the Darcy S0.01 approach.

The estimated total water make at the end of mining will aid in the decision making in terms of water management. The decisions include surface water dam volumes and whether or not a water treatment facility is required. The geometry of the coal floor in the pits allows only a small part of the pits to be filled with water before decanting can occur. Therefore, even though mining occur upgradient, no storage will be available and water management is critical.

At the East Block:

- Numerically estimated water make varies between 5.1 and 6.1 Mm^3 as determined by the different numerical approaches.
- According to the analytical approaches the total water make can vary between 2.9 and 14.3 Mm^3.

At the West Block:

- Numerically estimated water make varies between 2.5 and 2.9 Mm^3 as determined by the different numerical approaches.
- According to the analytical approaches the total water make can vary between 1.2 and 3.8 Mm^3.

10. Conclusion

The following conclusions can be drawn from the study:

- The scope of this study was to compare analytically and numerically estimated groundwater inflow rates to the opencast pits and the estimated recharge volumes to the pit. The results of this study will therefore conclude whether or not the analytically and numerically obtained results correlated with each other.

- Comparing the recharge rates as determined by the analytical and numerical approaches, indicated that the recharge as determined with the analytical approach was, and in some cases much higher than that determined with the numerical model. Overall, the analytical approach to determining recharge can be used to quickly determine and get an estimate of the recharge volume to the mining area. Since the average recharge percentage to an opencast pit has been determined by scientists in the field of geohydrology (eg. Hodgson), it is a quick, safe and fairly accurate method to determine the recharge rate by using the analytical approach. However, each study site is unique and exact recharge rates cannot be determined accurately.

- According to the Marinelli & Nicolli (2000) approach the groundwater inflow to the pit is predominantly from the pit floor and not the walls. This is also the major problem with this approach, as water in a coal mining environment is predominantly from the pit walls. Water from the floor is generally only expected when a geological structure such as a dyke and a fault are intersected, and even then only minimally.

- In determining the groundwater inflows to the mine, the Darcy + recharge method with two approaches was used. Firstly the groundwater inflow to the pits was determined by using a radius of influence as determined with S=0.1 (R=100m). In the thesis this approach is referred to as the Q Darcy S=0.1. The second approach using the Darcy + recharge method was using a radius of influence as

determined by S=0.01. A radius of influence of 314 meters was used. In the thesis this approach is referred to as Q Darcy S=0.01.

- It should be noted that the changes in storativity gives very different answers in the Darcy method. Determining the radius of influence analytical for a mining environment is very difficult and the method used during this study (Cooper-Jacob) was assumed to be the best representative method. One way of more accurately determining the radius of influence is by making use of observation boreholes and actually measuring the drawdown in the boreholes. This will aid in giving a groundwater gradient, which can be used especially in the Darcy method where Q=KiA (i= hydraulic gradient).

- Correlation between the numerical and various analytical approaches are very poor and in fact in some cases no correlation at all.

- At the East Block correlation vary between 41 and 57 %, with the lowest correlation between the numerical and Vandersluis *et al*. (1995) methods while the highest correlation was between the numerical and the Q Darcy S=0.01.

- At the West Block the correlation is also poor and varies between 53 and 71%. The lowest correlation at this block was between the numerical and Marinelli & Nicolli (2000) approaches. This is once again proof that the theory of this approach is not applicable to the Belfast project. Water in a coal mining operation in the project area will flow predominantly from the pit walls into the pit.

- The numerical and analytical approaches displayed similar trends in terms of groundwater inflow.

- As said before, the numerical model incorporates all factors that might not be covered by the analytical approaches. For the purpose of this study it is assumed that the numerical results are the closest to reality.

- With the very poor correlation and varying inflow rates between the numerical and analytical approaches determined during this study, it can be concluded that the analytical methods used during this study does in fact not give a good representation of the expected groundwater inflow rates.

- It is very important to note that this conclusion is made by assuming that the numerical approach gives the most realistic answers.

- The fact that the analytical approaches did not reveal representative values for the groundwater inflows and do not correlate well with the numerical model, does not mean that this will be the case at another site with different geohydrological characteristics.

- It is expected that the numerical approach in any coal mining area will give a better estimate provided that the model has been constructed according to a sound conceptual understanding of the aquifer and related characteristics. The numerical model incorporates all the input data and work on exact values rather than averages, estimates or assumptions. The accuracy of the numerical model still depends on the input data and the ability of the modeller. It should be noted that for the purpose of this thesis the values as obtained from the numerical model was assumed to be the closest to reality and analytical approaches was compared to the numerical approach. The Belfast study site is a 'greenfields' project and therefore indicate that mining has not yet occurred in the area. Therefore the results obtained from this investigation are based on available data only and needs to be compared to actual measured inflow rates once mining has begun and figures becomes available.

11. Recommendations

The following recommendations are made for the Belfast study site after the results from this thesis have been obtained:

- It is suggested that further research be conducted in relation with analytical and numerical modelling of opencast mines.

- Research should be performed at several mines to determine whether the relation between the numerical and analytical approaches display similar trends than was found during this study.

- These mines should preferably be in similar geological regions to compare with each other.

- The best way to determine whether the analytical methods can in fact be used to get a representative result is by repetition on several mining sites and most important comparing these values with the numerical model results and also the actual inflow rates as pumped from the mine once mining has started.

- Monitoring of monitoring boreholes may give an indication on the groundwater gradient which can aid in determining groundwater gradients and the radius of influence.

All said, analytical approaches, although in some cases giving answers close to the numerical results, cannot be used in a successful first estimate to estimate groundwater related queries in the Belfast mining environment.

12. References

Aryafar, A., Doulati Ardejani, F., Singh, R., Jodeiri Shokri, B., 2007. Prediction of groundwater inflow and height of seepage face in a deep open pit mine using numerical finite element model and analytical solutions. *IMWA Symposium 2007: Water in Mining Environments, 27th – 31st May 2007*, Cagliari, Italy.

Cogho, V.E. and van Niekerk, A.M., 2009. Optimum Coal Mine Water Reclamation Project. Abstracts of the International Mine Water Conference. Pretoria.

Dennis I., 2008, Introduction to groundwater modelling- Class notes. IGS, Bloemfontein.

DWA, 2008.Groundwater Dictionary. Department of Water Affairs.

environmental-agency.info/static/documents/Research/appendices_904700

Exxaro Coal Mpumalanga Limited, 2009. Mining Work Programme for the Proposed Belfast Coal Mine.

Grobbelaar R., Usher B., Cruywagen L-M., de Necker E. and Hodgson FDI., 2004. Long-term impact of intermine flow from collieries in the Mpumalanga Coalfields. *Report to the Water Research Commission, 1056/1/04*. Water Research Commission, Pretoria.

Hanna, T.M., Elfadil, A.A. and Atkinson, L.C., 1994. Use of an analytical solution for preliminary estimates of groundwater inflow to a pit. *Mining Engineering* 46. No. 2: 149-152.

Heath, R.C. (1987). Basic Groundwater Hydrology. *Geological Survey water-supply paper ; 2220.*USGS

Jeffrey, L.S. (2005). Characterization of the coal resources of South Africa. *The Journal of the South African Institute of Mining and Metallurgy*, 95-102.

Macmillan, S., 2004.Earth's Magnetic Field. Geophysics and Geochemistry, Encyclopedia of Life Support Systems, Developed under the Auspices of the UNESCO, Eolls Publishers, Oxford, UK, (www.eolls.net).

Marinelli, F. and Nicolli, W.L., 2000. Simple analytical equations for estimating groundwater inflow to a Mine Pit. Groundwater Vol. 38, No. 2 (pgs. 311-314).

McIntosh J., 2010. news.guelphmercury.com/options/editorialopinion/article/

594802.

Singh, R.N. and Reed, S.M., 1988. Mathematical modelling for estimation of mine water inflow to a surface mining operation. *International Journal of Mine Water,* Vol. 7, No.3. (pgs. 1-34).

Singh, R.N., Ngah, S.A., Atkins A.S., 1985. Applicability of current groundwater theories for the prediction of groundwater inflows to surface mining excavations. *Proceedings of the Second International Congress of the International Mine Water Association*, Granada, Spain, 553-571.

Soil Classification Working Group, 1991. Soil Classification- A taxonomic system for South Africa. Pretoria

Van Tonder, G.J. and Kirchner, J., 1990. Estimation of natural groundwater recharge in the Karoo aquifers of South-Africa. *Journal of Hydrology*, 121(1-4), (pgs. 395-419).

Van Zijl, J.S.V. and Köstlin, E.O., Field Manual for Technicians No.3, the Electromagnetic Method. South African Geophysical Association.

Vandersluis, G.D., Straskraba, V., Effner, S.A., 1995. Hydrogeological and geochemical aspects of lakes forming in abandoned open pit mines*. Proceedings on Water Resources at Risk, W.R. Hotckkiss, J.S. Downey, E.D. Gutentag and J.E. Moore (Eds.),* American Institute of Hydrology, 162-177.

World Coal Institute, 2005. The coal resource: A comprehensive overview of coal. UK.

Aquila Resources (2010) http://www.aquilaresources.com.au/ images/waterberg lrg.jpg

British Columbia Government (2011), http://www.env.gov.bc.ca/wsd/plan_protect_sustain/groundwater/gwbc/CO2_origin.html

SA Explorer (2010) http://www.saexplorer.co.za/south-africa/climate/belfast_climate.asp

South Africa Info (2010) http://www.southafrica.info/about/geography/mpumulanga

Agis (2009) http://www.agis.agric.za

Appendix A: Geological Borehole Logs

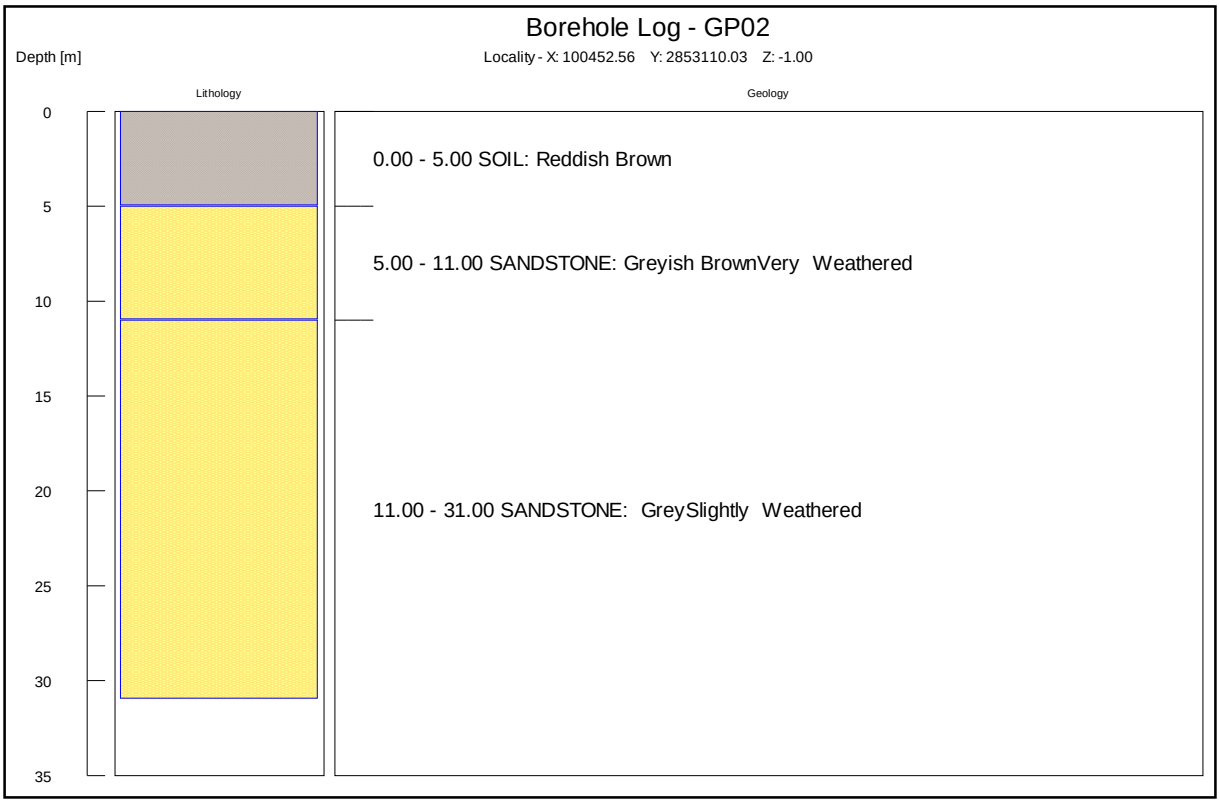
Borehole Log - GP02
Depth [m]
Locality - X: 100452.56 Y: 2853110.03 Z: -1.00
Lithology
Geology
0
5
10
15
20
25
30
35
0.00 - 5.00 SOIL: Reddish Brown
5.00 - 11.00 SANDSTONE: Greyish BrownVery Weathered
11.00 - 31.00 SANDSTONE: GreySlightly Weathered

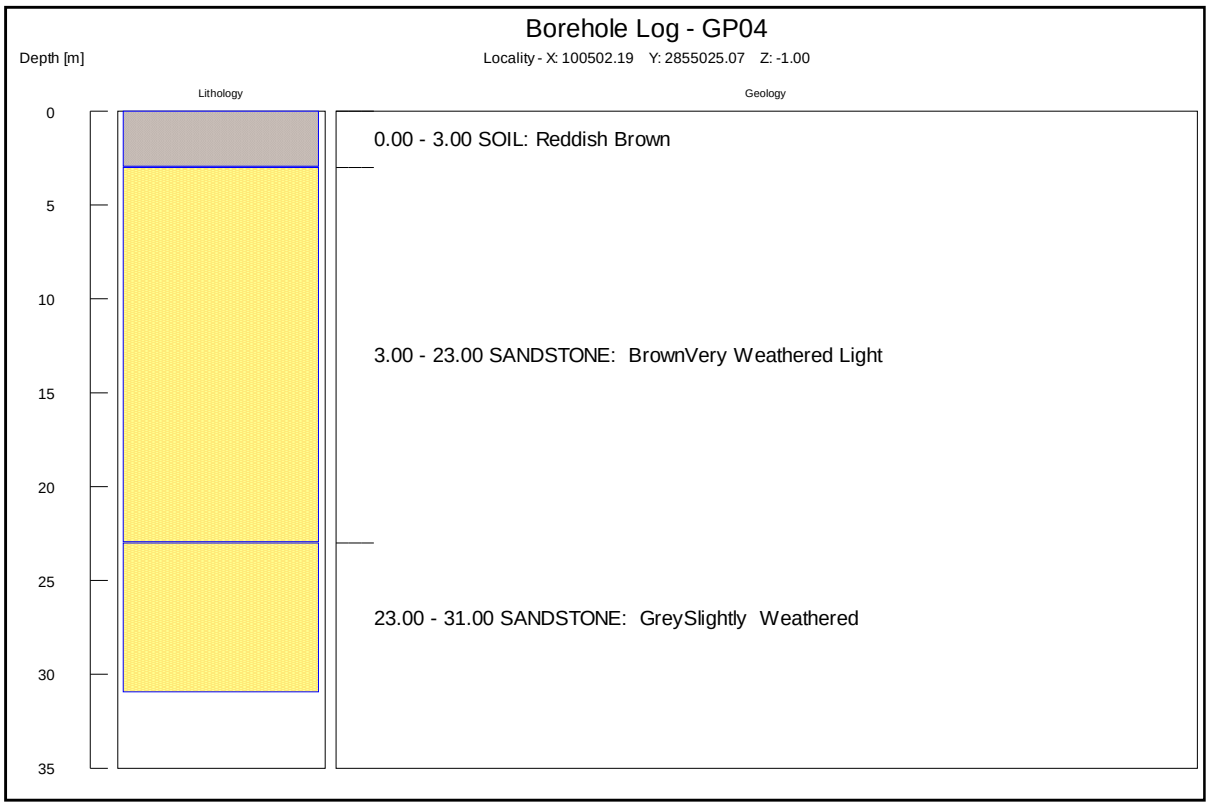
Borehole Log - GP04
Depth [m]
Locality - X: 100502.19 Y: 2855025.07 Z: -1.00
Lithology
Geology
0
5
10
15
20
25
30
35
0.00 - 3.00 SOIL: Reddish Brown
3.00 - 23.00 SANDSTONE: BrownVery Weathered Light
23.00 - 31.00 SANDSTONE: GreySlightly Weathered

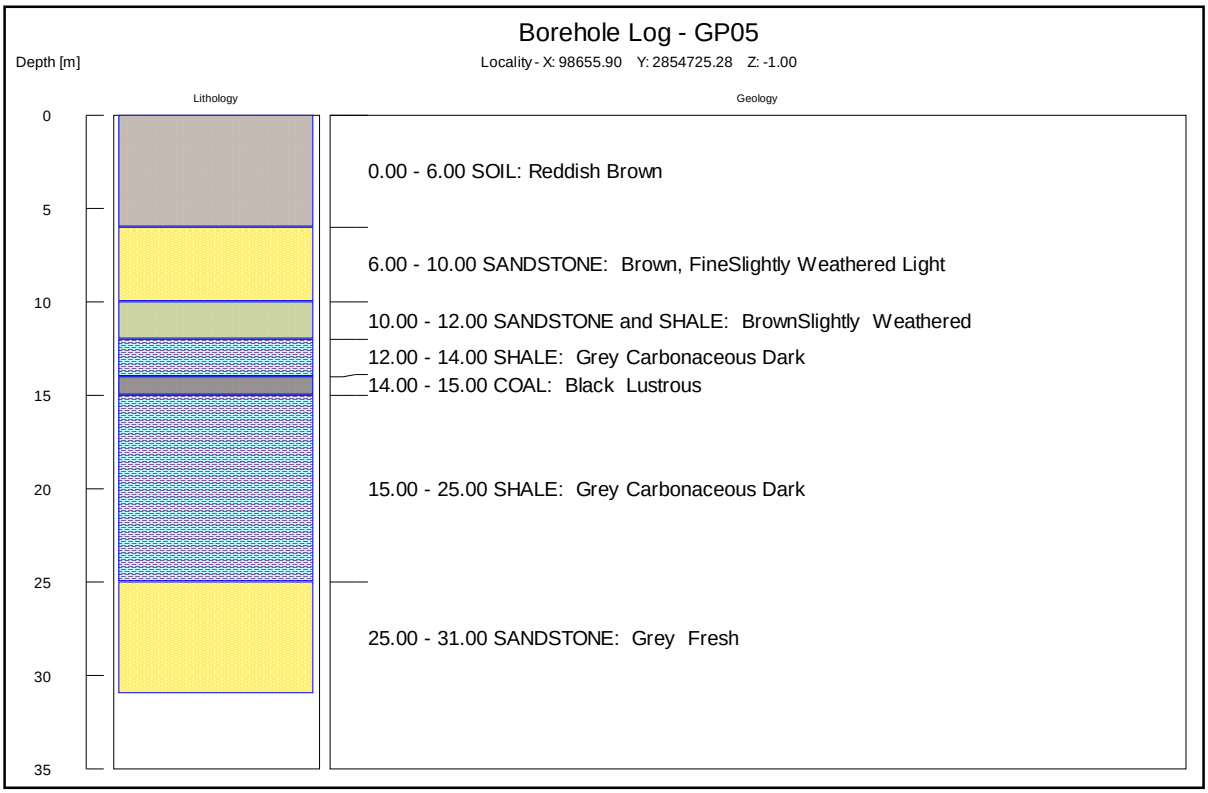
Borehole Log - GP05
Depth [m]
Locality - X: 98655.90 Y: 2854725.28 Z: -1.00
Lithology
Geology
0
5
10
15
20
25
30
35
0.00 - 6.00 SOIL: Reddish Brown
6.00 - 10.00 SANDSTONE: Brown, FineSlightly Weathered Light
10.00 - 12.00 SANDSTONE and SHALE: BrownSlightly Weathered
12.00 - 14.00 SHALE: Grey Carbonaceous Dark
14.00 - 15.00 COAL: Black Lustrous
15.00 - 25.00 SHALE: Grey Carbonaceous Dark
25.00 - 31.00 SANDSTONE: Grey Fresh

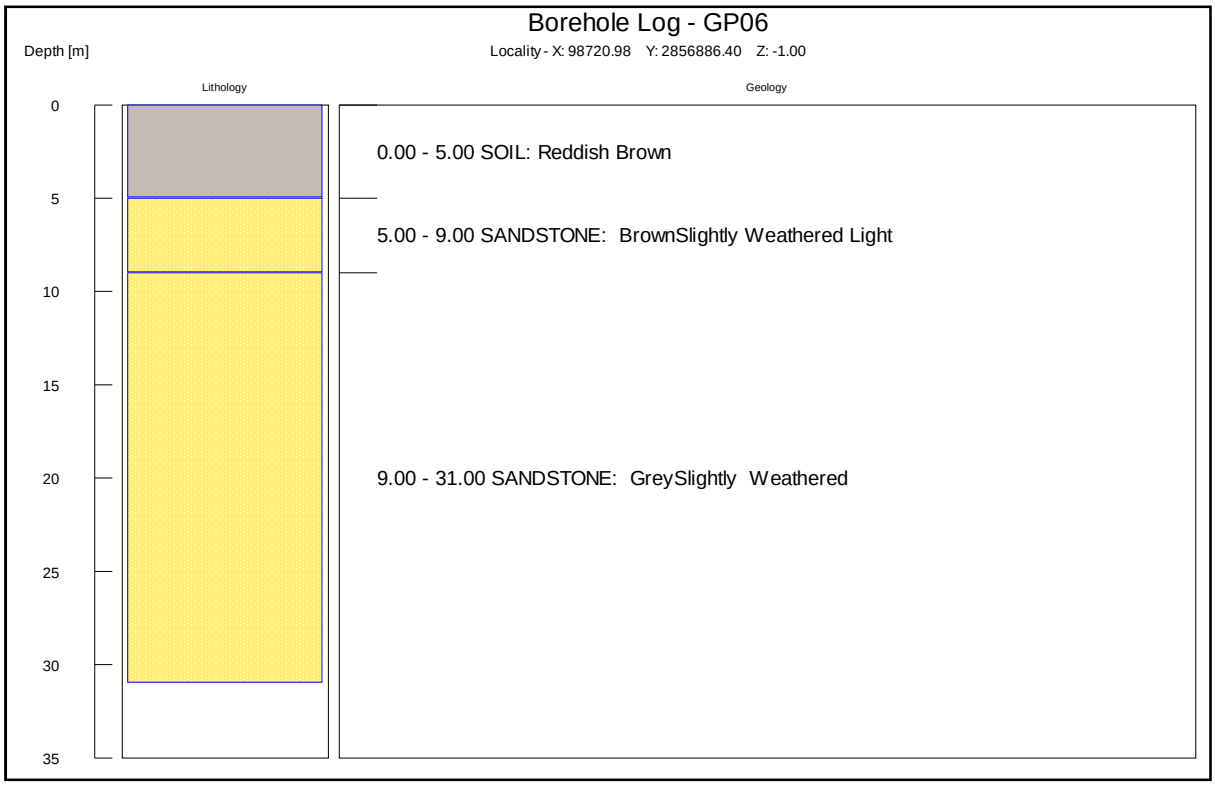
Borehole Log - GP06
Depth [m]
Locality - X: 98720.98 Y: 2856886.40 Z: -1.00
Lithology
Geology
0
5
10
15
20
25
30
35
0.00 - 5.00 SOIL: Reddish Brown
5.00 - 9.00 SANDSTONE: BrownSlightly Weathered Light
9.00 - 31.00 SANDSTONE: GreySlightly Weathered

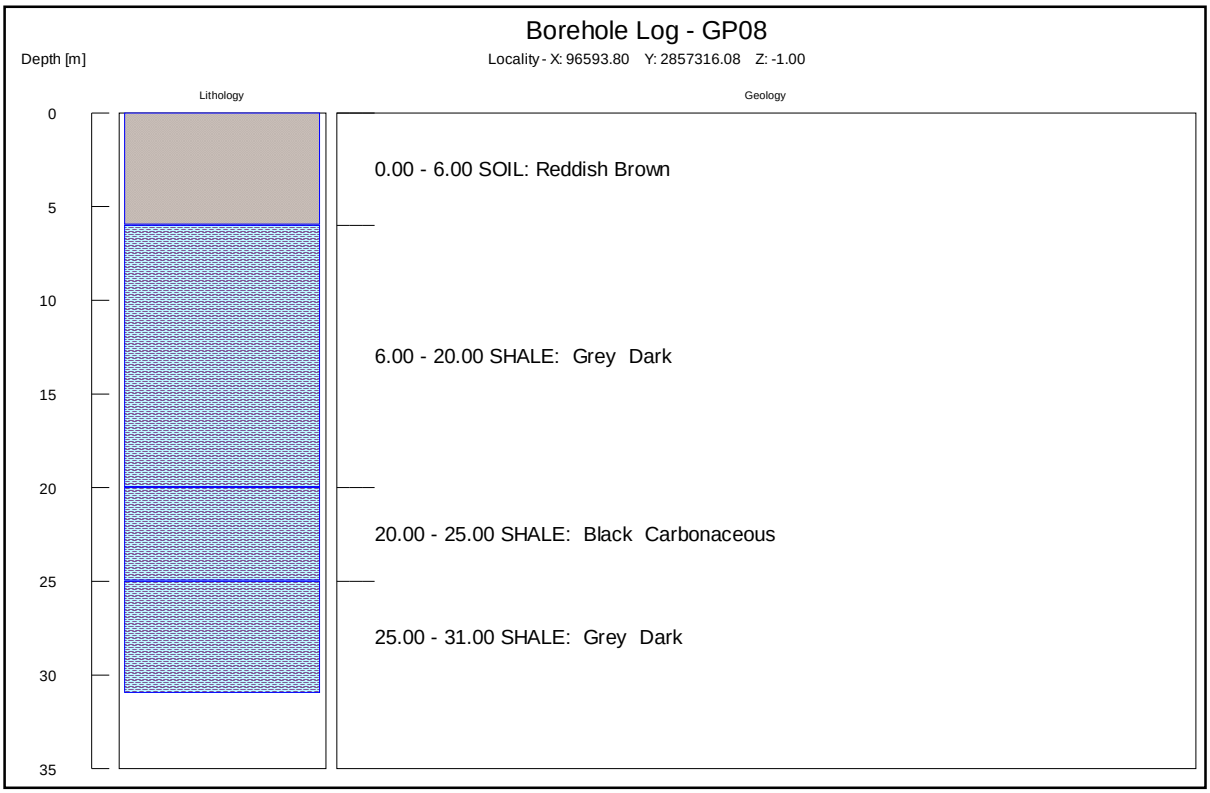
Borehole Log - GP08
Depth [m]
Locality - X: 96593.80 Y: 2857316.08 Z: -1.00
Lithology
Geology
0
5
10
15
20
25
30
35
0.00 - 6.00 SOIL: Reddish Brown
6.00 - 20.00 SHALE: Grey Dark
20.00 - 25.00 SHALE: Black Carbonaceous
25.00 - 31.00 SHALE: Grey Dark

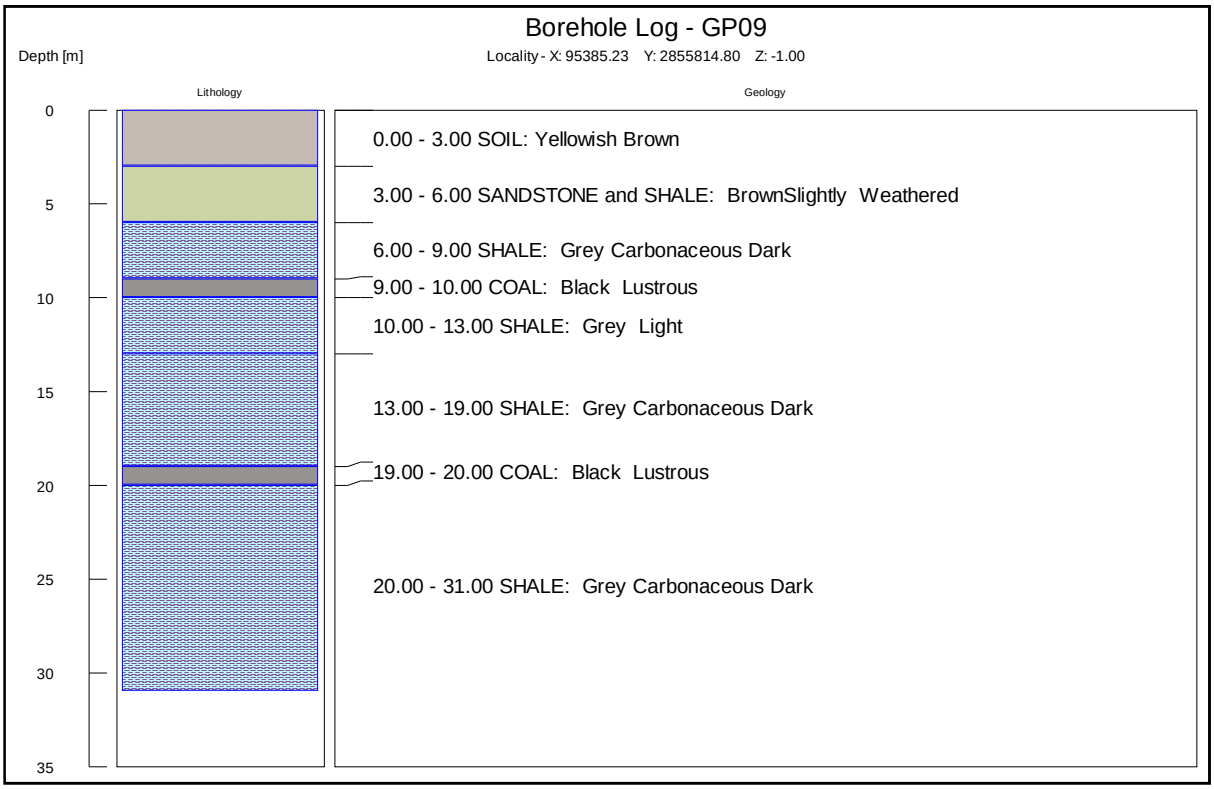
Borehole Log - GP09
Depth [m]
Locality - X: 95385.23 Y: 2855814.80 Z: -1.00
Lithology
Geology
0
5
10
15
20
25
30
35
0.00 - 3.00 SOIL: Yellowish Brown
3.00 - 6.00 SANDSTONE and SHALE: BrownSlightly Weathered
6.00 - 9.00 SHALE: Grey Carbonaceous Dark
9.00 - 10.00 COAL: Black Lustrous
10.00 - 13.00 SHALE: Grey Light
13.00 - 19.00 SHALE: Grey Carbonaceous Dark
19.00 - 20.00 COAL: Black Lustrous
20.00 - 31.00 SHALE: Grey Carbonaceous Dark

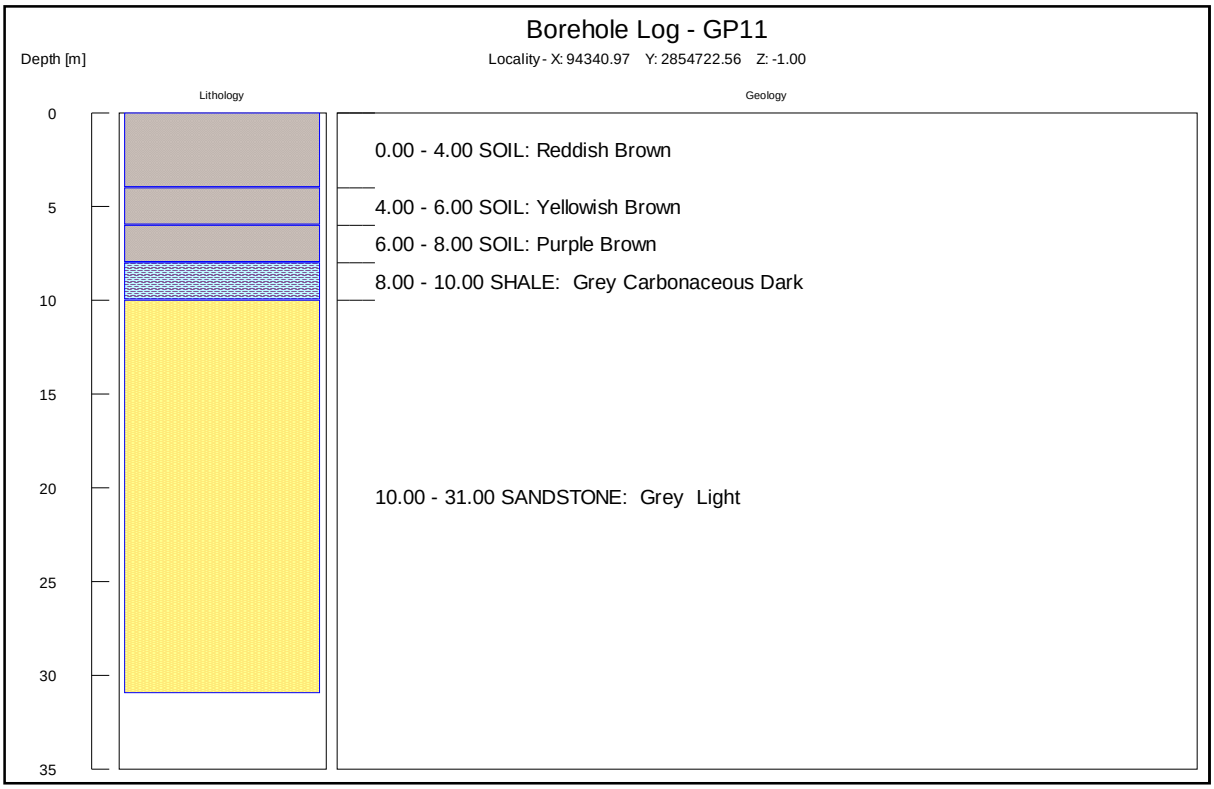
Borehole Log - GP11
Depth [m]
Locality - X: 94340.97 Y: 2854722.56 Z: -1.00
Lithology
Geology
0
5
10
15
20
25
30
35
0.00 - 4.00 SOIL: Reddish Brown
4.00 - 6.00 SOIL: Yellowish Brown
6.00 - 8.00 SOIL: Purple Brown
8.00 - 10.00 SHALE: Grey Carbonaceous Dark
10.00 - 31.00 SANDSTONE: Grey Light

Appendix B: Geophysical Results

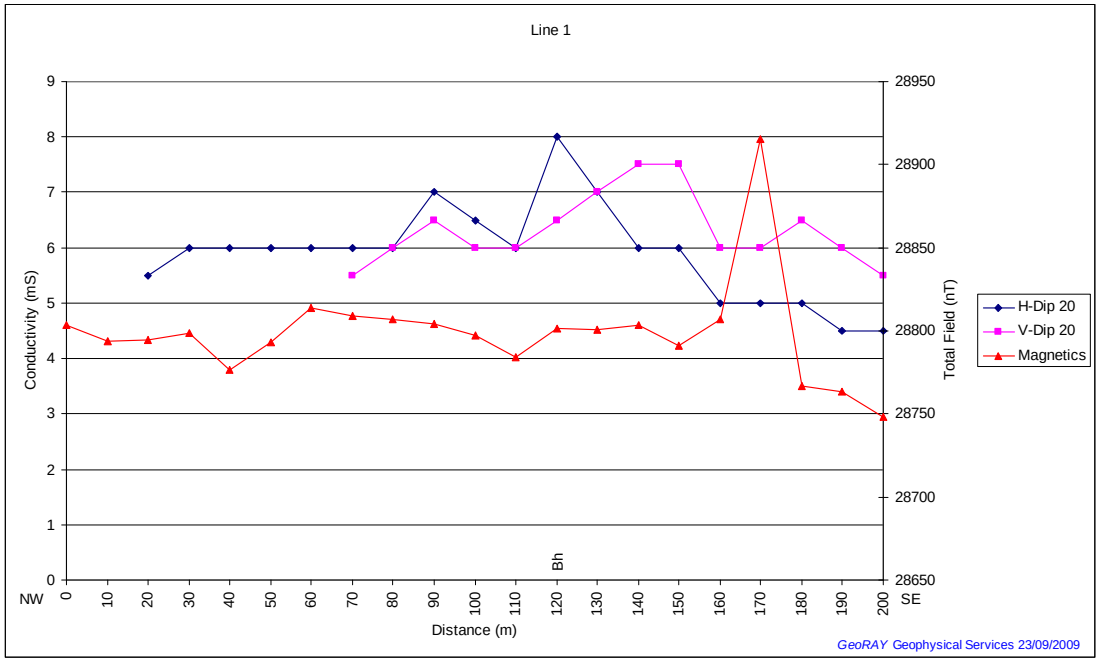
Line 1
Conductivity (mS)
Total Field (nT)
Distance (m)
NW
SE
Bh
H-Dip 20
V-Dip 20
Magnetics
GeoRAY Geophysical Services 23/09/2009

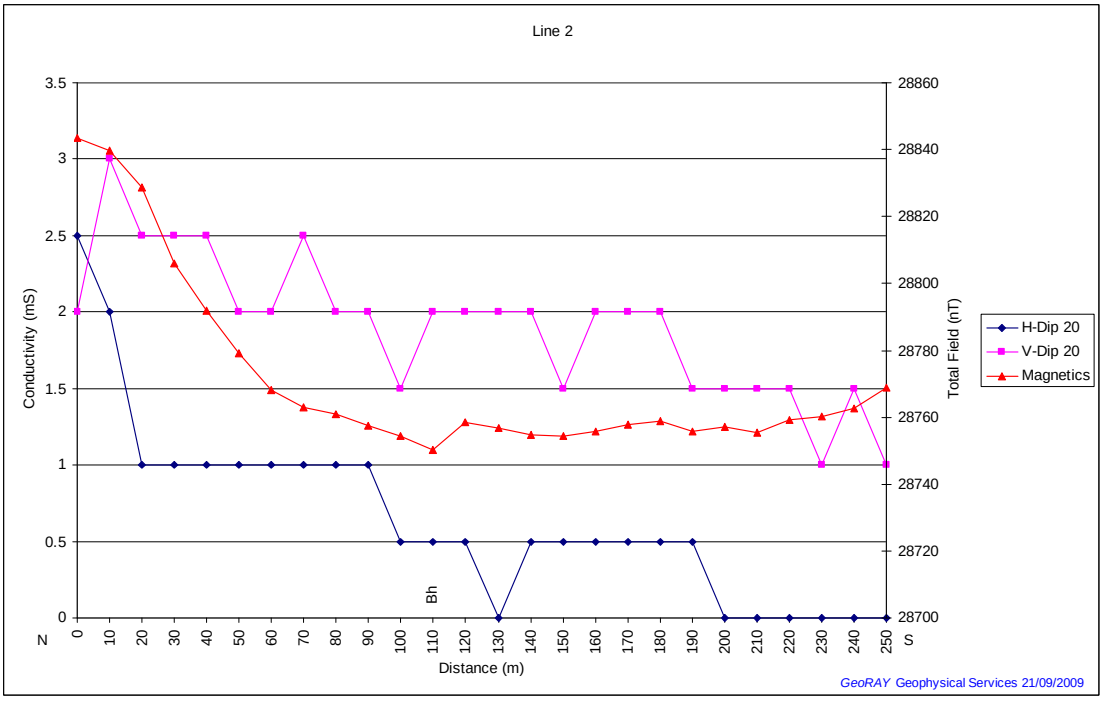
Line 2
Conductivity (mS)
Total Field (nT)
Distance (m)
N
S
Bh
H-Dip 20
V-Dip 20
Magnetics
GeoRAY Geophysical Services 21/09/2009

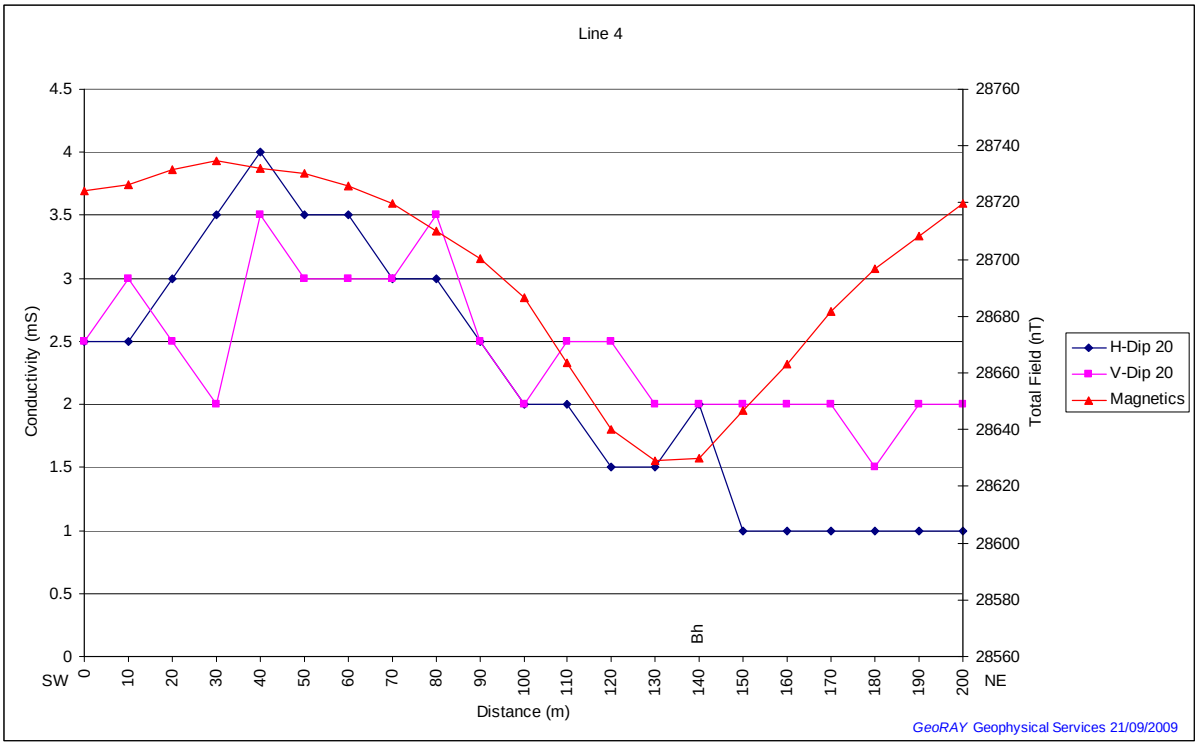
Line 4
Conductivity (mS)
Total Field (nT)
Distance (m)
SW
NE
Bh
H-Dip 20
V-Dip 20
Magnetics
GeoRAY Geophysical Services 21/09/2009

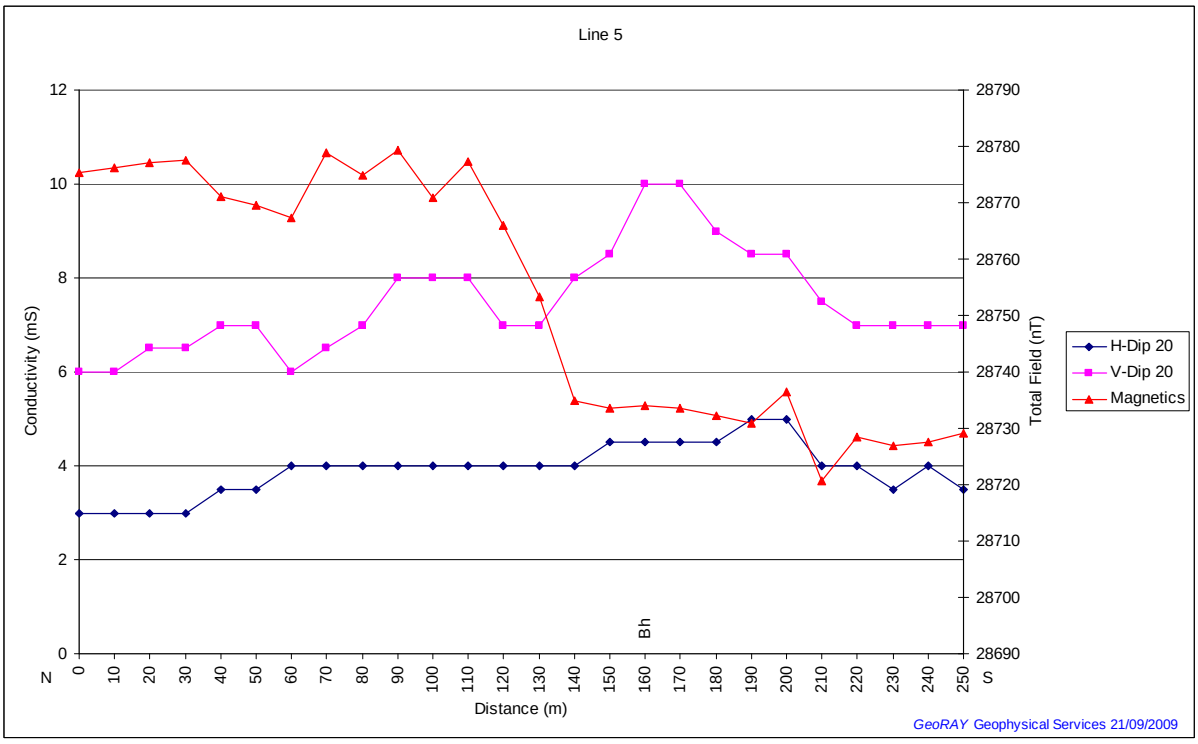
Line 5
Conductivity (mS)
Total Field (nT)
Distance (m)
N
S
Bh
H-Dip 20
V-Dip 20
Magnetics
GeoRAY Geophysical Services 21/09/2009

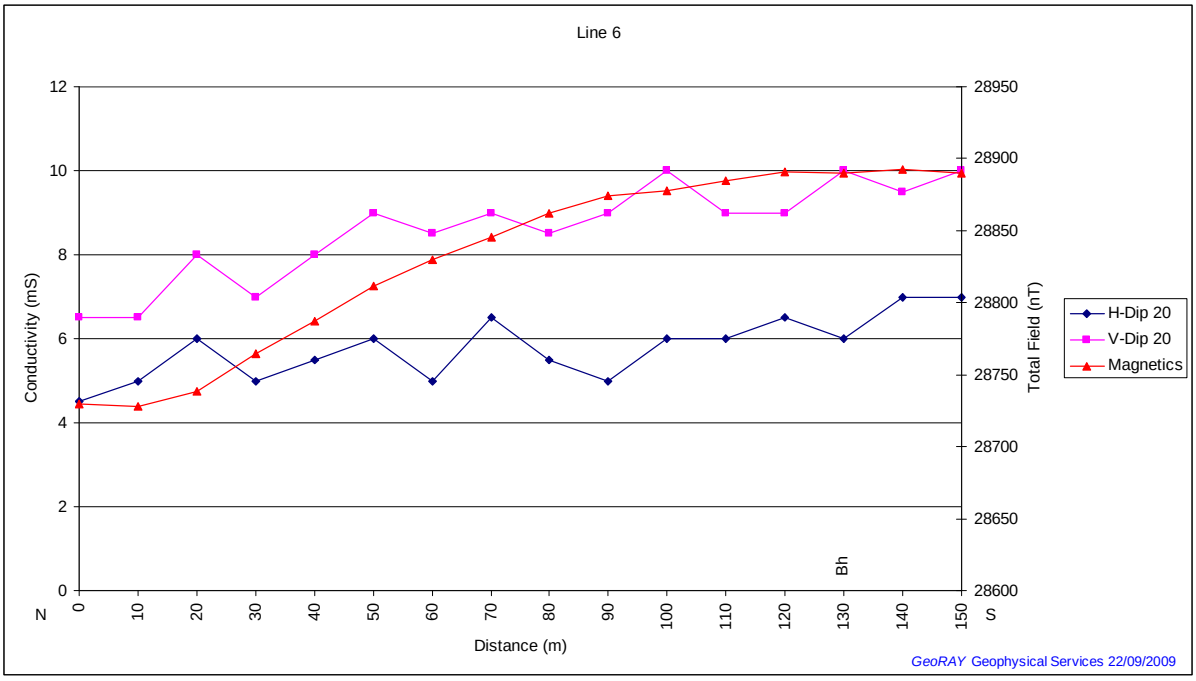
Line 6
Conductivity (mS)
Total Field (nT)
Distance (m)
N
S
Bh
H-Dip 20
V-Dip 20
Magnetics
GeoRAY Geophysical Services 22/09/2009

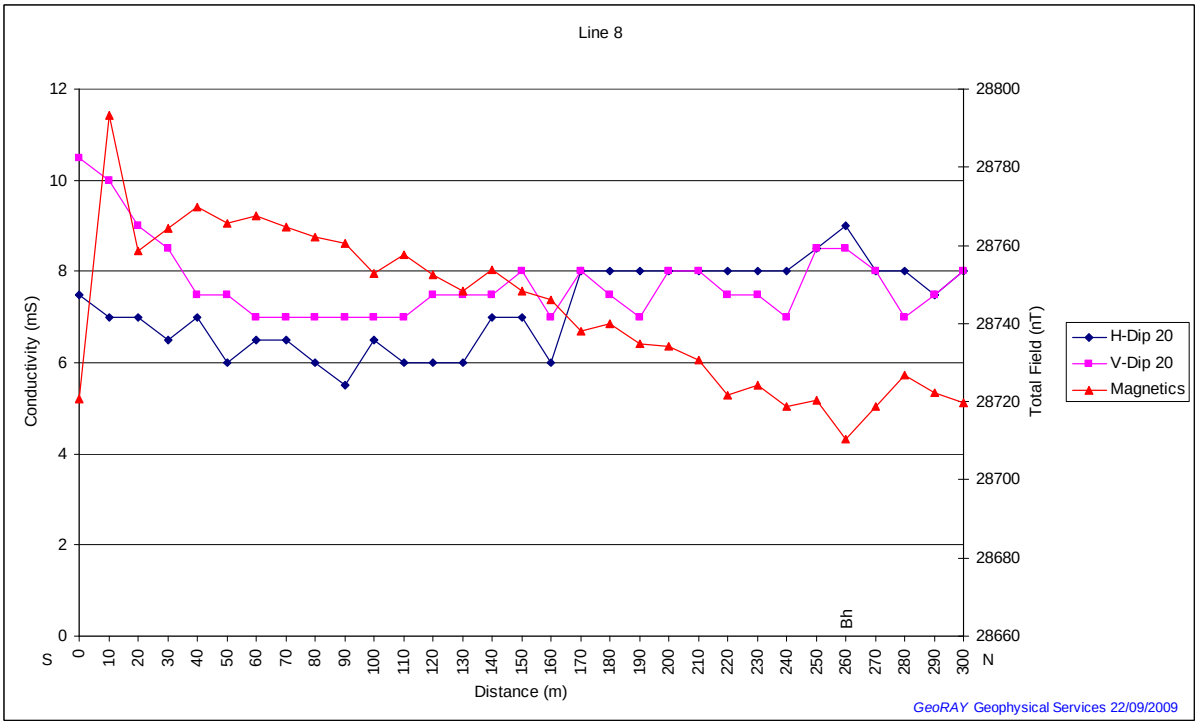
Line 8
Conductivity (mS)
Total Field (nT)
Distance (m)
S
N
Bh
H-Dip 20
V-Dip 20
Magnetics
GeoRAY Geophysical Services 22/09/2009

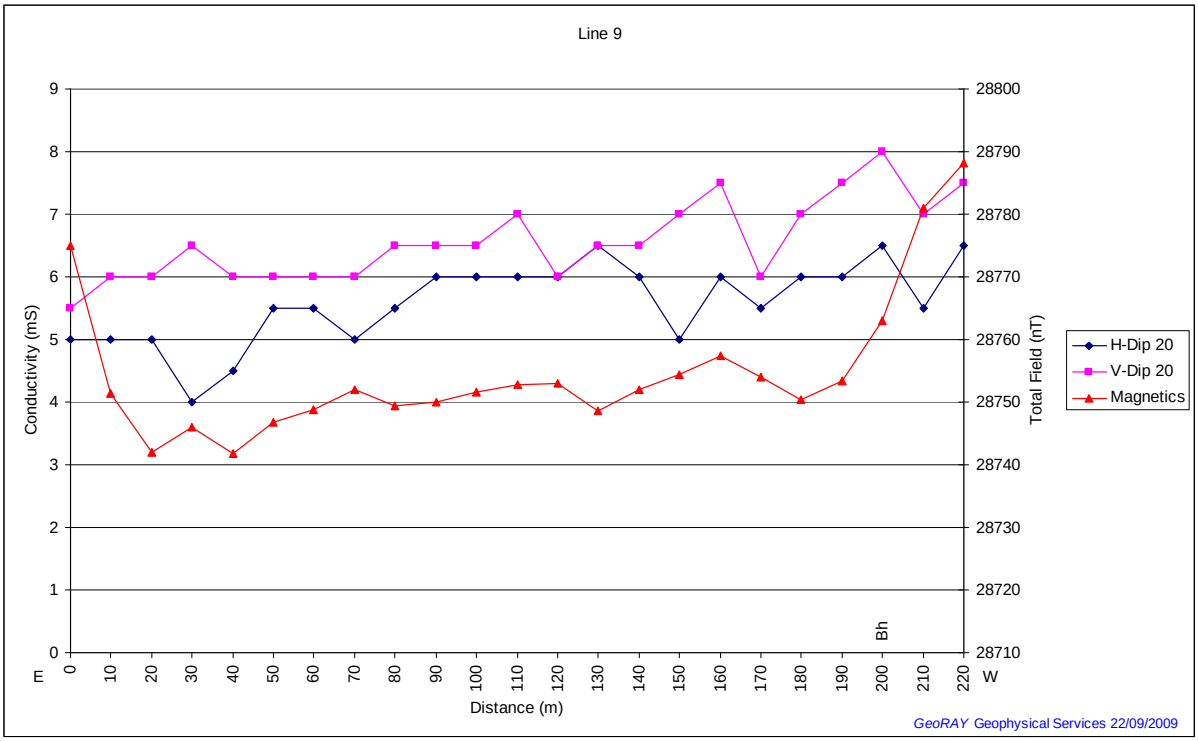
Line 9
Conductivity (mS)
Total Field (nT)
Distance (m)
E
W
Bh
H-Dip 20
V-Dip 20
Magnetics
GeoRAY Geophysical Services 22/09/2009

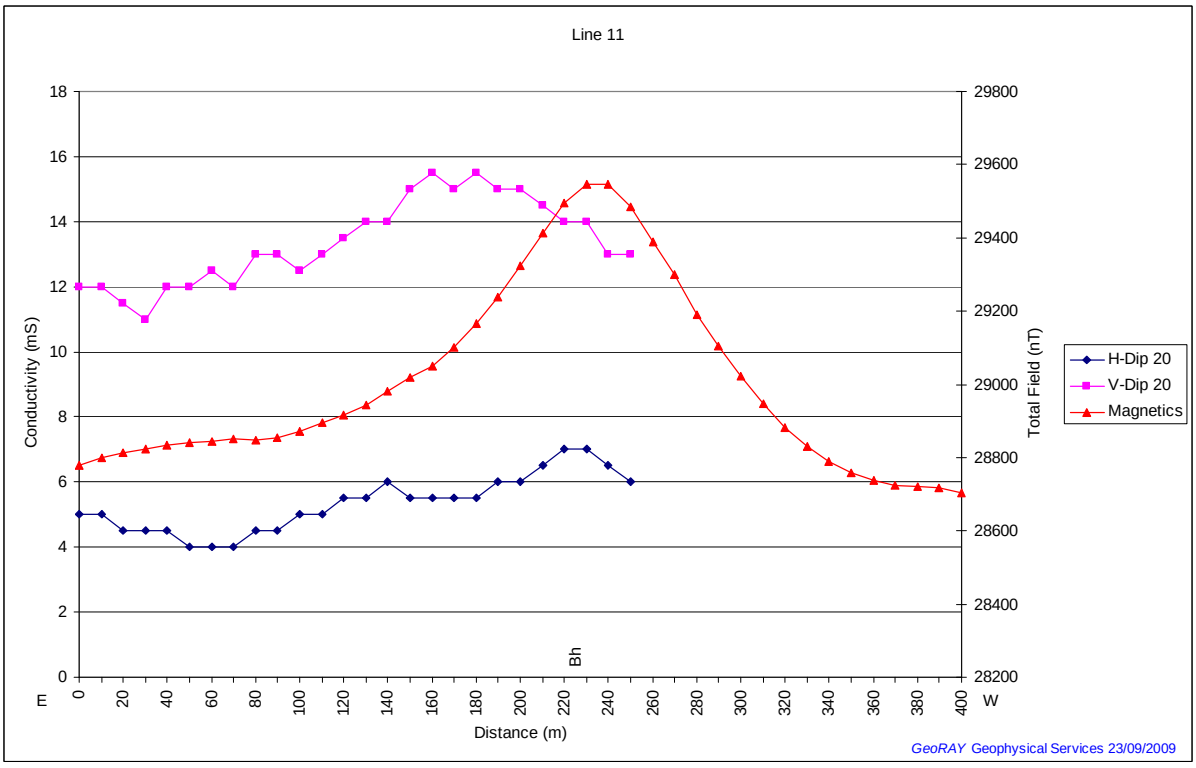
Line 11
Conductivity (mS)
Total Field (nT)
Distance (m)
E
W
Bh
H-Dip 20
V-Dip 20
Magnetics
GeoRAY Geophysical Services 23/09/2009

Appendix C: Pump Test Graphs

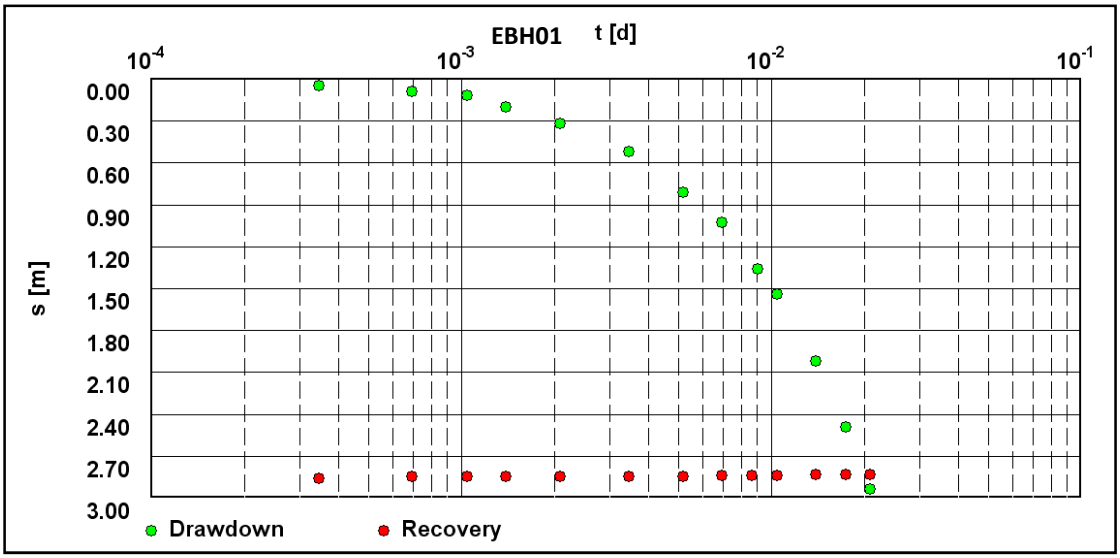
EBH01
t [d]
10-4
10-3
10-2
10-1
0.00
0.30
0.60
0.90
1.20
1.50
1.80
2.10
2.40
2.70
3.00
s [m]
Drawdown
Recovery

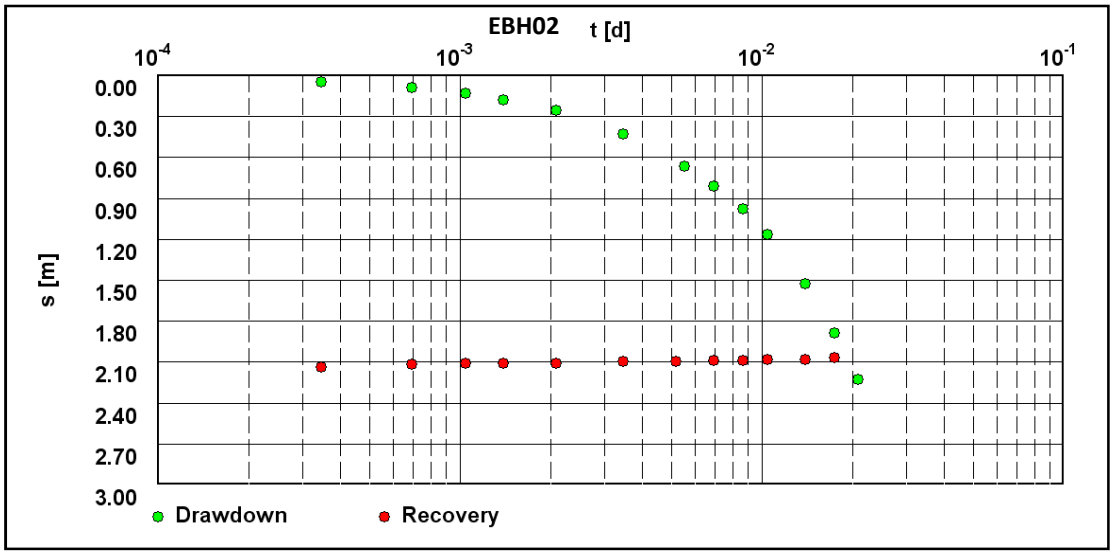
EBH02
t [d]
10-4
10-3
10-2
10-1
0.00
0.30
0.60
0.90
1.20
1.50
1.80
2.10
2.40
2.70
3.00
s [m]
Drawdown
Recovery

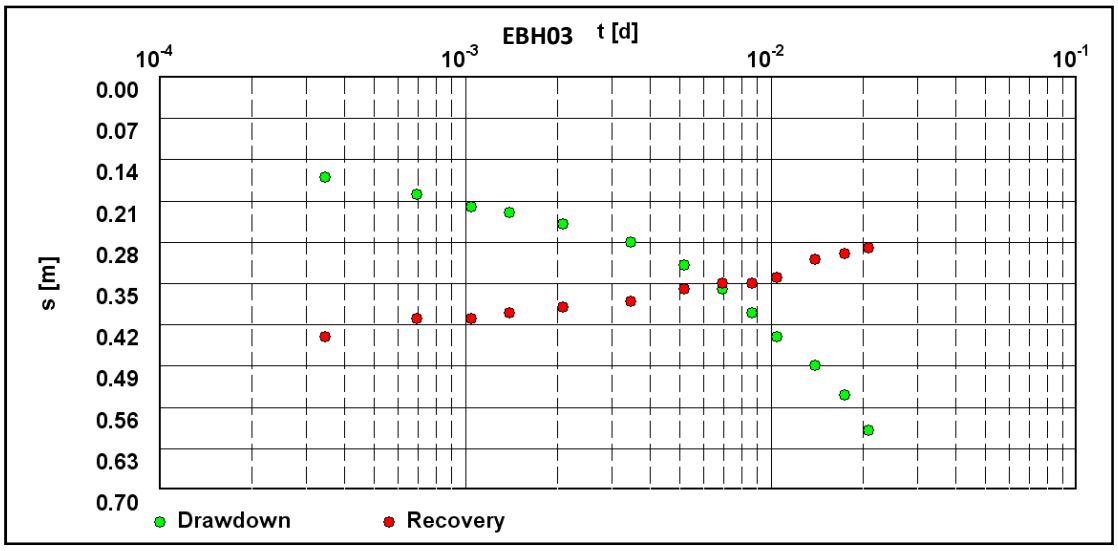
EBH03
t [d]
10-4
10-3
10-2
10-1
0.00
0.07
0.14
0.21
0.28
0.35
0.42
0.49
0.56
0.63
0.70
s [m]
Drawdown
Recovery

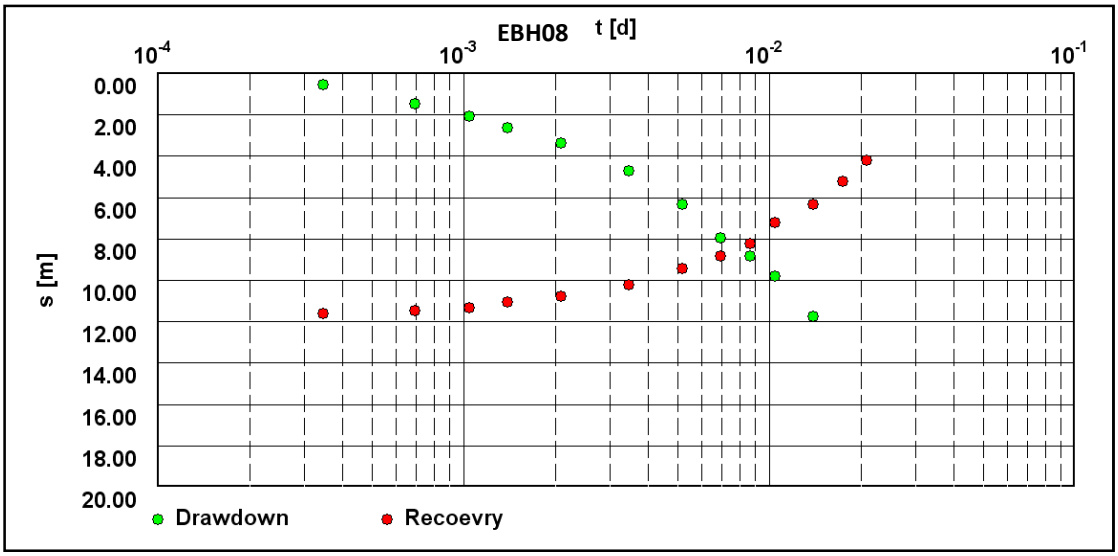
EBH08
t [d]
10-4
10-3
10-2
10-1
0.00
2.00
4.00
6.00
8.00
10.00
12.00
14.00
16.00
18.00
20.00
s [m]
Drawdown
Recoevry

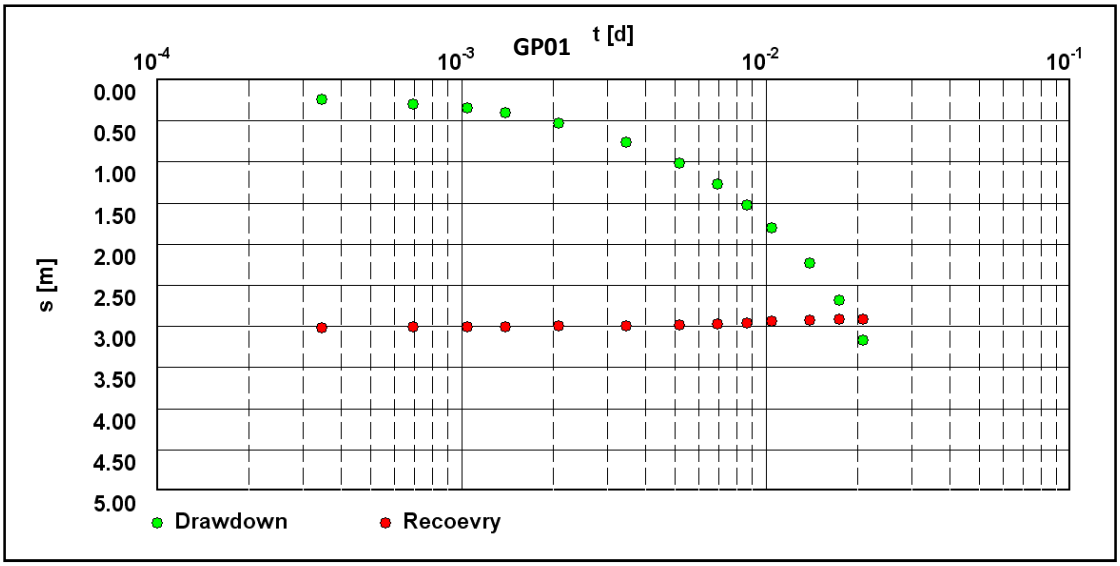
GP01
t [d]
10-4
10-3
10-2
10-1
s [m]
0.00
0.50
1.00
1.50
2.00
2.50
3.00
3.50
4.00
4.50
5.00
Drawdown
Recoevry

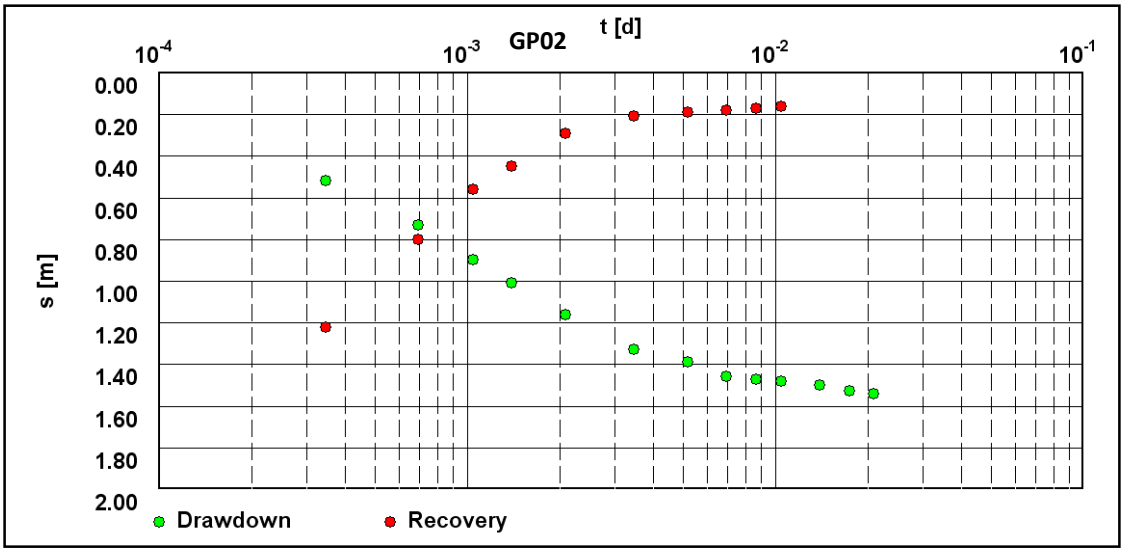
GP02
t [d]
10-4
10-3
10-2
10-1
s [m]
0.00
0.20
0.40
0.60
0.80
1.00
1.20
1.40
1.60
1.80
2.00
Drawdown
Recovery

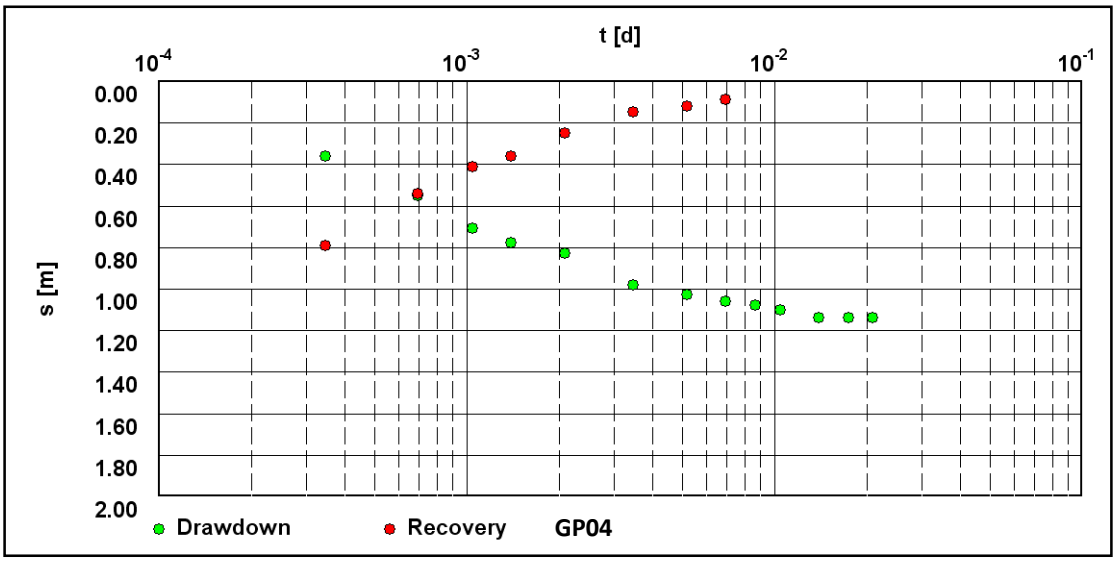
t [d]
10-4
10-3
10-2
10-1
0.00
0.20
0.40
0.60
0.80
1.00
1.20
1.40
1.60
1.80
2.00
s [m]
Drawdown
Recovery
GP04

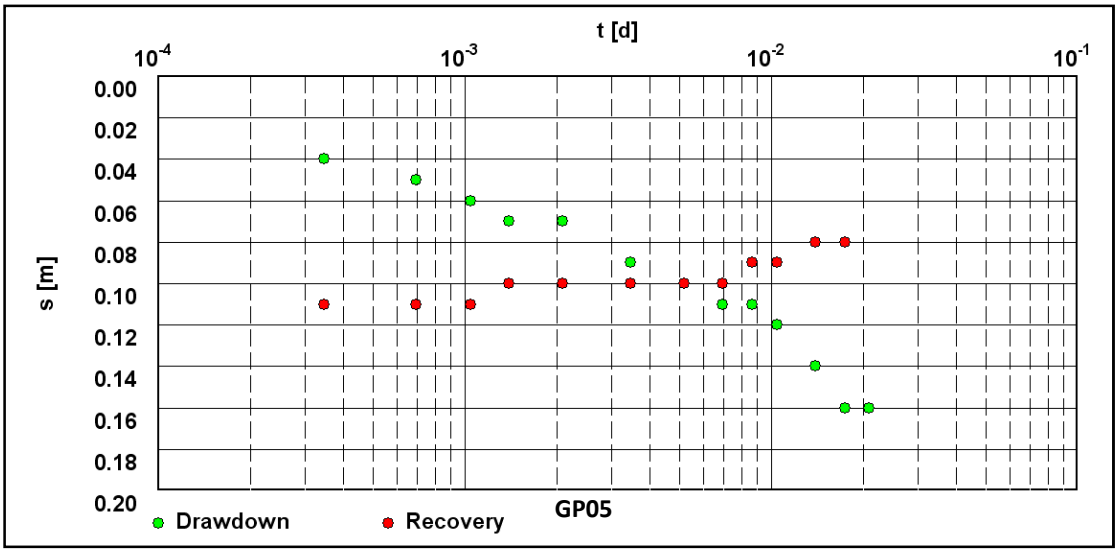
t [d]
10-4
10-3
10-2
10-1
0.00
0.02
0.04
0.06
0.08
0.10
0.12
0.14
0.16
0.18
0.20
s [m]
Drawdown
Recovery
GP05

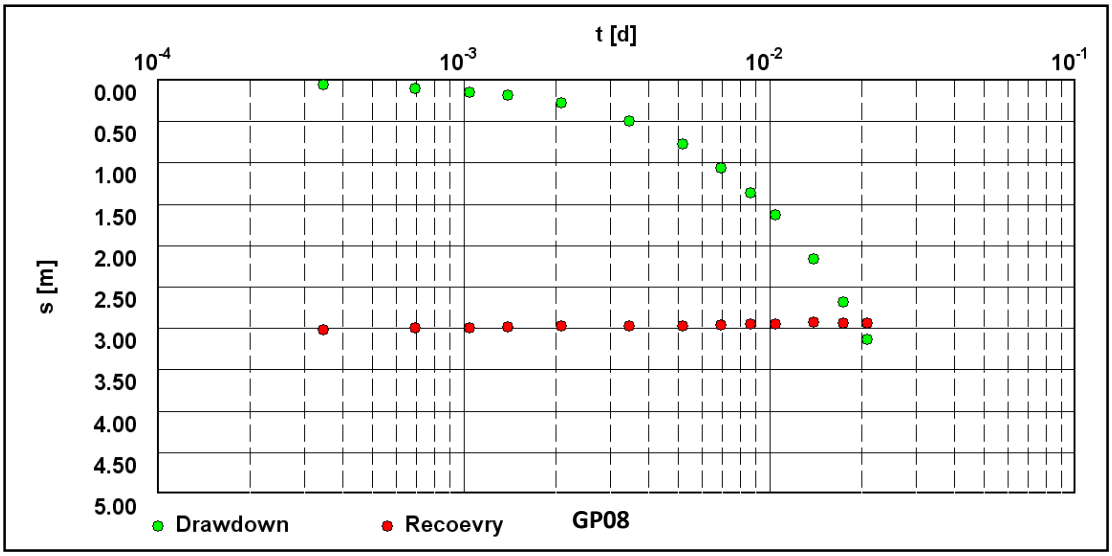
t [d]
10-4
10-3
10-2
10-1
0.00
0.50
1.00
1.50
2.00
2.50
3.00
3.50
4.00
4.50
5.00
s [m]
Drawdown
Recoevry
GP08

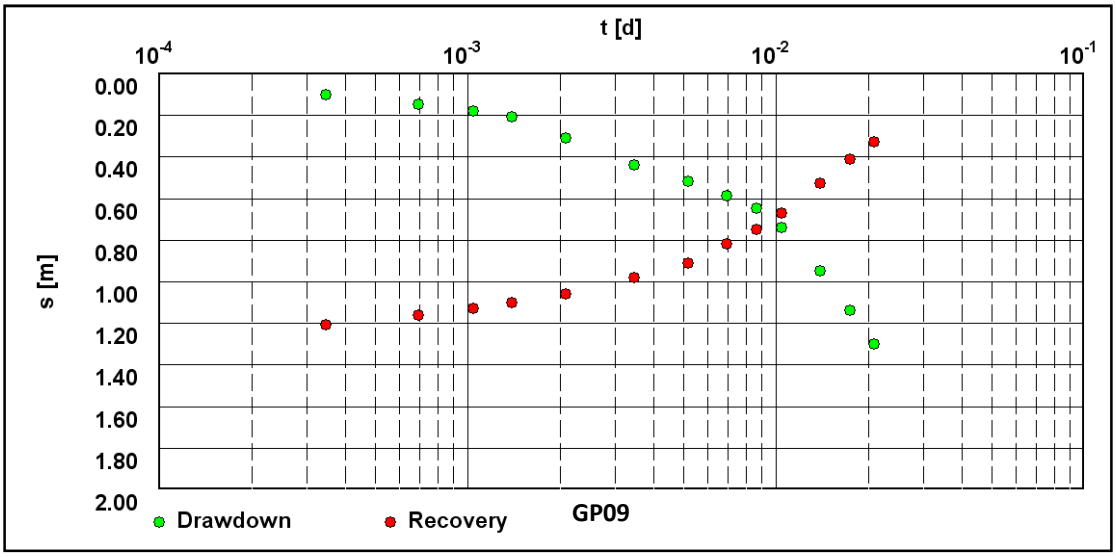
t [d]
10-4
10-3
10-2
10-1
0.00
0.20
0.40
0.60
0.80
1.00
1.20
1.40
1.60
1.80
2.00
s [m]
Drawdown
Recovery
GP09

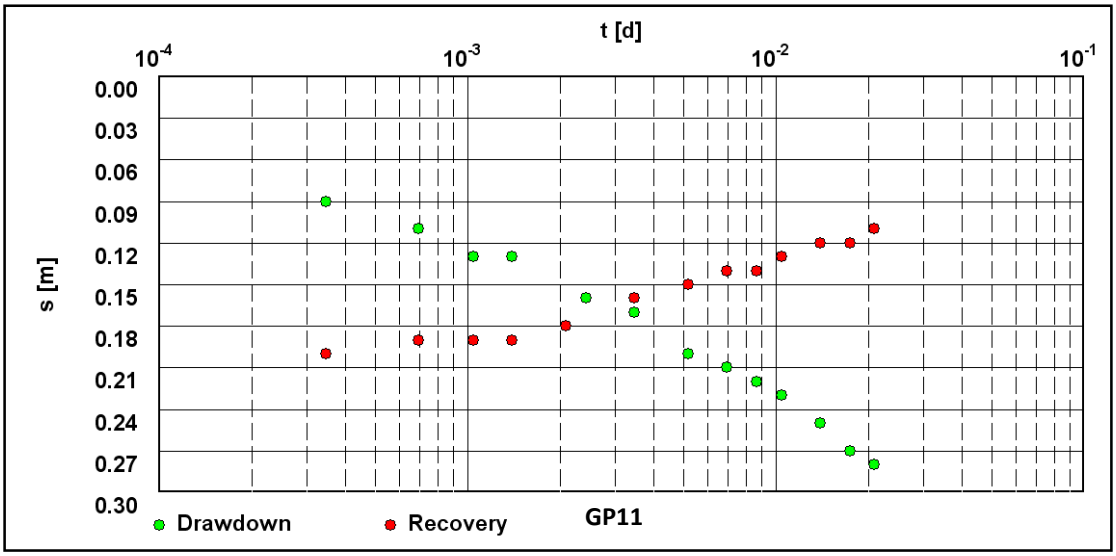
t [d]
10-4
10-3
10-2
10-1
0.00
0.03
0.06
0.09
0.12
0.15
0.18
0.21
0.24
0.27
0.30
s [m]
Drawdown
Recovery
GP11

Appendix D: Chemical analysis results of hydrocensus boreholes

	pH	TDS	Ca	Mg	Na	K	Alkalinity	Cl	SO4	N	F	Al	Fe	Mn
Ideal	5 - 9.5	1000	150	70	200	50	-	200	400	10	1.00	0.30	0.20	0.10
Maximum permissible	4 -10	2400	300	100	400	100	-	600	600	20	1.50	0.50	2.00	1.00
Bly01	6.6	29	3.3	3.2	3.02	1.99	16.93	6.60	<0.1	0.83	<0.48	<0.01	<0.01	<0.01
Bly03	7.4	10	0.7	1.0	1.85	1.09	8.48	<0.1	<0.1	<0.1	<0.48	<0.01	<0.01	0.03
Bly05	7.6	50	4.7	4.1	8.20	1.84	31.72	11.97	<0.1	<0.1	0.55	0.27	0.49	<0.01
Blyvoor 04	6.8	78	0.8	0.4	6.09	1.29	20.82	9.45	<0.1	<0.1	0.60	0.19	4.31	<0.01
Blyvoor05	8.0	74	5.8	4.4	4.41	1.60	40.89	1.80	<0.1	1.16	<0.48	<0.01	<0.01	<0.01
Blyvoor06	8.1	90	5.8	4.5	4.29	1.58	42.50	1.86	<0.1	1.28	<0.48	<0.01	<0.01	<0.01
Bv01	7.0	21	2.0	1.6	3.21	0.34	16.32	0.35	3.36	0.13	<0.48	0.33	0.60	<0.01
BV1	6.9	25	1.6	1.4	5.76	<1	13.30	6.70	0.82	<0.057	<0.183	0.07	0.02	<0.001
Bv2	7.7	28	2.6	2.1	5.20	0.95	17.19	6.26	<0.1	<0.1	<0.48	0.60	0.80	<0.01
Coet01	7.1	20	0.9	1.0	4.03	1.44	15.50	2.20	0.40	0.19	<0.183	<0.037	<0.001	<0.001
EBH01	7.8	148	23.1	16.8	7.67	4.94	150.9	3.2	1.47	<0.057	<0.183	<0.037	0.046	0.207

EBH02	7.9	732	100.4	70.5	51.36	8.53	332.5	11.5	289.91	<0.057	0.202	<0.037	0.029	0.126
EBH03	8.6	202	3.0	2.1	78.37	1.08	179.9	6.3	1.12	<0.057	2.114	0.094	0.866	0.007
EBH08	7.6	173	7.0	5.3	46.02	1.98	169.6	5.9	3.04	<0.057	2.204	7.028	4.649	0.025
Ef01	7.2	24	2.9	2.7	3.76	1.72	12.50	1.50	0.39	3.90	<0.183	<0.037	<0.001	<0.001
Ef07	7.0	47	6.0	3.6	4.68	2.51	40.40	1.50	4.25	<0.057	<0.183	<0.037	<0.001	<0.001
Ef2	7.2	28	1.0	1.0	6.60	1.92	14.80	7.60	1.07	<0.057	<0.183	0.09	0.28	<0.001
Ef5	7.1	1436	168.5	195.4	25.62	31.97	249.30	5.10	859.83	<0.057	<0.183	<0.037	<0.001	<0.001
Eg02	7.2	40	4.1	3.9	6.03	<1	13.10	14.60	1.17	1.38	<0.183	<0.037	<0.001	<0.001
Eg03	7.8	44	6.2	4.6	4.71	<1	29.30	9.80	1.01	<0.057	<0.183	<0.037	0.01	<0.001
GD 01	6.8	138	4.9	3.8	7.06	2.00	42.33	21.93	<0.1	0.15	0.80	0.13	18.06	1.03
GD 02	6.4	96	3.8	2.6	12.43	4.67	4.73	30.29	4.31	3.37	<0.48	0.04	0.04	<0.01
GP01	7.8	196	22.9	15.9	23.03	3.74	114.1	7.5	54.06	0.381	0.219	0.439	0.164	0.054
GP02	7.0	33	3.0	2.8	7.476	1.63	16.6	2.2	1.37	4.42	<0.183	0.66	0.252	0.01
GP04	6.5	28	2.5	1.8	4.39	2.27	17.4	2.6	3.11	0.823	0.337	5.061	1.554	0.067
GP05	6.9	21	1.6	1.0	3.601	2.08	15.8	<1.408	0.77	0.579	<0.183	<0.037	0.358	0.028
GP08	8.0	109	14.9	7.6	12.64	6.57	97.5	3.9	4.38	<0.057	0.639	0.217	0.056	0.024

GP09	7.2	72	10.3	3.8	4.343	5.11	50.8	6.4	10.92	0.126	0.918	26.54	3.804	0.033
GP11	7.2	98	10.8	4.9	14.42	4.03	79.5	5.6	9.83	<0.057	0.97	22.6	5.257	0.082
Grootpan 01	7.7	64	8.3	7.2	10.99	2.35	51.40	16.69	<0.1	1.74	<0.48	0.04	0.79	<0.01
Jou01	7.7	64	4.9	4.0	13.47	2.80	27.10	19.10	3.78	<0.057	<0.183	<0.037	<0.001	<0.001
JouG01	6.9	56	7.1	5.6	7.10	2.05	50.10	2.50	1.06	0.17	<0.183	<0.037	<0.001	<0.001
JP Pretorius	7.8	68	6.0	4.1	6.43	1.86	46.27	8.01	<0.1	<0.1	0.64	0.04	8.23	<0.01
Kotze 03	7.0	266	22.6	20.3	10.34	6.76	8.80	15.68	205.83	1.61	<0.48	<0.01	<0.01	<0.01
Kotze 06	7.9	1722	218.3	150.4	8.11	14.00	39.03	0.34	1177.43	<0.1	<0.48	<0.01	<0.01	<0.01
Kotze 07	7.8	1654	206.8	132.4	8.37	15.07	96.91	1.50	998.34	<0.1	<0.48	<0.01	<0.01	<0.01
Kotze01	7.7	66	6.9	3.0	6.32	6.64	<8.258	2.90	36.66	0.18	<0.183	<0.037	<0.001	<0.001
Kotze02	7.4	29	16.8	10.5	8.99	3.22	<8.258	2.60	85.60	<0.057	<0.183	<0.037	<0.001	0.32
Kotze04	7.9	111	18.6	7.5	7.45	3.53	22.60	<1.408	59.43	<0.057	<0.183	<0.037	<0.001	<0.001
Kotze05	6.2	154	14.1	8.7	12.84	4.74	<8.258	14.20	95.08	4.19	<0.183	7.18	<0.001	0.37
KOTZE08	4.5	45	3.7	2.7	4.49	5.93	22.00	<1.408	13.39	<0.057	<0.183	<0.037	<0.001	0.03
Kuiper 01	8.3	336	40.4	26.3	15.63	4.90	104.34	18.78	156.47	1.02	<0.48	<0.01	<0.01	<0.01

Kuiper02	8.5	210	26.5	7.8	23.63	3.94	127.31	33.78	18.04	0.42	<0.48	<0.01	<0.01	2.51
Kuiper03	8.2	82	7.4	3.9	5.18	3.45	52.58	2.79	<0.1	0.30	<0.48	<0.01	0.01	<0.01
Lb01	7.6	106	15.2	6.5	15.30	4.12	51.60	19.90	14.28	<0.057	0.24	<0.037	<0.001	<0.001
Lb02	4.6	103	14.0	6.4	15.16	4.20	51.30	18.90	13.92	<0.057	<0.183	<0.037	<0.001	<0.001
Lb03	7.7	220	7.3	3.6	85.03	1.52	187.80	5.20	2.96	<0.057	1.91	<0.037	<0.001	<0.001
Lb07	8.0	76	10.7	3.2	12.44	5.12	53.60	3.60	8.57	<0.057	<0.183	<0.037	<0.001	<0.001
Lb08	7.8	26	3.9	2.2	2.61	3.46	20.92	<0.1	0.43	0.55	<0.48	<0.01	<0.01	<0.01
Lb5	7.9	32	3.1	3.3	5.85	<1	11.50	7.00	2.58	2.69	<0.183	0.38	0.01	<0.001
Lb6	7.8	81	5.3	5.4	14.22	2.37	24.21	37.35	<0.1	1.13	<0.48	<0.01	0.24	<0.01
Leeubank	7.8	156	10.6	11.8	15.21	2.45	61.75	43.61	<0.1	0.94	<0.48	<0.01	0.02	<0.01
Paarde 05	8.1	170	20.1	11.6	7.10	9.68	60.04	21.29	45.16	1.74	<0.48	<0.01	<0.01	<0.01
Paarde 06	7.6	128	8.4	3.7	21.15	3.13	22.28	37.75	29.92	0.26	<0.48	<0.01	0.01	<0.01
Paarde04	7.1	22	0.7	0.4	1.73	1.02	7.84	<0.1	<0.1	0.78	<0.48	<0.01	<0.01	<0.01
Paarde04	8.3	14	1.6	-0.3	3.08	1.40	<8.258	<1.408	1.91	0.56	<0.183	<0.037	<0.001	<0.001
Pp01	7.7	48	7.3	6.5	4.31	<1	45.90	<1.408	0.99	<0.057	<0.183	<0.037	<0.001	<0.001
Pp02	8.1	39	4.1	5.4	2.66	0.69	41.13	<0.1	<0.1	1.79	<0.48	<0.01	<0.01	<0.01

Pp02	7.0	49	7.1	6.5	4.62	<1	46.40	<1.408	1.33	<0.057	<0.183	<0.037	<0.001	<0.001
Vaal01	8.1	55	7.6	2.6	7.44	2.60	38.49	5.70	5.87	<0.1	<0.48	<0.01	0.02	<0.01
Vaal02	8.2	82	17.9	3.1	7.36	2.23	60.73	5.56	9.77	<0.1	<0.48	<0.01	0.02	<0.01
Vaal03	7.9	56	5.9	2.8	8.99	2.95	33.83	7.50	7.71	<0.1	<0.48	<0.01	0.04	<0.01
Vil 01	4.3	112	5.7	4.4	9.65	3.31	<0.1	24.52	38.63	<0.1	0.55	0.63	<0.01	0.44
Vil 02	6.9	64	3.6	2.5	8.70	1.92	8.25	21.03	11.76	1.10	<0.48	<0.01	<0.01	<0.01
Vil G01	7.4	24	1.5	0.4	2.93	0.43	9.91	<0.1	<0.1	1.36	<0.48	<0.01	<0.01	<0.01
Vil03	7.2	130	20.3	6.1	17.65	8.23	76.90	19.10	12.05	<0.057	0.40	<0.037	0.01	<0.001
VW 01	7.7	84	3.7	3.0	10.00	2.94	25.63	19.76	<0.1	0.14	0.57	0.90	5.48	<0.01
VW 02	6.9	64	4.0	3.6	9.33	4.07	8.54	23.82	9.59	0.46	<0.48	0.18	0.40	<0.01
VW 03	7.7	96	5.7	5.1	13.51	1.79	23.92	37.37	<0.1	0.47	<0.48	<0.01	0.04	<0.01
VwG01	7.8	138	9.6	4.8	8.24	2.28	21.70	14.52	<0.1	8.00	<0.48	<0.01	<0.01	<0.01
VwG01	7.0	65	10.5	5.2	9.86	2.77	29.60	9.50	4.01	5.26	<0.183	<0.037	<0.001	<0.001
Welt1	7.0	60	5.8	3.4	6.98	7.02	22.95	21.07	0.46	1.01	<0.48	<0.01	0.14	<0.01
Wt02	7.5	49	7.7	5.2	4.97	<1	44.00	3.20	1.12	<0.057	<0.183	<0.037	<0.001	<0.001
Wt1	7.8	14	-0.5	0.3	3.60	1.69	9.30	1.50	1.14	<0.057	<0.183	<0.037	0.09	<0.001

Wt5	7.7	11	0.8	0.5	2.54	<1	<8.258	1.50	0.98	0.20	<0.183	0.04	<0.001	<0.001
Z04	7.3	49	2.5	3.2	11.54	6.24	<8.258	14.00	0.94	6.77	<0.183	<0.037	<0.001	<0.001
Z05	8.0	17	1.0	2.0	2.60	3.58	<8.258	2.80	0.75	4.17	<0.183	<0.037	<0.001	<0.001
Z06	8.4	10	-0.5	-0.3	2.99	1.17	<8.258	2.80	0.92	0.08	<0.183	<0.037	<0.001	<0.001
Z07	7.2	35	2.9	2.4	4.13	5.72	26.10	<1.408	2.95	<0.057	0.23	<0.037	0.010	<0.001
Z08	6.3	31	-0.5	0.5	8.68	4.04	<8.258	11.90	1.12	<0.057	<0.183	<0.037	<0.001	<0.001
Z1	7.0	45	3.2	3.1	8.91	4.40	10.40	11.50	5.56	2.30	<0.183	<0.037	<0.001	<0.001
Z10	7.9	40	5.1	3.8	5.29	0.93	32.98	4.47	<0.1	<0.1	0.63	0.04	0.27	<0.01
Z11	8.0	61	7.0	5.6	9.05	2.88	55.60	1.80	1.09	<0.057	<0.183	<0.037	<0.001	<0.001
Z12	6.9	138	16.1	20.9	11.01	2.44	111.80	19.20	1.20	<0.057	<0.183	<0.037	<0.001	<0.001
Z2	7.1	25	1.8	1.4	5.24	1.55	10.40	7.56	0.86	<0.1	<0.48	0.03	1.82	<0.01
Z3	8.1	774	11.4	11.9	246.00	43.00	311.25	196.13	128.32	1.33	1.18	67.00	42.42	0.22
Z9	8.0	41	5.0	3.7	5.39	1.35	31.89	5.75	<0.1	<0.1	<0.48	0.06	0.46	<0.01
Zk01	6.9	169	4.7	0.9	64.93	2.28	150.50	2.80	1.78	<0.057	1.31	<0.037	<0.001	<0.001
Zk07	7.8	36	0.8	0.8	7.48	7.33	16.00	6.80	2.34	0.85	<0.183	<0.037	0.52	<0.001
Zk4	7.3	75	4.9	4.8	14.05	3.10	18.26	37.16	<0.1	0.19	<0.48	<0.01	0.70	<0.01

Zk5	5.7	19	1.3	0.7	1.75	1.73	5.24	3.13	3.88	0.40	<0.48	0.59	<0.01	0.02
Zk6	7.5	78	5.7	5.6	13.69	4.79	15.00	37.10	<0.1	1.40	<0.48	<0.01	0.02	<0.01
Zoekop 02	7.5	228	5.9	7.1	28.35	32.37	77.35	73.68	<0.1	1.75	0.59	<0.01	2.49	<0.01
Zoekop 03	7.5	54	2.8	1.9	6.06	2.46	13.85	10.06	<0.1	<0.1	<0.48	0.03	2.01	<0.01
Zoekop 07	6.9	316	6.2	8.2	16.13	52.32	79.48	56.33	0.15	2.68	0.76	1.07	1.60	0.52
Zoekop01	8.8	296	2.7	1.0	101.40	2.65	175.27	5.58	20.38	0.92	2.39	<0.01	<0.01	<0.01
Zoekop04	7.2	18	0.7	0.4	4.43	1.31	11.00	3.10	1.01	0.22	<0.183	<0.037	<0.001	<0.001
Zoekop04	7.5	40	1.8	0.9	3.13	1.37	7.41	1.61	<0.1	2.21	<0.48	<0.01	<0.01	<0.01
Zoekop05	8.2	66	4.4	2.6	4.24	3.01	29.45	1.50	<0.1	0.14	<0.48	0.06	0.05	<0.01
Zoekop06	7.6	194	31.5	14.6	22.67	7.22	61.90	65.20	11.81	3.72	<0.183	<0.037	<0.001	<0.001

Appendix E: Analytical Calculations Spreadsheets

Vandersluis et al. Approach

East Block

	East Block			
Year	r	H	R	Q +recharge
2011	316	12	416	103
2012	430	15	530	144
2013	413	16	513	157
2014	378	22	478	201
2015	498	16	598	217
2016	246	17	346	113
2017	294	17	394	117
2018	297	18	397	127
2019	304	18	404	124
2020	294	19	394	132
2021	295	19	395	131
2022	295	19	395	130
2023	308	20	408	139
2024	312	20	412	142
2025	295	21	395	150
2026	317	21	417	152
2027	295	21	395	151
2028	292	22	392	160
2029	286	23	386	169
2030	432	23	532	251
2031	426	24	526	248
2032	417	24	517	245
2033	448	24.5	548	251
2034	420	24.5	520	253
2035	348	24	448	201
2036	353	24	453	207
2037	413	23	513	252
2038	523	22.5	623	272
2039	524	22	624	280
2040	538	21	638	282
2041	470	21	570	250
2042	485	21	585	234
2043	427	22.5	527	246
2044	494	24	594	266
2045	515	26	615	310

2046	475	27	575	308
2047	459	27.5	559	297
2048	416	27.5	516	282
2049	237	27.5	337	203

West Block

Year	West Block			
	r	H	R	Q + recharge
2011	-	-	-	-
2012	-	-	-	-
2013	-	-	-	-
2014	-	-	-	-
2015	-	-	-	-
2016	550	7.5	650	182
2017	544	7.5	644	177
2018	483	6	583	141
2019	465	5.5	565	128
2020	465	5.5	565	130
2021	411	6.5	511	108
2022	391	7.5	491	123
2023	519	9.5	619	164
2024	436	11	536	138
2025	377	12	477	118
2026	389	13	489	122
2027	390	14	490	130
2028	412	15	512	140
2029	454	17	554	182
2030	287	18	387	115
2031	274	19.5	374	125
2032	303	21	403	140
2033	248	22	348	139
2034	251	23	351	147
2035	343	25.7	443	221
2036	359	29	459	262
2037	180	30	280	197
2038	-	-	-	-
2039	-	-	-	-
2040	-	-	-	-
2041	-	-	-	-
2042	-	-	-	-
2043	-	-	-	-
2044	-	-	-	-
2045	-	-	-	-

2046	-	-	-	-
2047	-	-	-	-
2048	-	-	-	-
2049	-	-	-	-

Krusseman and De Ridder approach

East Block

	East Block				
Year	Length (Y)	r	H	R	Q + Recharge
2011	770	316	12	416	189
2012	950	430	15	530	336
2013	840	413	16	513	365
2014	880	378	22	478	556
2015	1700	498	16	598	474
2016	1870	246	17	346	240
2017	1940	294	17	394	275
2018	1980	297	18	397	306
2019	2070	304	18	404	307
2020	2370	294	19	394	329
2021	2380	295	19	395	328
2022	2380	295	19	395	327
2023	2340	308	20	408	370
2024	2400	312	20	412	376
2025	2390	295	21	395	392
2026	2480	317	21	417	415
2027	2380	295	21	395	392
2028	2340	292	22	392	422
2029	2240	286	23	386	448
2030	2300	432	23	532	703
2031	2800	426	24	526	733
2032	3300	417	24	517	719
2033	3300	448	24.5	548	787
2034	3100	420	24.5	520	750
2035	2990	348	24	448	585
2036	2800	353	24	453	597
2037	2800	413	23	513	681
2038	3060	523	22.5	623	810
2039	3380	524	22	624	795
2040	2300	538	21	638	765
2041	2480	470	21	570	666
2042	2520	485	21	585	664

2043	2640	427	22.5	527	673
2044	2870	494	24	594	840
2045	2970	515	26	615	1016
2046	2930	475	27	575	1003
2047	2880	459	27.5	559	990
2048	2840	416	27.5	516	900
2049	2780	237	27.5	337	520

West Block

	West Block				
Year	Length (Y)	r	H	R	Q + recharge
2011	-	-	-	-	-
2012	-	-	-	-	-
2013	-	-	-	-	-
2014	-	-	-	-	-
2015	-	-	-	-	-
2016	1490	550	7.5	650	231
2017	1620	544	7.5	644	226
2018	1440	483	6	583	168
2019	1720	465	5.5	565	150
2020	1440	465	5.5	565	152
2021	1540	411	6.5	511	135
2022	1570	391	7.5	491	157
2023	1660	519	9.5	619	239
2024	1800	436	11	536	220
2025	1840	377	12	477	200
2026	2070	389	13	489	222
2027	2200	390	14	490	247
2028	2200	412	15	512	282
2029	2120	454	17	554	388
2030	1850	287	18	387	247
2031	1850	274	19.5	374	272
2032	1890	303	21	403	334
2033	1900	248	22	348	304
2034	1940	251	23	351	330
2035	1930	343	25.7	443	557
2036	1760	359	29	459	713
2037	1590	180	30	280	399
2038	-	-	-	-	-
2039	-	-	-	-	-
2040	-	-	-	-	-
2041	-	-	-	-	-
2042	-	-	-	-	-

2043	-	-	-	-	-
2044	-	-	-	-	-
2045	-	-	-	-	-
2046	-	-	-	-	-
2047	-	-	-	-	-
2048	-	-	-	-	-
2049	-	-	-	-	-

Marinelli and Nicolli Approach

East Block

Year	East Block				
	rp	ro	Qwall	Qfloor	total Q
2011	316	416	15	288	303
2012	430	530	20	490	509
2013	413	513	19	501	520
2014	378	478	17	631	648
2015	498	598	22	605	627
2016	246	346	12	318	330
2017	294	394	14	380	394
2018	297	397	14	406	420
2019	304	404	14	415	430
2020	294	394	14	424	438
2021	295	395	14	425	439
2022	295	395	14	425	439
2023	308	408	15	468	482
2024	312	412	15	474	488
2025	295	395	14	471	485
2026	317	417	15	506	521
2027	295	395	14	470	484
2028	292	392	14	488	502
2029	286	386	14	499	513
2030	432	532	20	754	774
2031	426	526	19	777	796
2032	417	517	19	760	779
2033	448	548	20	833	854
2034	420	520	19	780	799
2035	348	448	16	634	651
2036	353	453	16	644	660
2037	413	513	19	721	739
2038	523	623	23	892	916
2039	524	624	23	874	898
2040	538	638	24	857	881
2041	470	570	21	750	771
2042	485	585	22	773	795
2043	427	527	19	729	748

2044	494	594	22	901	923
2045	515	615	23	1016	1039
2046	475	575	21	974	995
2047	459	559	21	957	978
2048	416	516	19	868	887
2049	237	337	12	496	507

West Block

	West Block				
Year	rp	ro	Qwall	Qfloor	Q total
2016	550	650	24	313	337
2017	544	644	24	310	334
2018	483	583	22	220	242
2019	465	565	21	194	215
2020	465	565	21	194	215
2021	411	511	19	203	221
2022	391	491	18	223	241
2023	519	619	23	374	397
2024	436	536	20	364	384
2025	377	477	17	343	360
2026	389	489	18	384	402
2027	390	490	18	414	432
2028	412	512	19	469	488
2029	454	554	21	586	607
2030	287	387	14	393	406
2031	274	374	13	405	419
2032	303	403	14	483	498
2033	248	348	12	415	427
2034	251	351	12	438	450
2035	343	443	16	668	684
2036	359	459	17	789	806
2037	180	280	9	409	418

Darcy Approach

	East Block		West Block	
Year	Q Darcy S=0.1	Q Darcy S=0.01	Q Darcy S=0.1	Q Darcy S=0.01
2011	350	150		
2012	530	230		
2013	590	250		
2014	890	340		
2015	640	300		
2016	410	160	350	220

2017	470	180	250	180
2018	550	210	190	140
2019	570	210	160	130
2020	750	270	170	130
2021	660	240	150	110
2022	620	230	190	130
2023	640	230	320	190
2024	680	250	290	160
2025	710	260	280	140
2026	780	280	360	170
2027	730	260	400	180
2028	770	270	450	200
2029	810	290	620	270
2030	1170	450	490	180
2031	1370	500	520	190
2032	1480	540	620	220
2033	1440	520	650	230
2034	1390	510	740	260
2035	1180	420	990	360
2036	1210	430	1200	420
2037	1350	510	910	300
2038	1350	521		
2039	1380	540		
2040	1100	460		
2041	1090	440		
2042	1100	430		
2043	1340	500		
2044	1370	510		
2045	1570	590		
2046	1640	600		
2047	1610	580		
2048	1530	550		
2049	480	480		

Summary

A new opencast coal mining operation is proposed in the Belfast region in Mpumalanga, South Africa. This proposed operation is the study site that was investigated in this thesis. The Belfast opencast operation is expected to be operational for 29 years and coal from mainly the number 2 and 3 seams will be mined.

The inflow rate of the groundwater was determined by using both analytical and numerical groundwater methods. The rate at which groundwater flows into the mine voids are important to estimate before mining commence since this will determine at what rate groundwater needs to be pumped from the mining pits to ensure dry and safe working conditions.

In order to obtain site specific data for the study area, several field investigations have been conducted. These investigations include a geophysical survey, drilling of monitoring boreholes and pump testing of the monitoring boreholes. These investigations are done to obtain a better overview of the aquifer conditions in the study area.

For the study area a numerical groundwater flow model was constructed and the groundwater inflow was determined by making use of a water budget function. The analytical approach to determining the inflow included four different methods. A sensitivity analysis was done on the recharge with the numerical and analytical methods.

The results from the numerical and analytical approaches were compared to determine whether the analytical approach is in fact a good way of obtaining values that relates with the numerically obtained results. If there is a good correspondence between the analytical and numerical results, the analytical approach can be regarded as a save and representative way to obtain groundwater related values. Especially during the early stages of mine planning analytical methods would be supportive to quickly determine mine related issues as this will assist in decision making and related cost estimates.

From the results obtained in this thesis it can be concluded that the analytical approaches used during this study, although giving close to numerical answers, cannot be used in an effective manner in determining groundwater inflows during the early planning of mining.

The fact that the analytical approaches did not reveal representative values for the groundwater inflows and also do not correlate with the numerical model results, does not mean that this will be the case at another site with different geohydrological characteristics. It is important to note that assumptions are always made in analytical methods.

It is suggested that further research be conducted in relation with analytical and numerical modelling of opencast mines. Research should be performed at several mines to determine whether the relation between the numerical and analytical approaches display similar trends than was found during this study. These mines should preferably be on similar geological areas to compare with each other. The only way to determine whether the analytical methods can in fact be used to get a representative result is by repetition on several mining sites and also comparing these values with the numerical model results and also the actual inflow rates from the mine once mining has started.

Opsomming

‘n Nuwe oopgroefmyn word beplan in die Belfast omgewing, Mpumalanga, SuidAfrika. Hierdie beplande myn is die studie area wat tydens hierdie studie bestudeer is. Dit word verwag dat die Belfast projek operasioneel sal wees vir 29 jaar en Steenkool sal hoofsaaklik vanuit die 2 en 3 soom gemyn word.

Die groundwater invloei tempo is bepaal deur gebruik te maak van beide analitiese en numeriese grondwater metodes. Dit is belangrik om die geskatte tempo van grondwater invloei na die oopgroef te bereken voordat mynbou begin aangesien hierdie geskatte waardes sal bepaal teen watter tempo grondwater vanuit die groef gepomp moet word om te verseker dat mynbou op ‘n veilige en droë manier plaasvind.

Verskeie veld ondersoeke is in die studie area uitgevoer om data eie aan die omgewing te verkry. Hierdie ondersoeke sluit in ‘n geofisiese ondersoek, boor van moniterings boorgate asook pomptoetse op die nuwe moniterings boorgate. Hierdie ondersoeke word uitgevoer om ‘n beter oorsig van die akwifeer eienskappe in die studie area te verkry.

‘n Numeriese grondwater model is opgestel vir die studie area en die grondwater invloeie is bepaal deur gebruik te maak van die ‘water budget’ funksie. Vier verskillende analitiese metodes is gebruik gedurende die studie om die invloeie na die groef te bepaal. ‘n Sensitiwiteits analiese van die akwifeer aanvulling is uitgevoer deur gebruik te maak van die analitiese en numeriese metodes.

Die resultate van die numeriese en analitiese metodes is vergelyk om te bepaal of die analitiese metodes wel ‘n goeie manier is om resultate te verkry wat in verhouding is met die waardes wat numeries verkry is. In die geval van ‘n goeie verhouding tussen hierdie twee metodes, kan die analitiese metode geag word as ‘n veilige en verteenwoordigende manier om grondwater verwante syfers te verkry. Veral gedurende die vroeë stadiums van beplanning van die myn, sal dit

handig wees om vinnig mynverwante kwessies te bepaal en dit sal dus besluite en verwante koste beramings ondersteun.
Vanaf die resultate wat verkry is tydens hierdie studie kan die gevolgtrekking gemaak word dat die analitiese metodes wat gebruik is tydens hierdie studie nie, alhoewel daar soms waardes verkry is wat naby aan die numeriese waardes is, nie gebruik kan word op ‘n effektiewe manier om die grondwater invloeie te bereken tydens die vroeë stadiums van myn beplanning.

Die feit dat die analitiese metodes nie verteenwoordige syfers verskaf het nie en nie met die numeriese syfers vergelyk nie, beteken nie dat dit die geval sal wees in alle omgewings met verskillende geohidrologiese eienskappe nie. Aannames word altyd gemaak in analitiese berekeninge. Dit is dus die hoof aanbeveling dat die waardes wat tydens hierdie studie verkry is (veral numeries), vergelyk sal word met die feitlike invloeie wat deur die myn gemeet word wanneer mynbou in die operasionele fase is.

Verdere studies in die analitiese en numeriese bepaling van grondwater invloeie na die groewe word voorgestel. Navorsing moet gedoen word op verskeie myne om te bepaal of die verwantskap tussen die analitiese en numeriese benaderings ook in ander omgewings eenderse resultate verkry. Die enigste manier om te bepaal of hierdie analitiese metodes wel verteenwoordigende syfers verskaf is deur die herhaling van die metodes op verkeie ander studie areas en ook die vergelyking met werklike pomp tempos verkry vanaf die myn wanneer mynbou alreeds begin het.